NORCE Norwegian Research Centre AS
www.norceresearch.no

Satellite-Based National Intertidal-Zone Mapping of Continental Norway with Sentinel-1&2

Sluttrapport: Fjernmålingsbasert kartlegging og overvåking av tidevannssonen.
Opsjon-2: Nasjonalt kartlegging
April 2021

Jörg Haarpaintner, Corine Davids, Heidi Hindberg, Ingar Arntzen & Njål Borch

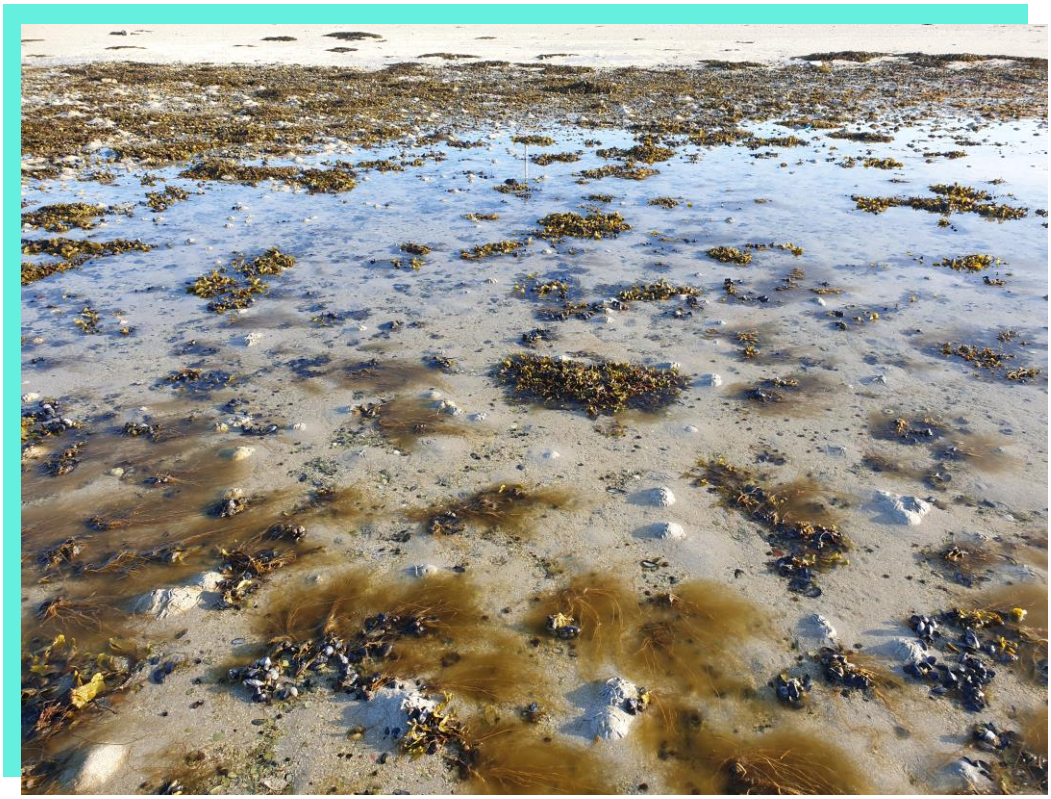

Final REPORT 1-2021
NORCE Klima

Project title:	Fjernmålingsbasert kartlegging og overvåking av tidevannssonen.
Project number:	101800
Institution:	NORCE – Norwegian Research Centre AS
Client/s:	Miljødirektoratet (MD) Project: M-1994 I 2021 Satellite Based Intertidal-Zone Mapping from Sentinel-1&2 Contact person: Tomas Holmern
Classification:	Public
Report no.:	1-2021 (NORCE KLIMA)
ISBN:	978-82-8408-147-2
Number of pages:	91
Publication month:	April 2021
Citation:	Haarpaintner, J. & C. Davids. Satellite-Based National Intertidal-Zone Mapping of Continental Norway with Sentinel-1&2. Final Report, NORCE Klima Report nr. 1-2021, Norwegian Environment Agency report M-1994, 30 March 2021.
Captions and credits:	Contains modified Copernicus Sentinel-1&2 data (2018-2019), processed by NORCE

Summary:
The report describes updated methods that were originally developed in Haarpaintner & Davids (2020) to map the intertidal zone, in terms of atmospheric exposure, type and areal extent, based on radar and optical high resolution (10m) satellite imagery from Sentinel-1A/B (C-band synthetic aperture radar, C-SAR) and Sentinel-2A/B (multi-spectral instruments) of the European Copernicus Program. It further presents the application of the method to create products covering the whole Norwegian coast and describes some limitations and error sources. The project resulted in a first version of national products of the intertidal zone area, type and its atmospheric exposure.

Revisions

Rev.	Date	Author	Checked by	Approved by	Reason for revision
V 0.1	2.12.2020	J. Haarpaintner	C. Davids		Foreløpig rapport
V1-1	15.03.2021	J. Haarpaintner	C. Davids		Final Report
V2.1	09.04.2021	J. Haarpaintner	C. Davids		Reviewed final report

Tromsø, 09.04.2021

Jörg Haarpaintner	Corine Davids	Tomas Holmern
Project manager	*Quality assurance*	*Contact person at MD*

Disclaimer – limitation of liability

The authors assume no responsibility or liability for any errors or omissions in the content of this research report. The information contained in this report is provided "as is", based on their best knowledge and effort during the work of the project with no guarantees of completeness, and accuracy.

Preface

In 2019, the Norwegian Environment Agency issued a call for tender to map and monitor the intertidal zone of Norway with free remote sensing data. In a first phase, the winning tender should develop methods and algorithms that are able to map the intertidal zone area, distinguish between different types and environmental parameters of the intertidal zones in order to be able to do this operationally on a periodic basis. The methods were demonstrated on Trondheimsfjord. This has been reported in Haarpaintner & Davids (2020).

In a second phase, presented by this report, the goal is to apply the developed methods on the whole Norwegian coastline to develop a first version of a national map of the intertidal zone including a minimum accuracy and quality assessment.

The continuation in the following phases should then lead to an operational system that leads to a national intertidal zone map that can be updated periodically, as well as the potential to detect changes in this area.

NORCE – the Norwegian Research Centre AS successfully responded to the tender proposing to develop methods focusing on the use of Sentinel-1 and Sentinel-2 of the European Copernicus Program. This is the final report after the second phase (Option 2) about the national mapping of the intertidal zone under contract M-1994|2020.

Table of Contents

List of figures

List of tables

Summary for Policy Makers: Satellite-Based National Intertidal-Zone Mapping of Continental Norway with Sentinel-1&2

Background and Objectives

The intertidal zone (ITZ) (Figure A) is a vulnerable coastal ecosystem with high biodiversity providing important ecosystem services. The ITZ, defined as the area between the lowest and the highest tidal level water line, is under strong pressure due to changes in land use (e.g., new constructions, habitat destruction, coastal erosion, contamination), changes in marine use (e.g., aquaculture), as well as climate change and sea-level rise. Because of it its highly dynamic nature, it is a challenging area to map and monitor on a national scale and the only possibility to observe it at different tidal stages is with dense time-series data from air or space. Aerial observations are costly and therefore limited in time and space, which makes satellite observation the only viable solution. Over Norway, the European Copernicus Program provides near-daily radar (cloud independent) and optical imagery of 10m resolution that can sample the tidal cycle on a national scale.

The main objective of the project is to develop efficient methods to map and monitor the ITZ based on freely available satellite data and apply this on a national scale to deliver a first version of national ITZ products.

In the first phase of this project, satellite-based methods to map the ITZ area, atmospheric exposure and type were developed using high resolution (10m) radar and optical satellite imagery from the Sentinels-1&2 of the European Copernicus Program (Haarpaintner and Davids, 2020). In the second phase, reported here, the objective is to refine the methods and apply them on a national scale to produce a first version of national map products of the ITZ over Norway.

Figure A. Examples of ITZ types from left to right: sand beach, stone beach, mudflats, rocks, seaweed

Methods and Results

The overall approach is to use long, dense times-series of satellite acquisitions and the fact that the frequency of satellite acquisition is different than the tidal period of ~12.25h, to ensure acquisitions and sampling over the full range of tidal cycle levels (Figure B). Both sensors, Sentinel-1's C-band synthetic aperture radars (CSAR), S1A and S1B, and Sentinel-2's MultiSpectral Instruments (MSI) (S2A and S2B) can distinguish between water covered areas and land. As SAR is independent of cloud cover and sunlight, it can sample the tidal levels at a much higher rate than optical sensors that need cloud free conditions to observe the earth's surface. At the latitude of Trondheimsfjorden, which was the study site during the first method developing phase, each pixel is covered on a near-daily basis by 240 to 360 acquisitions per year with Sentinel-1 (S1). On the

other hand, optical data acquires information from several meters below the water surface and can, therefore, be used to map the ITZ with fewer acquisitions, although too few available acquisitions enhance any errors in cloud masking.

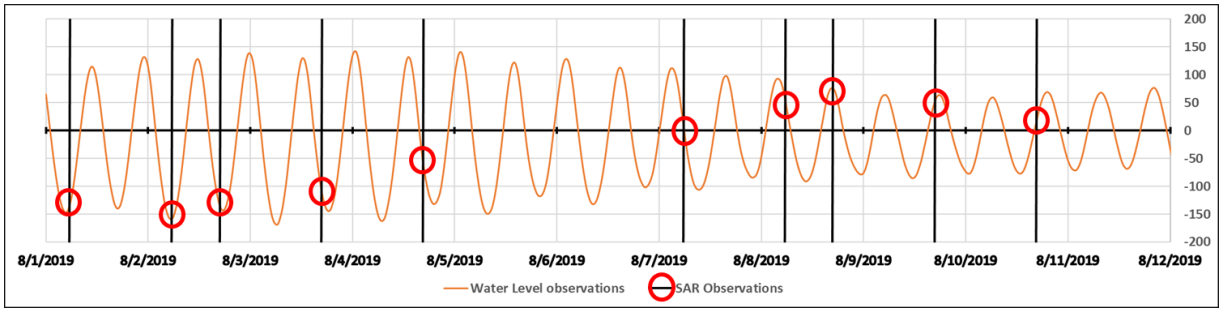

Figure B. Near-daily sampling of the tidal level with Sentinel-1 in Tromsø Kommune.

In the second phase these methods were reviewed, refined and updated with the help of field data, collected in Tromsø Kommune, in order to apply them on the whole coast of continental Norway and produce a first version of national ITZ products. We focused on the high sampling rate of S1 to map the atmospheric exposure of the ITZ and on Sentinel-2 (S2) to classify the ITZ into types. Both sensors provide independently the area of the intertidal zone which can then be combined into one S1/S2 combined ITZ area product.

To map the atmospheric exposure, all S1 (A&B) data from the ice-free months (June to November) over the Norwegian coast from 2018 and 2019 were processed and statistically analysed. Percentile values of the radar backscatter in co- and cross polarization, VV and VH, were extracted for each pixel at 2%, 5%, 25%, 50%, 75%, 95% and 98% percentiles. The method is based on the fact that in SAR imagery, water and land can be relatively easily separated by simple thresholding; pixels in the intertidal zone can then be classified as land or water depending on the percentile image and can thereby be associated to a tidal level and the atmospheric exposure. Specific thresholds to divide between water and land for each percentile are extracted to best fit GPS tracks from water lines collected during fieldwork at different tidal levels. Each threshold contour line corresponds then directly to a certain tidal level. The water line of the 2% percentile will correspond to the (near-) highest tide, the 50% percentile to Mean Sea Level (MSL) and the 98% percentile to the near-lowest tide waterline. The area in between defines the intertidal zone area. Extracted water lines at other percentile values, i.e., 95%, 75%, 25% and 5%, correspond to the tidal levels mean low water spring (MLWS), MLW neap (MLWN), mean high water neap (MHWN) and spring (MHWS), respectively, and therefore to the atmospheric exposure.

As the extraction of the statistical values and percentiles is computational resource-demanding at 10m resolution over a large area, the Norwegian coast has been divided into 20x20 km tiles that were subsequently mosaicked together into 9 county products (Figure C). All S1 processing in this study was done in-house but can be exported into the cloud or a large processing facility like one of the Copernicus Data & Information Access Services (DIAS) currently developed through the European Space Agency (ESA).

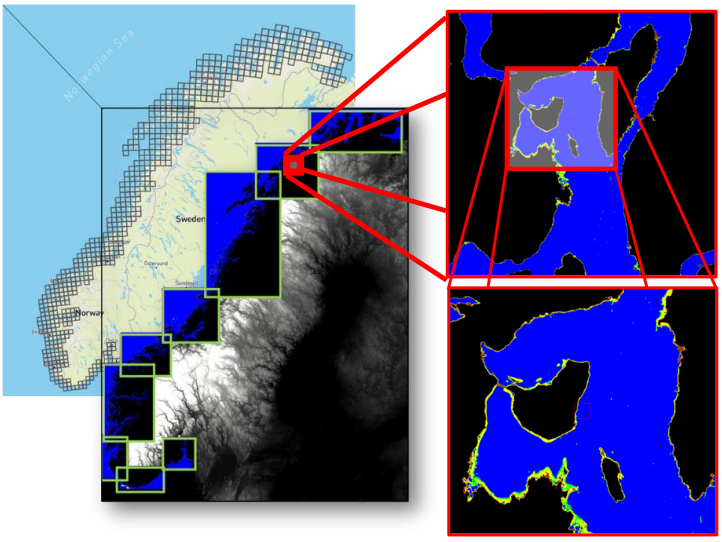

Figure C. Processing of the whole Norwegian coast in 20 x 20 km² tiles and mosaicking into 9 county products (left) and detailed view of the tile around Tromsø (right).

Similar to the S1 approach, the methodology used for the analysis of Sentinel-2 data is based on statistical analysis of dense time series. For the purpose of mapping ITZ types, statistical parameters are calculated from time series of several vegetation and water indices. A supervised classification using a random forest classifier and a training dataset is then applied to classify into permanent water, shallow water, mudflat, sandy/gravel beach, rocky shoreline, seaweed, and land. The training dataset was acquired by visually interpreting aerial photographs from norgeibilder.no, and the classes were chosen based on what appeared possible to identify from aerial photographs without further knowledge of the area. Due to cloud cover and dark winter months in Norway, the number of cloud free acquisitions varies mainly between 15 to 65 times per pixel for 2019. The ITZ area detected by S1 and S2 correspond well in general, with some expected variations between the two methods. It turns out that S2 can better detect large areas of mudflats than S1, particularly if the mudflats remain water saturated during the tidal cycle. Suspended sediments from river outflows can locally cause misclassification of water as shallow water and will require more specific training data. S2 processing and analysis was done using Google Earth Engine.

Combining the S1 and S2 intertidal areas can better delineate the whole ITZ area and provides a measure of confidence in the accuracy of the mapped areas where both methods agree. On the other hand, areas which are mapped as ITZ area by only one of the methods provide either complementary information (e.g. the presence of intertidal pools, or areas with shallow water) or highlight errors in the classification. Generally, such ambiguities can visually easily be distinguished.

As mentioned in Haarpaintner and Davids (2020), aerial images from norgeibilder.no turned out not to be suitable to map the ITZ on a large scale for several reasons: the aerial mosaics are not consistently acquired, neither in space, nor in quality, nor in resolution, nor in similar light condition, and nor in time, which makes it nearly impossible to map the ITZ on a national scale; only acquisition dates are available for the mosaics and not exact acquisition times which makes it difficult to define the tidal level for interpretation; observations are too few to ensure acquisitions at highest and lowest tides; the water line is not clearly visible and shallow water areas can be easily misinterpreted as ITZ. This limits also the possibility to use the aerial image database directly for a direct validation, especially for the atmospheric exposure product, but they can be used for

comparison and type interpretation. Aerial photographs are, however, useful for more detailed local mapping of the ITZ if they are taken at suitable low tidal levels.

Field data (Figure D1) has been collected at 7 occasions in 5 large ITZ areas around Tromsø. The fieldwork focused on 1. mapping the extent of the ITZ by tracking the water line at spring low tides, 2. mapping atmospheric exposure by tracking the water line at several tidal stages during a half tidal cycle, and 3. documenting different land cover and soil types in the ITZ. The fieldwork also showed some additional challenges: on shallow mudflats, the water line is rarely a clear line but more a transitional zone with puddles on dry mud, and small topographic features like small rocks, seaweed, or sandbanks surfacing in shallow water. Mapping the water line in the field is therefore based on a subjective decision and will also have an uncertainty of several or up to tens of meters.

The validation based on this field data show that with S1 an accuracy of 99% can be achieved in detecting ITZ areas above MSL (Mean Sea Level); ITZ areas down to the MLW and MLWS water lines are detected with an accuracy of 84% and 64%, respectively. The MSL seems to be well detected in all field validations. The overall accuracy of the ITZ type product based on a validation set of 290 pixels of visual interpretation of aerial mosaics from norgeibilder.no has been assessed to 86%. The majority of the training and validation points are currently, however, from northern Norway, and the accuracy of the current products is, therefore, likely to be less in other parts of Norway. The results of this study have also been compared with the mudflat data set from the Norwegian Environment Agency's "Naturbase". This mudflat data set, based on visual aerial image interpretation, is however clearly incomplete and also includes mudflats in shallow waters.

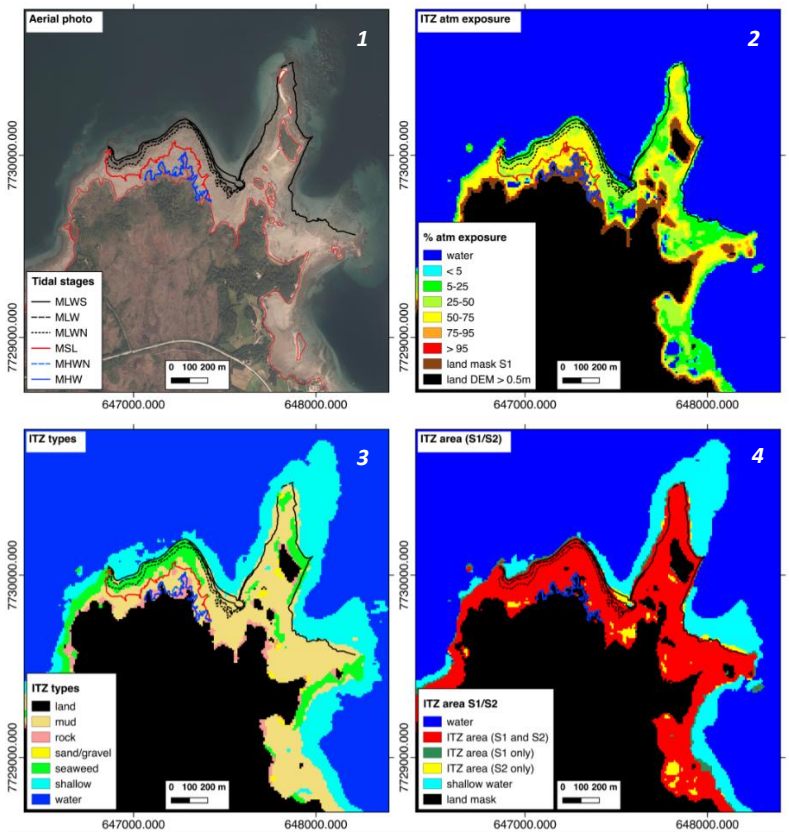

Figure D. Comparison between an aerial mosaic and field data of tidal level (1) and the different products from this project: ITZ atmospheric exposure (2), ITZ types (3), and combined S1/S2 ITZ area (4).

Discussion and Outlook

A first version of three national ITZ maps at 10m resolution representing ITZ atmospheric exposure,type and area (Figure D)have been produced in this project based on the analysis in the scale of 20 TB of satellite data. Each final national map product has a size of about 4.5 GB uncompressed and 50MB in compressed format. They have each been divided in 9 county products. These products clearly represent the best and most consistent ITZ data set currently available for Norway. A quantitative validation has been limited to Troms County due to a lack of funding and Covid-19 travel restrictions. Qualitatively, a number of challenges however were identified, including by a rough inspection of the other county products. Such challenges include misclassification of S1 results in areas with steep topography particularly in fjords in east-west orientation, the effect of ship traffic particularly around densely populated areas in southern Norway dominating the S1 signal of a generally smaller tidal range and the misclassification of fish farms as ITZ. Misclassification of S2 results can be generally associated with errors in cloud masking, the presence of suspended sediments in the water column, and the lack of training points in southern and mid Norway. An experienced user should be able to distinguish most of such misclassifications visually. To further improve the products, future studies should focus on the collection of field data in order to train, refine and better validate the methods on a county level, including a manual final “clean-up” of the results, in addition to extending the training/validation database based on visual interpretation of aerial photographs and other available data. Due to a generally lower tidal range and therefore a less significant ITZ in southern Norway, priority might be given to mid and northern Norway counties. Further combining S1 and S2 could be explored to improve the current products or develop new products, e.g. combining atmospheric exposure with type could be used to further delineate different areas. Furthermore, the methods need to be more automized if ITZ maps should be produced on a periodic basis in order to detect changes.

The current products can be used in the identification and delineation of important ITZ areas. The bathymetry in the ITZ is clearly represented in the ITZ AtmExp product and could be used for planning boat landings and new constructions. High biodiversity areas can be associated with the presence of seaweed and mudflats in the ITZ type product. After a manual clean-up, the total area of ITZ per county should also be quantifiable. The position as well as the size of fish farms are clearly identifiable in the products. As boat traffic detection dominates the ITZ in southern Norway where the tidal range is relatively low, particularly the products around densely populated areas are likely less accurate than our accuracy assessment in Troms county suggests.

The study also revealed new potential opportunities to map fish farms, suspended sediments, kelp forest and to estimate boat traffic or harbor occupancy in populated areas.

Utvidet Sammendrag (Norsk): Fjernmålingsbasert kartlegging og overvåkning av økosystemet våtmark – tidevannssonen ved bruk av Sentinel-1/2.

Bakgrunn og Mål

Tidevannssonen (TVS) (Figur A) er et sårbart kystøkosystem med høyt biologisk mangfold som gir viktige økosystemtjenester. TVS er området mellom laveste og høyeste tidevann, som dekkes av vann ved høyvann og kommer i kontakt med luft ved lavvann. Dette området er under sterk press fra arealendringer (for eksempel nye konstruksjoner, kysterosjon, habitatødeleggelse), endringer i marint bruk, forurensning, klimaendringer og havnivåstigning. Det er krevende å kartlegge og overvåke tidevannssonen på nasjonalt nivå pga. den store dynamikken i tidevannet. Den eneste muligheten for å observere TVS på ulike tidevannsnivåer er å bruke tidsserier med bilder fra fly eller satellitt. Å ta flybilder over hele Norge er dyrt og gjøres derfor mindre enn en gang i året. Derimot gir det europeiske Copernicus programmet oss nesten daglige satellitt bilder med 10m oppløsning over hele Norge.

Hovedmål i dette prosjektet er å utvikle effektive metoder basert på fritt tilgjengelige satellittbilder for å kartlegge og overvåke TVS og definere nasjonale kartprodukter.

I første fase av prosjektet ble metoder utviklet for å kartlegge areal, tørrleggingsvarighet, og naturtyper i TVS ved hjelp av høyoppløselig (10m) radar og optiske satellittbilder fra Sentinels-1 og 2 i det europeiske Copernicus-programmet (Haarpaintner og Davids, 2020). Målet i den andre fasen, rapportert her, er å forbedre metodene og bruke dem på nasjonalt nivå for å produsere en første versjon av nasjonale kartprodukter over Norge.

Figur A. Eksempler av TVS naturtyper. Fra venstre: sandstrand, steinstrand, bløttbunnfjære, fjell, tang.

Metoder og resultater

Den generelle tilnærmingen er å bruke lange, tette tidsserier av satellittdata; da frekvensen av satellittopptak er forskjellig fra tidevannsperioden på ~ 12,25 timer, får vi observasjoner over hele tidevannsyklusen (Figur B). Begge sensorer, avbildende C-bånd radar (CSAR) fra de to Sentinel-1 satellitter, S1A og S1B, og det multi-spektrale instrumentet (MSI) fra de to Sentinel-2 satellitter, S2A og S2B, kan skille mellom vann og land. Ettersom SAR er uavhengig av skydekke og sollys, kan den ta hyppigere opptak over tidevannsnivåene enn MSI, som trenger skyfrie forhold for å observere jordoverflaten. På breddegraden til Trondheimsfjorden, som var testområdet i utviklingsfasen, dekkes hver piksel nesten daglig med 240 til 360 opptak per år med Sentinel-1

(S1). Sentinel-2 (S2), derimot, ser også noen meter under vannoverflaten og kan derfor kartlegge TVS med færre opptak. Imidlertid kan for få tilgjengelige optiske opptak føre til økt feilklassifisering fordi mulige problemer med skymaskering vil ha økt påvirkning på resultatet.

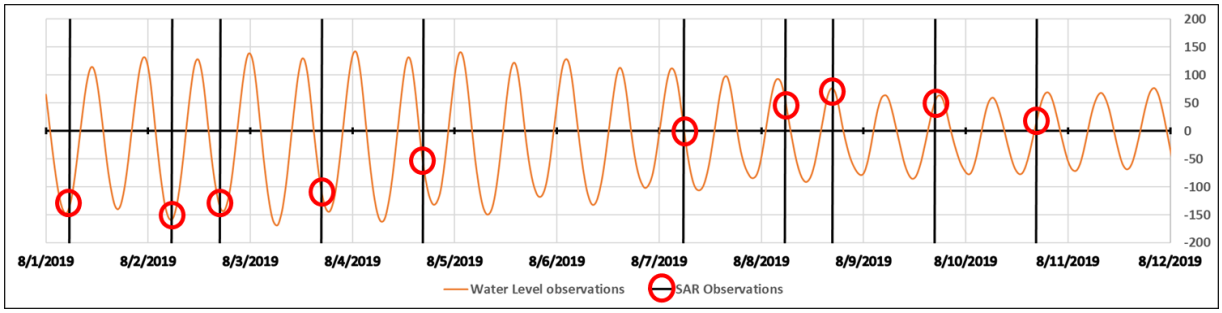

Figure B. Nesten daglige S1 opptak I forhold til tidevannsnivå i Tromsø Kommune gjennom en 12 dagers satellittsyklus.

I den andre prosjektfasen blir disse metodene gjennomgått, forbedret og oppdatert ved hjelp av feltdata innsamlet i Tromsø kommune, for så å bruke metodene langs hele den norske kysten til å lage nasjonale kart om TVS. Vi bruker den høye opptaksfrekvensen til S1 CSAR for å kartlegge tørrleggingsvarighet og den optiske S2 MSI for å klassifisere i naturtyper i TVS. Begge sensorene gir også TVS arealet uavhengig av hverandre som deretter kan kombineres til ett S1/S2 kombinert TVS areal produkt.

For å kartlegge tørrleggingsvarighet ble alle S1 (A&B) data fra de isfrie månedene (juni til november) over den norske kysten fra 2018 og 2019 prosessert og analysert statistisk. Persentilverdier av radar-tilbakespredning i co- og krysspolarisering, VV og VH, ble ekstrahert for hver piksel ved 2%, 5%, 25%, 50%, 75%, 95% og 98% persentiler. Metoden er basert på at i SAR-bilder kan vann og land relativt enkelt skilles fra hverandre ved enkel terskling; piksler i TVS kan deretter klassifiseres som land eller vann, avhengig av persentilbildet, og kan derved knyttes til et tidevannsnivå og tørrleggingsvarighet (i %). Under feltarbeidet ble det kartlagt vannlinjer ved ulike tidevannsnivåer med bruk av GPS. Disse GPS-spor fra vannlinjene fra forskjellige tidevannsnivåer er deretter brukt for å definere spesifikke terskler for å skille mellom vann og land for hver persentil. Hver terskelkonturlinje tilsvarer deretter direkte et bestemt tidevannsnivå. Vannlinjen til 2% persentilen vil tilsvare (nær) høyeste tidevann, 50% persentil til gjennomsnittlig havnivå (MSL) og 98% persentil til nærmest laveste tidevannlinjen. Området imellom definerer TVS arealet. Tidevannsnivåer ved andre persentilverdier som 95%, 75%, 25% og 5%, tilsvarer nivåer av henholdsvis middel spring lavvann (MLWS), og middel nipp lavvann (MLWN), middel nipp høyvann (MHWN) og middel spring høyvann (MHWS) og derfor til tilsvarende prosent tørrleggingsvarighet.

Ettersom beregning av statistiske verdier og persentiler er ressurskrevende i 10m oppløsning over hele Norge er den norske kysten delt inn i 20x20 km^2 fliser som deretter ble satt sammen til ni fylkesprodukter (Figur C). All S1-prosessering i denne studien ble utført med interne dataressurser men kan eksporteres til skybasert prosessering i for eksempel en av Copernicus Data & Information Access Services (DIAS) som er utviklet gjennom European Space Agency (ESA).

I likhet med S1-tilnærmingen er også S2 metoden basert på statistisk analyse av tette tidsserier. For å kartlegge TVS-naturtyper beregnes statistiske parametere fra tidsserier av flere vegetasjons- og vannindekser. En veiledet klassifiseringsmetoden «random forest» og et treningsdatasett er brukt for å klassifisere i permanent vann, grunt vann, bløtbunn, sandstrand / grusstrand, fjell, tang/tare og land. Treningsdatasettet er basert på visuell tolking av flyfoto fra norgeibilder.no, og klassene ble valgt ut fra det som syntes å være mulig å identifisere fra flyfoto uten ytterligere kunnskap om området. På grunn av skydekke og mørke vintermåneder i Norge, varierer antall

skyfrie opptak mellom 15 og 65 per piksel for 2019. TVS-areal oppdaget av S1 og S2 samsvarer generelt godt, med noen forventete variasjoner mellom de to metodene. Det viser seg at S2 detekterer bløtbunn områder bedre enn S1, spesielt hvis bunnen er vannmettet. Suspenderte sedimenter fra elveutstrømninger kan lokalt forårsake feilklassifisering av vann som grunt vann og vil kreve mer spesifikke treningsdata. S2-prosesseringen og analysen ble gjort ved hjelp av Google Earth Engine.

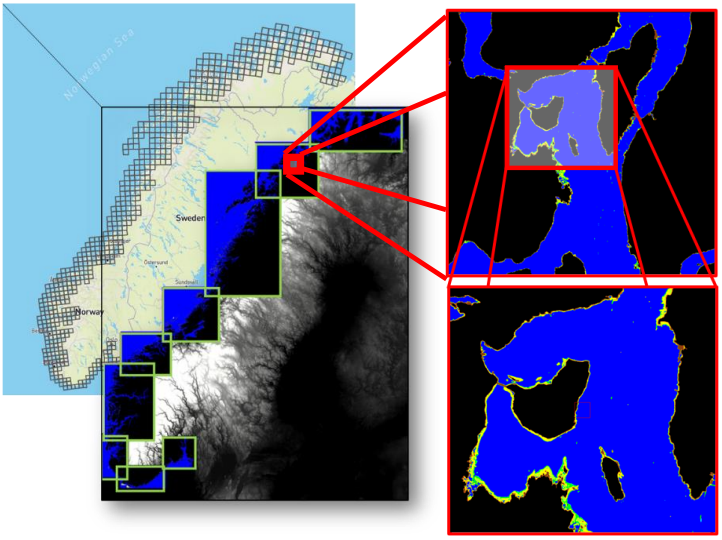

Figur C. Prosessering av S1 over hele norske kysten. Kysten deles i 20 x 20 km^2 blokker som til slutt er satt sammen i ni fylkesprodukter (venstre). Til høyre vises område rundt Tromsø mer detaljert.

Ved å kombinere resultatene fra S1 og S2 blir hele TVS-området bedre avgrenset, og det gir et høyere tillit i resultatene i de kartlagte områdene hvor begge metodene er enige. I tillegg gir TVS arealet som er kartlagt med bare en av metodene enten komplementær informasjon (f.eks. tilstedeværelsen av tidevannsbassenger eller områder med grunt vann) eller markerer feil i klassifiseringen. Generelt kan slike uklarheter lett skilles visuelt.

Som nevnt i Haarpaintner og Davids (2020) viste det seg at flyfoto fra norgeibilder.no ikke var egnet til å kartlegge TVS i stor skala av flere grunner: Flyfotomosaikkene er ikke konsekvent i opptak, verken i rom, tid, kvalitet, oppløsning, og heller ikke i lignende lysforhold, noe som gjør det nesten umulig å kartlegge TVS på nasjonal skala basert på flybilder. I tillegg er bare opptaksdatoer tilgjengelige for mosaikkene og ikke nøyaktige opptakstider som gjør det vanskelig å definere tidevannsnivået for tolkning. Oservasjoner er for få til å sikre opptak ved høyeste og laveste tidevann, vannlinjen er ofte ikke godt synlig, og grunne vannområder kan lett tolkes som TVS. Dette begrenser også muligheten til å bruke flybildedatabasen direkte til validering, og spesielt for tørrleggingsvarighetskart. Flybildene kan derimot brukes til sammenligning og til en viss grad til tolkning av TVS naturtyper. Flyfoto er imidlertid nyttig for mer detaljert lokal kartlegging av TVS hvis de er tatt på passende lave tidevannsnivåer.

Feltdata (Figur D1) er samlet inn ved sju anledninger i fem store TVS områder rundt Tromsø. Feltarbeidet fokuserte på 1) å kartlegge omfanget av TVS ved å kartlegge vannlinjen under lavvann, 2) å kartlegge tørrleggingsvarighet ved å kartlegge vannlinjen under flere tidevannsnivåer i løpet av en halv tidevannsyklus, og 3) å dokumentere forskjellige naturtyper. Feltarbeidet viste også noen ekstra utfordringer: i bløttbunnområder er vannlinjen sjelden en klar linje, men mer en overgangssone med små dammer og topografiske ujevnheter som flytende tang eller sandbanker som dukker opp på grunt vann. Kartlegging av vannlinjen i feltet er derfor basert på en subjektiv beslutning og vil også ha en usikkerhet på opptil en titalls meter.

Valideringen basert på disse feltdataene viser at det oppnås en nøyaktighet på 99% for å detektere TVS-områder over MSL (gjennomsnittlig havnivå) med S1; TVS-områder ned til MLW- og MLWS-vannlinjene oppdages med en nøyaktighet på henholdsvis 84% og 64%. MSL linjen ser ut til å bli godt detektert i alle feltvalideringer. Den totale nøyaktigheten til TVS naturtyper er vurdert til 86% basert på et valideringssett på 290 piksler som er visuelt tolket fra flybilder fra norgeibilder.no. Flertallet av trenings- og valideringspunktene er imidlertid fra Nord-Norge, og nøyaktigheten til de produktene er derfor sannsynligvis lavere i andre deler av Norge. Resultatene av denne studien har også blitt sammenlignet med bløttbunndatasettet fra Miljødirektoratets "Naturbase". Dette datasettet, som er basert på visuell tolkning av flybilder og tegning av polygoner for hånd, er tydelig ufullstendig og inkluderer også bløttbunn på grunt vann.

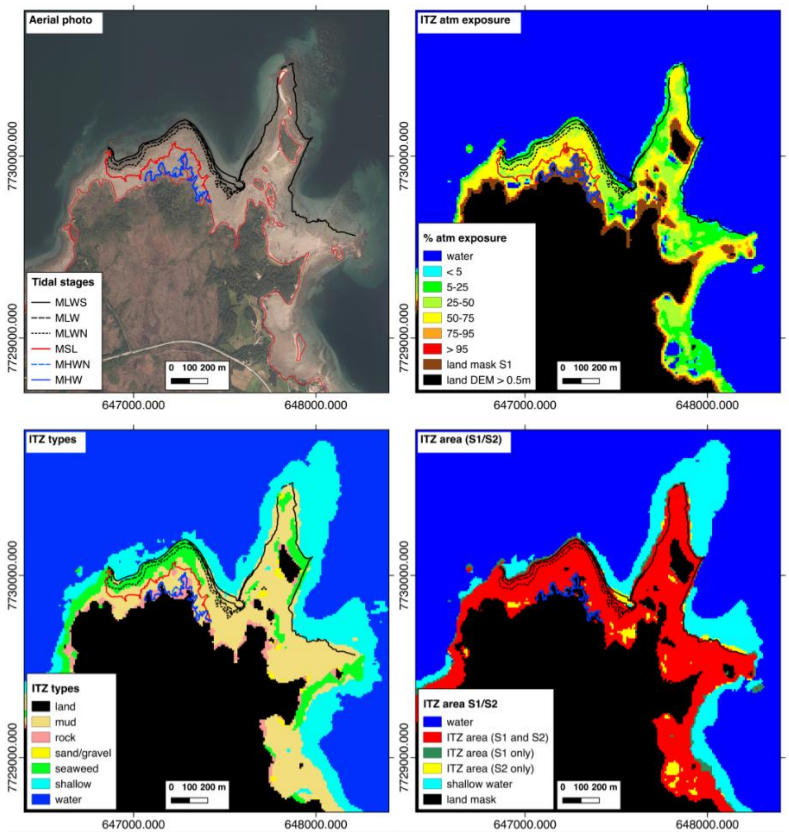

Figur D. Sammenligning mellom flyfoto med tidevannslinjer kartlagt gjennom feltarbeid (øverst til venstre) og de forskjellige kartprodukter fra dette prosjektet: TVS tørrleggingsvarighet (øverst til høyre), TVS naturtyper (nederst til venstre) og kombinert S1/S2 TVS areal (nederst til høyre). Området er Lille Grindøya sør-vest fra Tromsø.

Konklusjon og framtid

En første versjon av tre nasjonale TVS-kart i 10m oppløsning som representerer TVS tørrleggings-varighet, naturtype og areal (Figur C og D) er produsert basert på analysen av mer enn 20 TB satellittdata. Hvert endelige nasjonale kartprodukt har en størrelse på ca. 4,5 GB ukomprimert og 50 MB i komprimert format. Kartproduktene over hele Norge er delt opp i 9 fylkesprodukter. Disse produktene representerer klart det beste og mest konsistente TVS-datasettet som er tilgjengelig for Norge per i dag. En kvantitativ validering har vært begrenset til Troms Fylke på grunn av manglende finansiering og reisebegrensninger pga. Covid-19. Kvalitativt ble det imidlertid identifisert en rekke utfordringer, blant annet ved en grov inspeksjon av de andre fylkesproduktene. Slike utfordringer inkluderer feilklassifisering av S1-resultater i områder med bratt topografi, særlig i fjorder i øst-vest-orientering, effekten av skipstrafikk, spesielt rundt tettbebygde områder i Sør-Norge, som dominerer S1-signalet og hvor tidevannshøyde er lavere og feilklassifisering av oppdrettsanlegg i TVS. Feil klassifisering av S2-resultater kan generelt være assosiert med feil i skymaskering, tilstedeværelse av suspenderte sedimenter i vannsøylen og mangel på treningspunkter i Sør- og Midt-Norge. En erfaren bruker skal kunne skille visuelt de fleste av slike feilklassifiseringer. For å forbedre produktene ytterligere, bør fremtidige studier fokusere på innsamling av feltdata for å trene, forbedre og bedre validere metodene på fylkesnivå, inkludert en manuell opprydding av resultatene. Det er behov for å utvide trenings- og valideringsdatabasen basert på visuell tolkning av flyfoto, feltarbeid og andre tilgjengelige data. På grunn av et generelt lavere tidevannsområde og derfor en mindre signifikant TVS i Sør-Norge, bør muligens Midt- og Nord-Norge fylkene prioriteres. Videre kombinasjon av S1 og S2 kan utforskes for å forbedre de nåværende produktene eller utvikle nye produkter, f.eks. kombinere tørrleggingsvarighet og naturtyper til å avgrense forskjellige naturtyper ytterligere. Videre må metodene automatiseres ytterligere hvis TVS-kart skal produseres med jevne mellomrom for å kartlegge endringer.

De nåværende produktene kan brukes til å identifisere og avgrense viktige TVSer. Batymetrien i TVS er tydelig i tørrleggingsvarighets produktet og kan brukes til planlegging av båtlandinger og nybygg. Områder med høyt biologisk mangfold kan assosieres med tilstedeværelse av tang og bløttbunn i TVS. Etter en manuell opprydding bør også det totale arealet av TVS per fylke kunne estimeres. Plasseringen og størrelsen på oppdrettsanlegg er tydelig identifiserbar i produktene. Ettersom deteksjon av båttrafikk dominerer TVS i Sør-Norge der tidevannsforskjellen er relativt lavt, er spesielt produktene rundt tettbebygde steder sannsynligvis mindre nøyaktige enn vår nøyaktighetsvurdering i Troms Fylke antyder. Metodene bør også kunne brukes enda lengre nord, som for eksempel på Svalbard, men da må det tas hensyn til sjøis langs kystene, lav solvinkel og polar natt.

Studien avdekket også nye potensielle muligheter for å kartlegge oppdrettsanlegg, suspenderte sedimenter, tareskog og å estimere båttrafikk eller havneanlegg i befolkede områder.

1. Background

1.1 Mapping of coastal ecosystems

The report 'Global Assessment on Biodiversity and Ecosystem Services', published by IPBES (IPBES, 2019), concludes that coastal ecosystems are vulnerable for strong pressures from both changes in land use (e.g. new constructions, habitat destruction, coastal erosion, contamination), changes in marine use (e.g. aquaculture), and climate change. Coastal ecosystems deliver important ecosystem services, such as coastal protection, coast stabilisation, recreation, and food production (Murray et al., 2018) and climate mitigation by carbon sequestration (Macreadie et al., 2019). In addition, intertidal zones, in particular mudflats, can have a large biodiversity and are often important areas for shorebirds and seabirds. The intertidal zone is defined as the area which is exposed to air at low tide and covered by water at high tide. The intertidal zone comes in various forms and types and includes, for example, mudflats, sandy beaches, rocky beaches and steep cliffs. With respect to the 'Naturtyper i Norge' (NiN) system, the main types that occur in the intertidal zone are: M3 fast fjærebelte-bunn, M4 eufotisk marin sedimentbunn, and M8 helofytt-saltvannssump.

Norway has a long coastline with locally extensive intertidal zones. According to regjeringen.no (online), Norway has the second longest coastline in the world after Canada, with a length of 100,915 km including all the islands. The coast stretches across 14 degrees in latitude, from 58° to 71°N, and encompasses therefore a range of climatic conditions, nature types and biodiversity (Lundberg, 2013). Intertidal mudflats and mires, in particular, are important foraging areas for birds and fish and several large mudflat areas have therefore been designated as 'Wetlands of International Importance' (RAMSAR sites) (https://www.ramsar.org/wetland/norway) (Direktoratet for naturforvaltning, 2007). Norway has 45 marine or coastal wetlands that are designated RAMSAR sites, including Målselvutløpet and the Balsfjord Wetland System that are used as examples in this report (e.g. Figure 41). Intertidal zones are also important areas for recreational activities, fishing and grazing, and can therefore be affected by pressure for development (e.g. Vesterbukt et al., 2013).

Traditional mapping and monitoring of the intertidal zone is a challenge and use of remote sensing data can therefore be a good solution for both mapping and monitoring. Intertidal zones are highly dynamic and one of the challenges with the use of remote sensing data is therefore the time of acquisition relative to the tidal state. Additional challenges include the high spatial resolution needed for mapping, the separability of the spectral properties of the different zones and bottom conditions, and regular cloud cover. As a result of the increased availability of satellite images in recent years, there has been a focus on national and global level satellite-based mapping of wetlands and coastal areas (Davidson et al., 2019; Murray et al., 2018; Rebelo et al., 2018). For example, EU project Satellite-based Wetland Observation Service (SWOS) developed tools to map wetlands based on both radar and optical satellite data (SWOS toolbox). Based on time series of Landsat images, Murray et al. (2019) produced a map showing the global extent (between +/- 60° latitude) of intertidal zones. Similarly, Sagar et al. (2017) extracted the intertidal extent and topography of the Australian coastline from a 28-year time series of Landsat observations. The Copernicus Land Monitoring Service (CLMS) currently runs a program to map Europe wide

thematic hotspot in coastal zones. Land cover classes from this study that are part of the intertidal zone are intertidal flats, salt marshes, and maybe salines.

There are many types of remote sensing data: from different platforms, such as satellite, aerial or drone; and with different sensors, such as radar (SAR), optical, lidar, or thermal. Historically, optical aerial and satellite data has been the most important for the mapping of vegetation and landscape types. In particular, Landsat satellites, which have optical bands in the visible, near infrared and shortwave infrared part of the spectrum, with 30 m spatial resolution, have been used extensively in land use and vegetation mapping. The Landsat satellite image archive goes back to 1972 and is now freely available and therefore particularly useful for the mapping of changes. The first Sentinel satellites from the European Copernicus program were launched in 2014/2015; today, the program includes Sentinel-1A/B (S1), Sentinel 2A/B (S2) and Sentinel-3 (S3). S1 are two C-band radar satellites (SAR = synthetic aperture radar) with 10-20 m spatial resolution; S2 are two optical satellites with bands similar to Landsat, but with 10m spatial resolution. Since there are two radar and two optical satellites, images are acquired over Norway nearly every day for both radar and optical satellites; this produces large quantities of data and gives the possibility for dense time series and high temporal resolution.

Optical remote sensing measures the reflection of solar irradiation on surfaces; as different surfaces, or objects, have different spectral properties, the spectral signatures (reflection in the different parts of the spectrum) can be used to identify and separate different surfaces as long as the spectral signatures are separable. Optical remote sensing is dependent on cloud free conditions, which in Norway significantly influences the amount of data that can be used. Radar data, however, is independent of cloud cover or darkness and is acquired all year round. Radar data is sensitive to surface roughness, moisture and volume scatterers like vegetation, and is therefore particularly useful for the mapping of soil moisture, water surfaces, surface roughness and changes over time.

Tides are caused by the gravitational effects of the sun and moon and the rotation of the earth. Tidal water levels do, however, not only depend on the position of the sun and moon, but also on the bathymetry, coastline, fjords and straits, and can therefore also vary geographically at relatively short distances. This means that a single acquisition of satellite, aerial photo or LiDAR data does not capture the same tidal level across the whole area. Murray et al. (2019) calculated statistical parameters from time series of a number of vegetation and water indices and used these in combination with bathymetric and topographic data, expert knowledge to create a training/validation dataset and machine learning techniques (random forest) to differentiate between permanent water, tidal zones, and other (land, including vegetated tidal zones). In order to map the extent of tidal zones as accurately as possible, it is necessary to capture both the highest and lowest water levels. As satellite data is acquired at fixed times, which do not necessarily coincide with maximum/minimum tides, long times series of satellite data are required to capture the full tidal range.

In the first phase of this study, Haarpaintner and Davids (2020) showed that S1 SAR satellite data seems to be ideal for the mapping and monitoring of the extent of tidal zone at different tidal states and changes on a national scale. Zhao et al. (2020) confirms this in a similar study in Southern China. S2 optical satellite data seems to perform better at distinguishing variations and land types within the tidal zones. As SAR and optical satellite sensors observe different properties of the terrain, identifying their strengths and weaknesses with respect to the mapping of intertidal zones would help to develop methods to combine the datasets and improve the final products.

The Sentinel satellites have a spatial resolution of 10-20 m. For more detailed mapping of the intertidal zones, aerial photographs may be used. However, the available aerial photographs are limited to about one dataset per year, and the quality varies between the years. In addition, the timing relative to the tidal cycle is unknown and unlikely to coincide with the lowest tide. In addition to the mapping of the extent of intertidal zones and identification of different landscape types within, there is a need to monitor changes in the intertidal zones and the ecological condition. Relevant changes in coastal ecosystems include mainly man-made modifications, changes in land use and changes in the extent of tidal zones, but also changes in surface structure, elevation and water depth. The Group on Earth Observations – Biodiversity Observation Network (GEO BON) has developed a set of variables, the so called 'essential biodiversity variables' (EBV), for the monitoring of biodiversity on a global level. This is later extended with a set of 'satellite remote sensing EBVs' (SRS EBV) variables that can be mapped using satellite data (Pettorelli et al., 2016). Several of these may be relevant for the monitoring of the ecological condition of intertidal zones, such as extent, flooding or atmospheric exposure, or phenology.

1.2 Tides and intertidal zones

Tides

Tides are caused by the effects of the gravitational forces by the moon and the sun, and the rotation of the earth. As the tidal forces depend on the position of the moon and the sun, the tidal range varies both on a daily and a bi-weekly cycle. The maximum tidal range is called spring tide and occurs when the tidal forces of the sun and the moon reinforce each other (at full moon and new moon); on the other hand, the minimum tidal range is called neap tide and occurs when the sun's tidal force partially cancels the moon's tidal force (Figure 1 and Figure 2). Figure 1 illustrates the different terms that are used for the different tidal water levels.

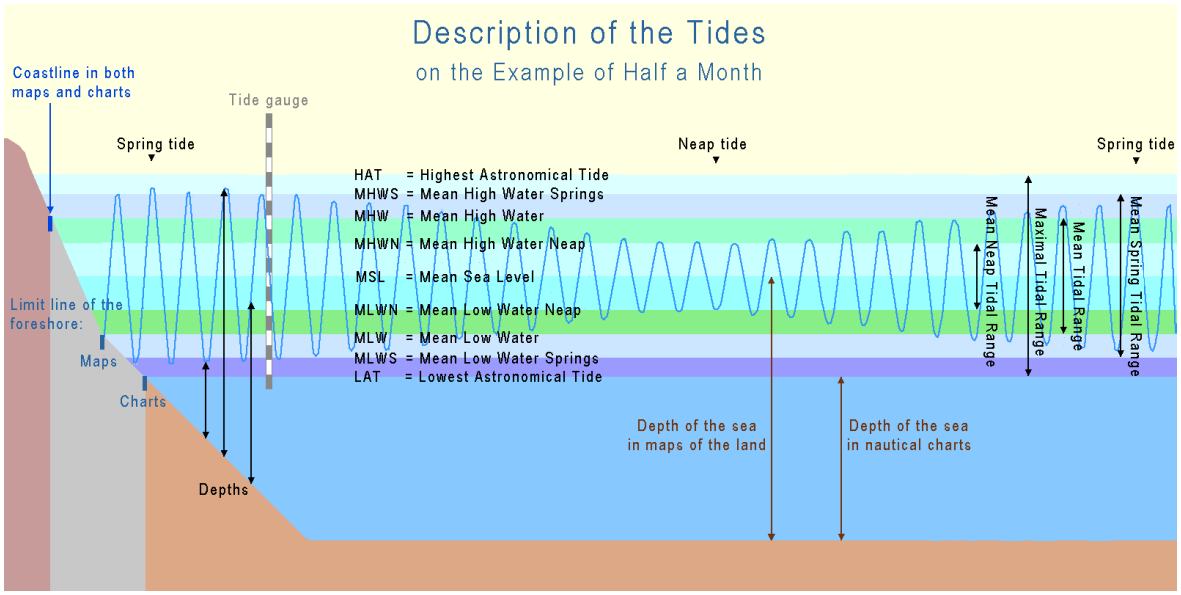

Figure 1. Illustration of tidal terms (Tide Terms by User: Ulamm / Wikimedia Commons / CC-BY-SA-3.0)

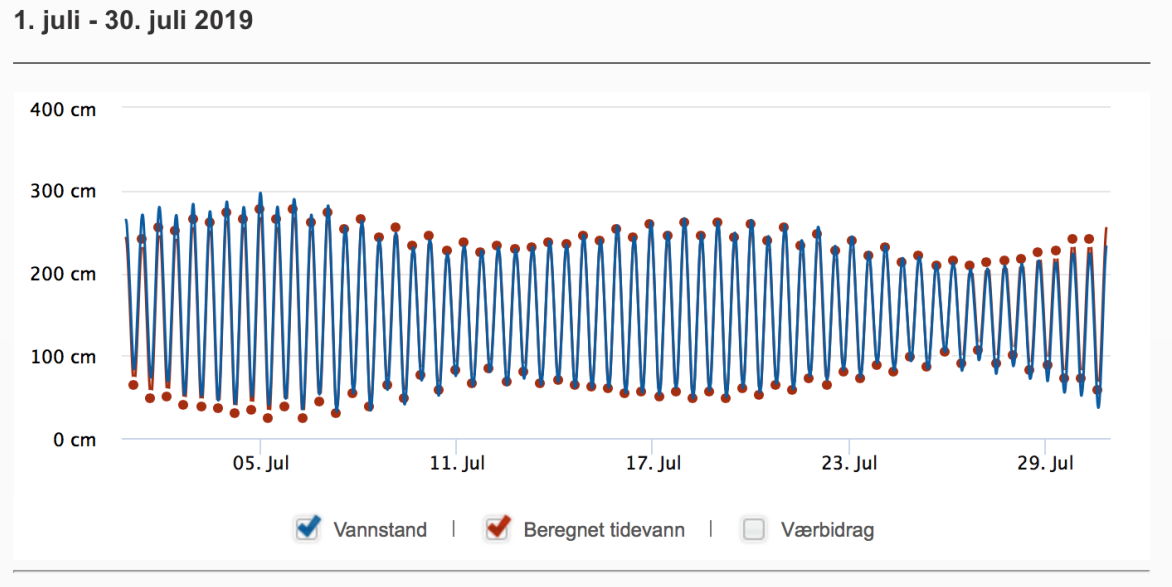

Figure 2. Tidal range variations in Tromsø, July 2019. Tidal data from Se Havnivå (http://www.kartverket.no).

In addition to the gravitational forces, the tidal range is also influenced by the weather, specifically the air pressure, and the local geography, such as the shape of the coastline and the bathymetry. The tidal ranges inside a fjord or along the outer coast can therefore vary significantly.

The intertidal zones

The intertidal zones are the coastal zones between the high tide and low tide levels; that is, the areas, which are under water at high tides and above water at low tides. Intertidal zones are highly dynamic ecosystems on the transition between marine and terrestrial ecosystems, with major variations in emersion, salinity, temperature, nutrients levels and wave action. The zones are often characterized as having either hard bottom or soft bottom substrates, and include rocky shores, sandy beaches, mudflats, estuaries and saltmarshes.

The intertidal zone is commonly subdivided into 3 zones, although the definition of the boundaries between these vary:

1. *low intertidal zone*: this zone is only above water at the lowest spring tides and is therefore mainly submerged. The low intertidal zone is mainly marine, rich in vegetation (particularly seaweed), and rich in biodiversity.
2. *mid intertidal zone*: this is the area roughly between the average low tide and the average high tide and is therefore regularly exposed and submerged.
3. *high intertidal zone*: this zone is only submerged during high spring tides and is therefore dry most of the time.

There is, however, no single definition or naming convention for the intertidal zone subdivision, and the zone is also often referred to as (eu)littoral zone or foreshore.

1.3 Intertidal zone ecosystems

In Norway, the 'Natur i Norge' (NiN) system (https://www.artsdatabanken.no/NiN/Systemet) was developed to describe the variation in nature at 3 different levels: landscape, natural system and environmental living conditions. The natural system is described at three hierarchical levels: the main division into 'hovedtypegrupper' (main type groups), 'hovedtyper' (main types), and 'grunntyper' (bottom types). The intertidal ecosystems fall on the transition between the two 'hovedtypegruppene' marine ecosystems and terrestrial ecosystems. The main 'hovedtypene' that occur in the intertidal zone are the marine ecosystems M1 'Eufotisk fast saltvannsbunn', M3 'Fast fjærebeltebunn', and M4 'Eufotisk marin sedimentbunn', and the terrestrial ecosystems T11 'Saltanrikingsmark i fjæresonen', T12 'Strandeng', and T29 'Grus og steindominert strand og strandlinje'. The main differences between these main types are the 1. type of bottom, rock (hard bottom) or unconsolidated sediment (soft bottom); 2. The duration of submersion/exposure: how much of the time is the area exposed to air versus submerged; 3. The presence and type of vegetation (seaweed, salt tolerant grasses).

Ecosystems can be described and distinguished by using a number of relevant environmental variables. Following on from the identification of the main differences between the main ecosystems, the environmental variables that are most relevant for the description of intertidal zone ecosystems are:

1. TV tørrleggingsvarighet: duration of exposure to air, i.e. the atmospheric exposure
2. VF vannpåvirkningsintensitet: index describing the influence of water
3. SA marin salinitet: salinity
4. S1 kornstørrelsesklasse: grain size
5. S3 sedimentsortering: indicator for erosion resistance
6. SF saltanriking: salt enrichment
7. IO Innhold av organisk material: organic material content

Not all of these environmental variables will be able to be mapped using remote sensing data, but it is expected that there are a number of variables or indicators that can be mapped which can help distinguish between some of the main ecosystems that occur in the intertidal zone:

1. Tørrleggingsvarighet (atmospheric exposure):
   "% of duration of exposure to air" = 100% - "% of duration of submersion"
2. Bottom type: distinction between rocky bottoms and soft sediment bottoms
3. The presence, and possibly type, of vegetation, such as zones rich in seaweed, or areas with salt tolerant vegetation (e.g. coastal meadows ('strandeng'))
4. Man made changes.

1.4 Project Objective

The main goal of the project is to develop an efficient method to map and monitor the intertidal zone based on freely available Copernicus satellite data.

The first objective was to develop and demonstrate such a method for the test area of Trondheimsfjorden. This has been documented in Haarpaintner and Davids (2020). The objective for this follow-up study is to apply these methods to produce a first version of a national map of the intertidal zones over Norway. The sub-goals are to:

1) Map the extent of the intertidal zone,
2) Identify and classify different types and environmental variables of intertidal zones,
3) Detect changes in the intertidal zones,
4) Assess the possible use of available aerial photos and processed LiDAR data,
5) Propose a concept for large-scale mapping of the intertidal zone for all of Norway on a regular basis.

Haarpaintner and Davids (2020) already described the methodological approach of 1-4. This report describes some improvements and the production of a national map of the intertidal zones of continental Norway.

2. Study Sites and Data

2.1 Study Sites

2.1.1 Demonstration Site - Trondheimsfjorden

The demonstration site to develop the methods was Trondheimsfjorden (Figure 3). The area is in UTM Zone 32N with the following limits:

E 510020 to E 630000,
N 7013000 to N 7112980.

Figure 3. Trondheimsfjorden (©GoogleMaps)

2.1.2 Field data collection sites in Tromsø Kommune

Due to the Covid-19 crises since March 2019 and the travel restrictions, field data was collected on seven occasions only in Tromsø Kommune at 5 different locations: Lille Grindøya (twice), Hillesøy (twice), Langnes, Finnvika and Grøtfjorden. A drone flight was performed over the Hillesøy site. The locations are indicated in Figure 4.

Figure 4. Field data collection sites in Tromsø Kommune.

2.1.3 Processing of continental Norway

For the Sentinel-1 processing of the whole of Norway, the Norwegian coast was divided into 20x20 km^2 tiles (Figure 5). All together there are 597 tiles. The maps are produced in UTM zone 33N at 10m resolution.

Figure 5. Division of the Norwegian coast in 20x20 km^2 tiles.

2.2 Satellite data

The use of satellite data is based on the freely available Copernicus program from the European Commission and specifically on the high-resolution radar and optical satellites Sentinel-1 and Sentinel-2.

2.2.1 Sentinel-1

"Sentinel-1 (S1) is a Synthetic Aperture Radar (SAR) mission, providing continuous all-weather, cloud independent, day-and-night imagery at C-band (centre frequency: 5.405 GHz), operating in four exclusive imaging modes with different spatial resolutions and coverages. Dedicated to Europe's Copernicus Programme, the mission supports operational applications in the priority areas of marine monitoring, land monitoring and emergency management services. The mission is based on a constellation of two identical satellites, Sentinel-1A (S1A) and Sentinel-1B (S1B), launched separately on 3 April 2014 and 25 April 2016. In the interferometric wide-swath mode used here, each S1 can map global landmasses once every 12 days. The two-satellite constellation can deliver a six- day repeat cycle at the equator. The baseline observation scenario is pre-defined. The plan systematically makes use of the same SAR polarization scheme over a given area to guarantee data in the same conditions for routine operational services. More information can be found at https://sentinel.esa.int/web/sentinel/missions/sentinel-1/observation-scenario .
Sentinel data products are made available systematically and free of charge to all data users including the general public, scientific and commercial users. All data products are distributed in the Sentinel Standard Archive Format for Europe (SAFE) format. More information can be found at https://sentinel.esa.int/web/sentinel/sentinel-data-access ." (ESA, online)
The original data format used in this project is Level-1 Ground Range Detected (GRD). "GRD products consist of focused SAR data that has been detected, multi-looked and projected to ground range using the Earth ellipsoid model WGS84. The ellipsoid projection of the GRD products is corrected using the terrain height specified in the product general annotation. The terrain height used varies in azimuth but is constant in range (but can be different for each IW/EW sub-swath).
Ground range coordinates are the slant range coordinates projected onto the ellipsoid of the Earth. Pixel values represent detected amplitude. Phase information is lost. The resulting product has approximately square resolution pixels and square pixel spacing with reduced speckle at a cost of reduced spatial resolution. For the IW and EW GRD products, multi-looking is performed on each burst individually. All bursts in all sub-swaths are then seamlessly merged to form a single, contiguous, ground range, detected image per polarization." (ESA, https://sentinel.esa.int/web/sentinel/user-guides/sentinel-1-sar/product-types-processing-levels/level-1)

All acquired Sentinel-1A&B data over the demonstration site Trondheimsfjorden (Figure 6) have been downloaded through the Copernicus Open Access Hub (https://scihub.copernicus.eu/) or the Alaska Satellite Facility (https://vertex.daac.asf.alaska.edu/#) from 1 January 2017 until 31 December 2018 as the demonstration was done in 2019.
Over Norway, the acquisition scenario reflects also the maximum acquisition possibilities, continuous acquisition of all paths both ascending and descending. As S1 is polar orbiting, the overlap of the adjacent paths is increasing with latitude and more than 50% around Trondheimsfjorden. Table 1 summarizes the covering paths for one cycle period of 12 days in August 2018, specifying the satellite S1A or S1B, the path number, and the flight direction of the satellite, i.e. 4 ascending (ASC) paths and 3 descending (DES) paths, and the time of overflight. Descending paths pass around 05.45, ascending paths pass around 16.45. All pixels are therefore covered at least 8 times per satellite cycle, i.e. more than 240 times per year. Most of pixels in

Trondheimsfjorden are covered at least 26 times per month. Figure 6 also shows the location of the paths and single scenes.

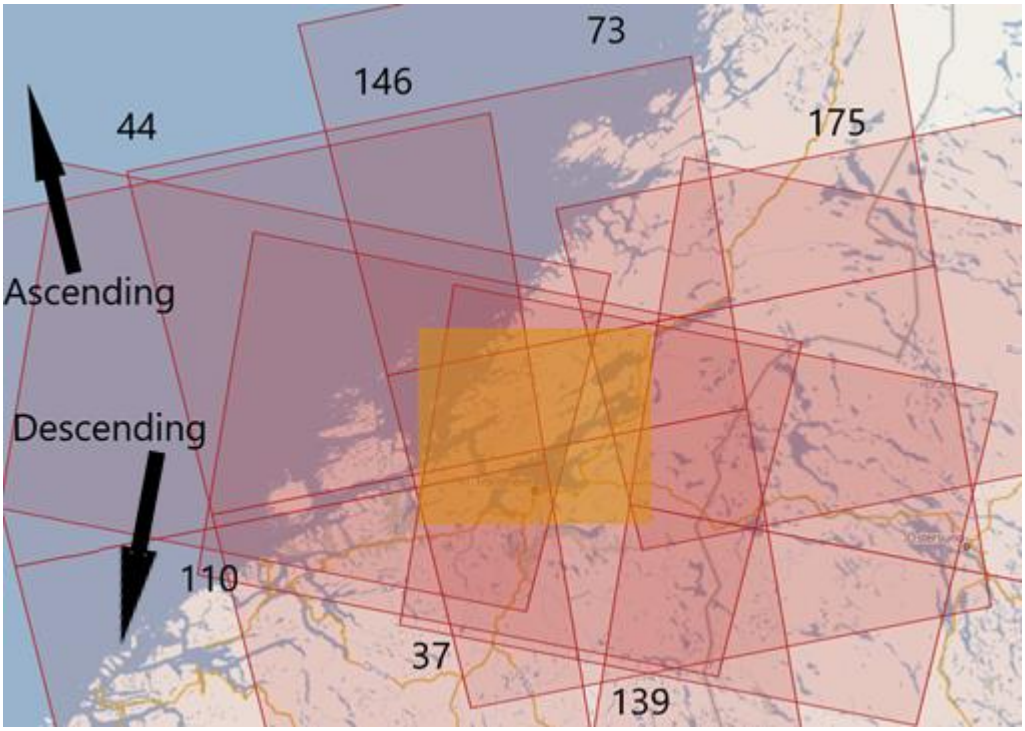

Figure 6. Example of Sentinel-1 path numbers (in black), flight direction and coverage of the demonstration area Trondheimsfjorden (yellow rectangle).

Table 1. Sentinel-1 path numbers off a 12-day cycle (starting 01.08.2019) covering Trondheimsfjorden specifying the satellite, path and direction.

Nr	Date	Satellite	Path	Direction
1	01.08.2019 - 05.38	S1B	139	DES
2	01.08.2019 - 16.54	S1B	146	ASC
3	02.08.2019 - 16.46	S1A	073	ASC
4	03.08.2019 - 16.38	S1B	175	ASC
5	05.08.2019 - 05.55	S1A	110	DES
6	06.08.2019 - 05.46	S1B	037	DES
7	06.08.2019 - 17.02	S1B	044	ASC
8	07.08.2019 - 05.38	S1A	139	DES
9	07.08.2019 - 16.54	S1A	146	ASC
10	08.08.2019 - 16.46	S1B	073	ASC
11	09.08.2019 - 16.38	S1A	175	ASC
12	11.08.2019 - 05.55	S1B	110	DES
13	12.08.2019 - 05.46	S1A	037	DES
14	12.08.2019 - 17.02	S1A	044	ASC

The whole Norwegian coast is covered by 31 satellite paths: 18 ascending and 13 descending satellite paths. Most paths require several individual scenes to cover the coast. Per 12-day cycle, this sums up to about 100 individual scenes per S1 satellite, i.e. about 200 individual scenes of S1A and S1B per 12 days. As some Norwegian fjords can be covered with sea ice during the winter months, we processed only ice-free months (June to November) but used the two years 2018 and 2019. In total, 6893 individual S1 scenes have therefor been processed to map the intertidal zone of whole continental Norway.

The ascending S1 path numbers are: 014, 015, 018, 029, 043, 044, 058, 072, 083, 087, 088, 102, 116, 117, 131, 145, 146, 160, 175.

The descending S1 path numbers are: 007, 008, 022, 037, 051, 066, 080, 081, 095, 110, 139, 153, 168.

2.2.2 Sentinel-2

The Copernicus Sentinel-2 mission acquires optical multispectral satellite imagery in 13 bands in the visible, near infrared and short wave infrared part of the spectrum (Table 2) at a high spatial resolution (10 - 60 m) and with a swath width of 290 km (https://sentinel.esa.int/web/sentinel/missions/sentinel-2). The mission consists of 2 polar-orbiting satellites, Sentinel-2A and Sentinel-2B, which provide a revisit time of 5 days at the equator and 2-3 days in Norway. The spectral bands are chosen such that they provide spatial information on land cover/land use, vegetation properties, cloud/snow separation, which can be used for applications in environmental monitoring (e.g. land cover change, effects of climate change), land management (e.g. crop monitoring for agriculture, forestry), estimation of vegetation biophysical parameters (e.g. leaf chlorophyll content (Ch), leaf area index (LAI)), mapping of coastal zones, monitoring of inland waters, snow cover, or risk management (e.g. flood mapping). The Sentinel-2 satellites provide continuity for the multispectral imagery provided by the Landsat TM and SPOT satellites, and, in addition, include three new narrow spectral bands in the red edge region (680 – 730 nm; Table 2), which significantly improve the estimates of biophysical parameters Ch and LAI (Delegido et al., 2011). The data is freely available from the Copernicus Open Access Hub or the national Norwegian hub (https://colhub.met.no/#/home). Sentinel-2 data is available for download in 2 main formats, level 1-C and level 2-A. The level 1-C product includes radiometric and geometric corrections and represents the top-of-atmosphere (TOA) reflectance; the level 2-A product includes an atmospheric correction applied to the level 1-C product and represents a bottom-of-atmosphere (BOA) reflectance.

In this study, all Sentinel-2A and 2B images from 2 seasons (1st June – 30th September 2019 and 2020) that cover the Norwegian coastline, with a cloud cover of less than 20% that were available as level 2-A surface reflectance products from the google earth engine database, were used. In addition, it was checked if using images from 2019 only (between 1st May and 30th October 2019) would give better results, but this resulted in very few images available for analysis in some areas, particularly in Vestland and Rogaland.

Band number	Description	Central wavelength (nm)	Band width (nm)	Spatial resolution (m)
1	Coastal aerosol	443	21	60
2	Blue	493	66	10
3	Green	560	36	10
4	Red	665	31	10
5	Vegetation red edge	704	15	20
6	Vegetation red edge	740	15	20
7	Vegetation red edge	783	20	20
8	NIR	833	106	10
8a	Vegetation red edge	865	21	20
9	Water vapor	945	20	60
10	SWIR – Cirrus	1374	31	60
11	SWIR1	1610	92	20
12	SWIR2	2190	180	20

Table 2. Band specifications Sentinel-2 (https://sentinel.esa.int/web/sentinel/user-guides/sentinel-2-msi/resolutions/radiometric).

2.3 Aerial and ground reference data

2.3.1 Aerial photos from Norgeibilder.no

Norgeibilder.no is a cooperation between Statens vegvesen, Norsk institutt for Bioøkonomi (NIBIO) og Statens kartverk, providing an overview of aerial photos over Norway that cooperating partners in the "Norge digital" program acquired as ortho-photo mosaics. Norge digital is a cooperation between the public agencies that have responsibilities for producing or using geodata. Publishing in Norgeibilder.no is also open to other data providers.

This project was given access to the database of the aerial mosaics. The aerial ortho-mosaics have each their individual meta data set and specifications and it is therefore not a homogenous data base with equal quality, resolution etc., nor predefined acquisition plans. The meta data provided for each mosaic has the following information:

Name and acquisitions year: f.e. Nord Trøndelag 2017
Fotodate: f.e. 2017-06-30
Publising date: f.e. 2017-12-15
Prosjektstart: f.e. 2017
Data owner: f.e. Omløpsfoto
Type: f.e. Ortofoto 50

Resolution: f.e. 0.25 (m)
Mappingnumber f.e. TT-14313
Image category: f.e. Color
Color coding: f.e. 24 bit/px
Acquisition method/sensor: f.e. Digital sensor
Picture format: f.e. TIFF
Orientation method: f.e. GNSS/INS med AAT
Coordinate system: f.e. UTM32 EUREF89
Flight: f.e. TerraTec AS
Producer: f.e. TerraTec AS
A product specification report.

The general resolution of the aerial data is in the range of 10cm to 1m. And the main type are aerial photos in visible wavelength. Some infra-red acquisitions are also available. Unfortunately, there is no specific time information or acquisition time period available, neither with the meta data, nor in the product specification reports, so it is not possible to compare this data set with the tidal charts without access to single aerial images. It is just by comparison between different data sets,i.e. aerial mosaics, over the same region that one can roughly estimate high, middle or low tide if available from different years.

Because of its high resolution, this data base is still a good source of ground truth data with regard to some tidal zone types and the presence of vegetation or algae. However, the waterline is generally difficult to see or extract exactly, especially in shallow waters. This data set is so inhomogeneous and misses necessary time information to be used operationally on large areas. It is, however, a good source to detect and identify changes, and to help interpret the different types of tidal zones.

2.3.2 Vector data from “Naturbase”

The GIS database Naturbase from the Norwegian Environment Agency combines GIS based environmental data from a range of different sources in Norway, including data from the Norwegian Environment Agency, NIBIO, NINA, Norwegian Polar Institute, Artsdatabanken, and Institute of Marine Research. Data available in this database that is relevant for tidal zone mapping includes data on protected sites, and data on selected ecosystems. This includes GIS data on marine ecosystems, such as mudflats (bløttbunn), large kelp forests, coastal meadows and wetlands and occurrences of shell sand. This data is potentially useful as ground truth data to either train or validate the results from the satellite image analysis. However, a challenge with these datasets is that the vector outlines are generally manually digitized, presumably based on visual interpretation of aerial photographs (according to the measurement method description in the metadata: ‘digitized on screen from orthophotos’). The vector outlines can be rather coarse and include other adjacent ecosystems, which can make it difficult to compare directly with the results of satellite image analysis. They are also not always complete, but often only include well known examples or important protected sites. On the other hand, they are useful as examples of where certain coastal and marine ecosystems are known to occur, which helps with the visual interpretation of aerial photographs to create training data. The most useful and complete vector dataset for this project is the mudflats dataset, which will be used for comparison.

2.3.3 In-situ data collection in Tromsø Kommune

Field data was collected on seven occasions at five sites in Tromsø Kommune (Figure 4). The field data collection aimed to 1. map the extent of intertidal zones by mapping the low tide water line on days with very low tides, 2. map the atmospheric exposure by mapping the water line at different tidal stages, and 3. identify and document different features within intertidal zones, to help visually interpret aerial images. The water line mapping was done by walking along the water line and recording the track by hand-held GPS or mobile phone. The recorded tracks have an estimated uncertainty of ca +/- 5 m, based on the difficulty of identifying the water line in the field and the uncertainty in the GPS measurements.

Lille Grindøya (19 July 2019 and 25 July 2020)

Grindøysundet is a nature reserve on Kvaløya, close to Tromsø. This area is part of the Ramsar site Balsfjord wetland system, with extensive mud- and sandflats with coastal meadows.

On 19 July 2019, low tide on the day was at 09:59, with a predicted water level of 49 cm (Se Havnivå: http://www.kartverket.no); the site was visited around low tide, from ca 09:30 to 11:20, with an estimated tidal water level between 49 and 68 cm, which is around the mean low water spring tide level of 51 cm in Tromsø (Kartverket, 2019). During the field visit, ground photography with GPS coordinates were taken to identify different ecosystems. A GPS track was recorded along the water line starting ca 30 min before the lowest tide until about 1.3 hour after the lowest tide. The track is shown under the validation section and is used for the accuracy assessment of the intertidal zone extent.

On 25 July 2020, the mudflat area to the west of Lille Grindøya was revisited and the water line was mapped using a handheld GPS at 7 stages during a half tidal cycle from low tide to high tide: the lowest water line on this day (LWL), Mean Low Water Spring (MLWS), Mean Low Water (MLW), Mean Low Water Neap (MLWN), Mean Sea Level (MSL), Mean High Water Neap (MHWN), and Mean High Water (MHW). These stages correspond to approximately 2%, 5%, 15%, 25%, 50%, 75% and 85% atmospheric exposure. At each stage, the waterline was tracked for about 20 min, from 10 min before to 10 min after the calculated time, to limit the change in tidal stage during the track. This tidal area is characterized by ca 300 m wide mudflats with and without seaweed, permanent pools, rocky outcrops with salt meadows, large boulders, sandy beaches and rocky coastline.

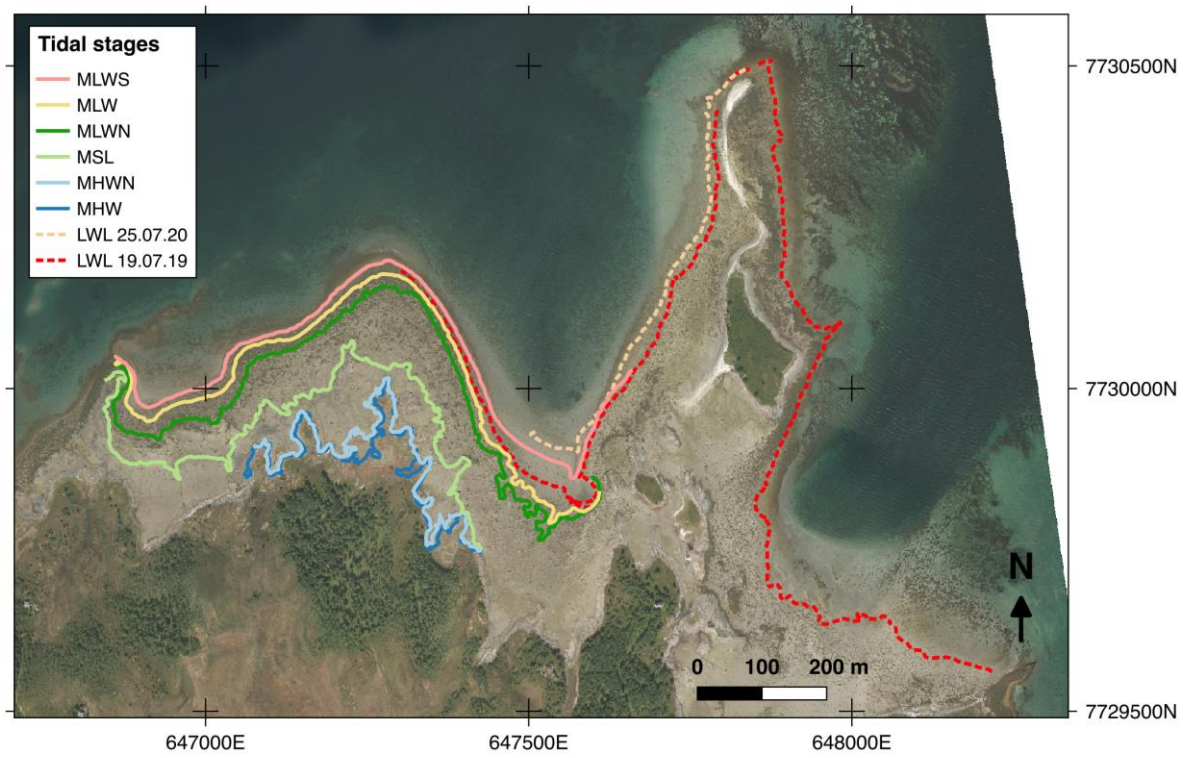

Figure 7. Aerial photograph (from Norge i Bilder) with the mapped tidal lines.

Langnes (8 May 2020)

Langnes is close to Tromsø Airport on Tromsøya (Tromsø Island). This region is quite variable and includes mudflats with and without vegetation (kelp and algae), a stone beach with and without kelp and algae, rocks with and without vegetation (kelp and algae), and a man-build stone dam. An adjacent small grassland area (coastal meadows) can be flooded at high spring tides. The field visit lasted half a tidal cycle from high to low tides from 3pm to 9pm on 8 May 2020, a spring tide day, during which the position of the water line has been taken nearly hourly by hand-held GPS while walking. Slippery rock and stones because of kelp and algae were very challenging to walk on. It is also clear that floating kelp in low waters challenges the definition of intertidal zone. Some waterline position can therefore vary by up to about 10m in accuracy. The same is valid for mudflats where small sand hills from crabs pass over the water line even if the rest is covered by water. Photos taken during the fieldwork (Figure 8) Illustrate some of these issues. The choice of where the “exact” waterline is under these conditions is therefore subject to the subjective interpretation of the observer and could be associated with an error of up to 10m.

Figure 8. Photos taken at Langnes showing the variability of intertidal zone type and challenges to access and define precisely the water line.

Finnvika (8 May 2020)

Finnvika is the estuary from Finnvikelva on Kvaløya, just N of Tromsøya. The tidal area is characterized by a ca 300 m wide area of mudflats, sand and permanent pools. The low water line was tracked using a handheld GPS for about an hour (30 min before and after peak low tide). The peak low tide this evening was at < 1% value of atmospheric exposure.

Hillesøy (6 June 2020 and 14 July 2020)

Avløsbukta at Hillesøya has been visited on two occasions, on 6 June and 14 July 2020.

On 6 June 2020, the site has been observed over a half tidal cycle from 8.20pm to 2.20am (7 June) by taking GPS tracks of the water line around the times of the predicted tidal levels of the lowest tide, mean low tide spring (MLWS), mean low tide (MLW), mean low tide neap (MLWN), mean sea level (MSL), mean high tide neap (MHWN), mean high tide (MHW) and mean high tide spring (MHWS) from kartverket.no, summarized in

Table 3. Figure 9 shows the scheme from kartverket.no of the tidal level in Avløsbukta at Hillesøy. On 14 July, the site was revisited taking one GPS track at 3.10pm during low tide. At the same time, aerial photos were collected using a small drone, a DJI Mavic Air quadcopter, that were then stitched together into an aerial photo mosaic. Two drone flights were needed to cover the area- The first flight lasted from 2.53pm to 3.04pm and the second from 3.32 pm to 4.44pm. Low tide (-62 cm, between MLWN and MLW) was at 2.40 pm on 14 July 2020. Figure 10 shows the aerial mosaic over Avløsbukta. Even on this very high-resolution aerial mosaic, it is difficult to see the water line, especially in the mudflat area in the norther part.

Table 3. Times and tidal levels of GPS tracks in Avløsbukta (Hillesøy)

Time	Water level (pred.) (ref. MSL)	Water level (obs.) (ref. MSL)	Tidal level
20.20-20.30 (6 June)	[-111cm; -110cm]	[-98cm; -96cm]	Minimum on 6 June
20.45-20.54	[-108cm; -106 cm]	[-95cm; -93 cm]	MLWS
21.38-21.53	[-87cm; -76 cm]	[-74cm; -62 cm]	MLW
22.12-22.19	[-65cm; -59cm]	[-51cm; -45cm]	MLWN
23.09-23.27	[-18 cm; -3cm]	[-4cm; +11cm]	MSL
23.59-00.08	[+24cm; +31cm]	[+39cm; +45 cm]	MHWN
00.32-00.52 (7 June)	[+48cm; +61cm]	[+60cm; +75cm]	MHW
01.08-01.25	[+70cm; +78cm]	[+85cm; +92cm]	MHWS

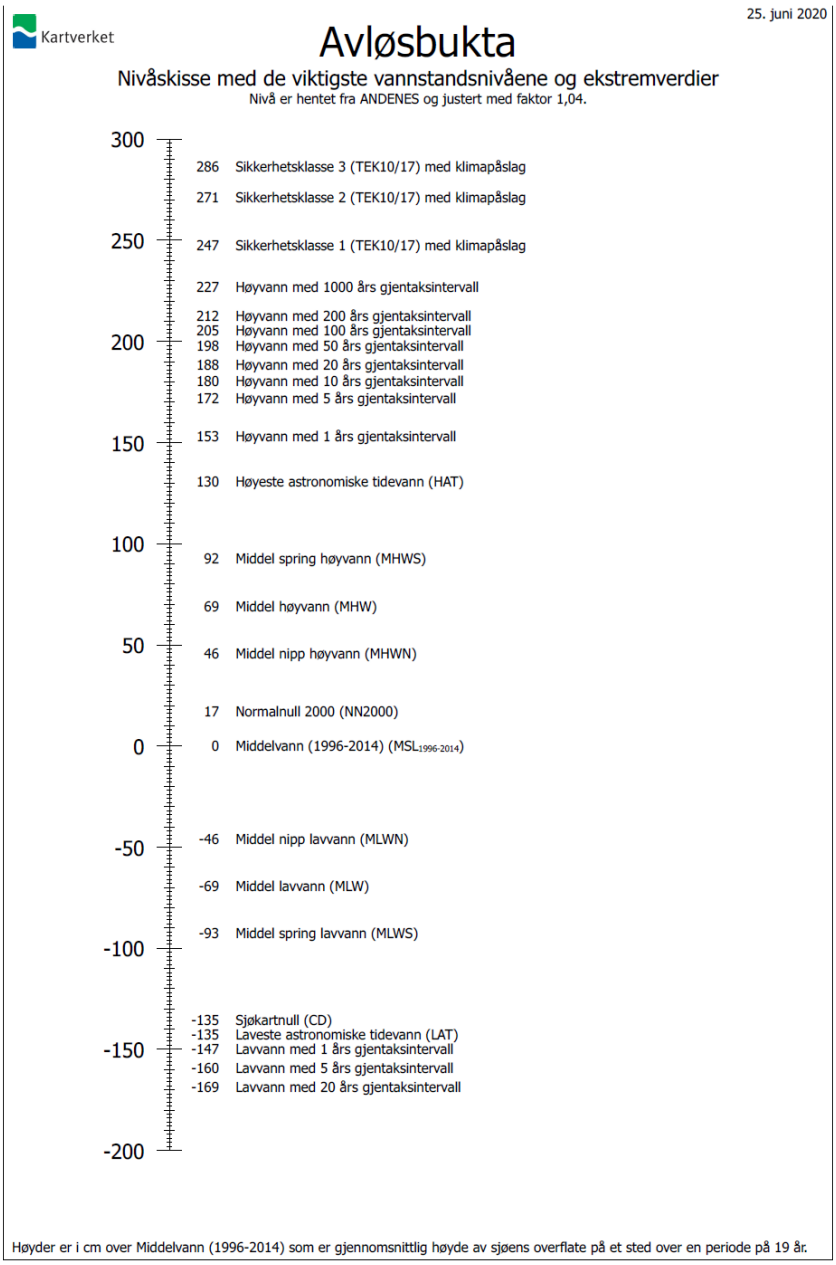

Figure 9. Tidal level in Avløsbukta at Hillesøy.

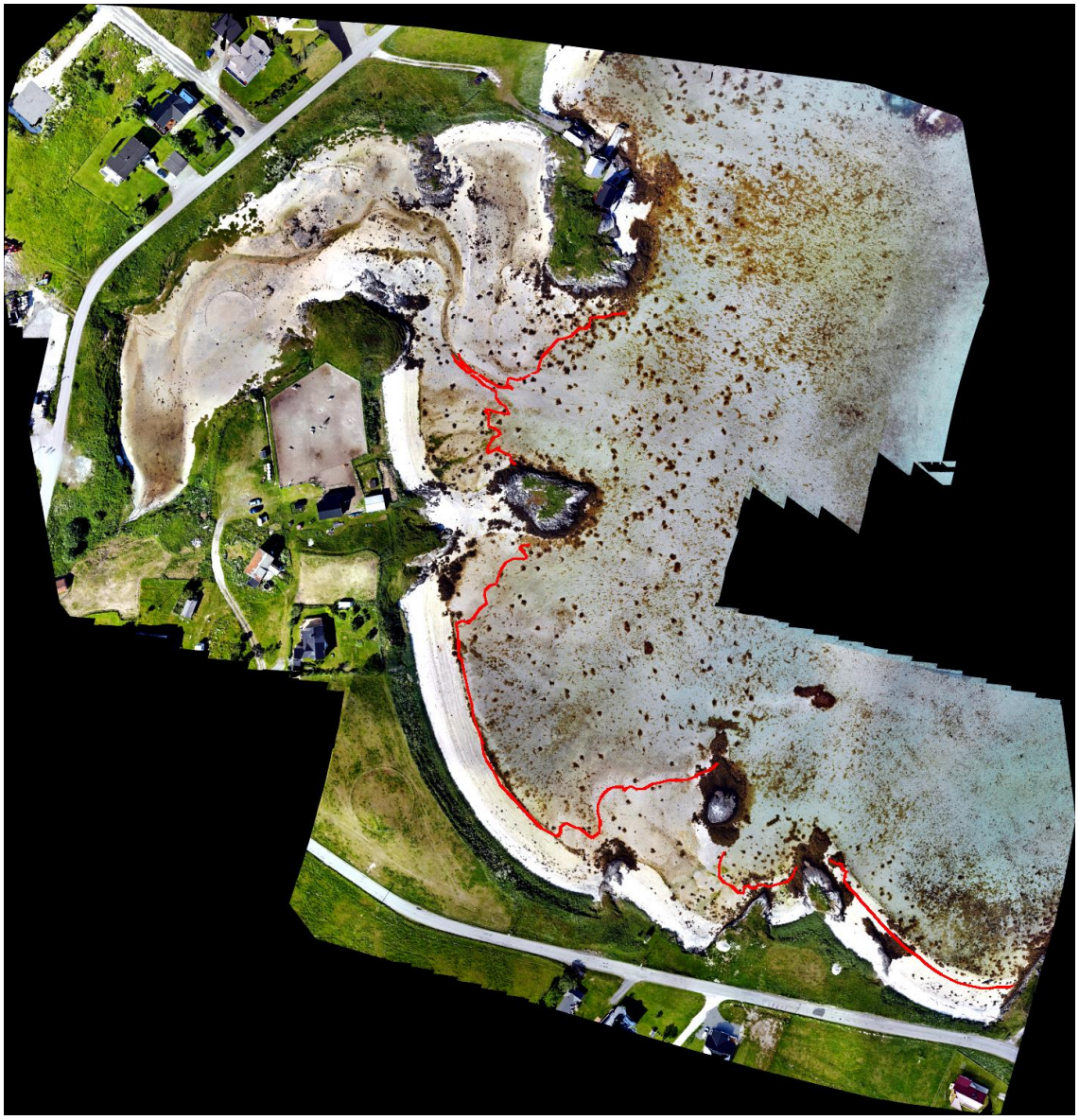

Figure 10.Aerial mosaic over Avløsbukta at Hillesøy (Tromsø Kommune, Troms).

Grøtfjord

The beach at Grøtfjorden was visited on 21 Jun 2020 during a family excursion and a GPS track was recorded between 6.10 pm and 6.15 pm, about 2h before low tide. The tidal level corresponded to -63cm which is between MLWN and MLW.

3. Methods

The processing methods have already been described in Haarpaintner & Davids (2020) and are mainly repeated here. The intertidal zone mapping methods (section 3.2.) however have been refined and updated during this second phase of the study using field observation.

3.1 Pre-processing

3.1.1 Sentinel-1 CSAR

Norut's (now NORCE's) GSAR/GDAR SAR processing system is used in this project as it allows operational processing of big data sets. The system had been earlier set-up for Troms and adapted to Trondheimsfjorden during the first phase of the project and the process has been streamlined into the three following steps:

1) Geocoding and radiometric calibration
2) Radiometric slope correction according to Ulander (1996).
3) Yearly and monthly statistical analysis of data stack and mosaics production

For the second phase of the project, reported here, the processing line has been semi-automized and scripted in order to process 597 individual 20x20 km^2 tiles over the whole Norwegian coast.

The S1 GRD data was pre-processed with NORCE's geocoding software (Larsen et al., 2005) using the 10m Norwegian digital elevation model (DEM). Header information in the S1 *.SAFE folder include the necessary parameters for radiometric calibration and the exact satellite orbit information for georeferencing and terrain correction with the DEM. GRD files are therefore directly converted into georeferenced, radiometrically corrected gamma-naught γ° radar backscatter images in dB for both polarization, co-polarization VV and cross-polarization VH, γ°(VV) and γ°(VH), respectively. Adjacent single scenes of the same orbit are directly processed together into one seamless continuous image.
Once the GRD data are processed into georeferenced and radiometric corrected images an additional radiometric slope correction according to Ulander (1996) is applied. This is less relevant in this project as the topography in the intertidal zone is not resolved in the DEM. An important issue however is to mask the areas without reliable data due to SAR shadow and overlay occurring at steep hillsides along the coast perpendicular to the SAR range direction.

Instead of using NORCE's internal software that is set up for large scale operational monitoring, the pre-processing step can also be done with ESA's free openly available Sentinel 1 Toolbox from the Sentinel Application Platform (SNAP). Preprocessed Sentinel-1 SAR data is also available on Google Earth Engine (GEE). As far as we understand should the Norwegian Ground segment also provide such pre-processed data, but the usage of this data has not been evaluated in this project. Also the pre-processed S1 data from GEE has been reported of not resolving well enough the Norwegian topography.

3.1.2 Sentinel-2

Most of the processing and analysis of the S2 images is done in Google Earth Engine (GEE) (https://earthengine.google.com). GEE is a cloud-based platform that combines image processing capabilities that directly link to Google's satellite image databases and is therefore highly suited for the processing of large datasets. In this tidal zone mapping project we use the S2 surface

reflectance dataset (level-2A) available on GEE, which is a dataset produced by ESA by processing S2 Top-Of-Atmosphere data (level-1C) using ESA's Sen2Cor processor. S2 surface reflectance data are radiometric, atmospheric, geometric and terrain corrected.

Preprocessing includes filtering the dataset to exclude scenes with more than 50% cloud cover prior to further processing. This is followed by pixel-based cloud masking by using the QA60 band, which is created during the level-2A processing by Sen2Cor and contains information about the probability of clouds and cirrus.

In addition, some auxiliary products were prepared in QGIS (https://www.qgis.org), an open source GIS system, and uploaded as assets into GEE:

- Detailed coastline vector data was extracted from AR50 products downloaded from Geonorge.
- A land mask was made, >0.5 m, based on digital elevation models (DEM10 products) from Geonorge.
- A training/validation dataset with 750 points, based on visual interpretation of aerial photographs from Norge I Bilder and experience from several field visits to tidal zones around Tromsø. During the analysis in GEE, the training/validation dataset is randomly split in 80% training and 20% validation.

The coastline was used to delimit the area of interest to 5 km around the coastline, and the land mask to exclude land higher than 0.5 m above sea level.

3.2 Intertidal-zone mapping

The intertidal zone can be observed with both optical and radar satellite imagery. Since the intertidal zones are highly dynamic areas with twice daily submersion and exposure, it is necessary to use satellite time series to catch the range of tidal stages. Optical satellite data has the additional challenge with frequent cloud cover in Norway, which reduces the number of cloud free images available and requires additional preprocessing to mask pixels that are affected by cloud cover. In this section we describe in detail the methods used to analyze optical and radar satellite imagery to identify intertidal zones and distinguish different ecosystems.

3.2.1 Intertidal-zone area mapping with Sentinel-1 CSAR

The approach to map the intertidal zone with Sentinel-1 is straight forward. The radar backscatter signature from water and land are quite distinguishable and can be generally separated by simple thresholding between a water and a land mode in the backscatter histogram. As the tidal phase is half a moon-day, i.e. 12h 25.2 min, and Sentinel-1 passes are approximately at the same times of the day, either around 5.45 for descending paths or 16.45 for ascending paths, the phase difference and a long time series ensure that acquisitions are taken both at low and high tides. Every 12-day satellite cycle corresponds to a tidal phase shift of 4.8 min. Inside a 12-day satellite cycle, if both S1A and S1B are operational, each pixel is generally observed at least 8 times as the overlay over adjacent satellite paths is more than 50% over all Norway, i.e. two observation from ascending paths, and two observations from descending paths from each S1A and S1B. At the northern tip of Norway, the number of observations can increase to up to 16 observation per 12-day cycle.

Inside the intertidal zone area, the signatures will vary strongly between low backscatter when covered by water and generally a higher backscatter when exposed to the atmosphere. The highest and lowest waterline can therefore be extracted by thresholding the image representing the highest and lowest percentile of a backscatter time series. Figure 11 shows the minimum and maximum backscatter images from the 2017-2018 data series over Trondsheimsfjorden. Figure 12 illustrated the thresholding between a water and a land mode in a SAR backscatter histogram.

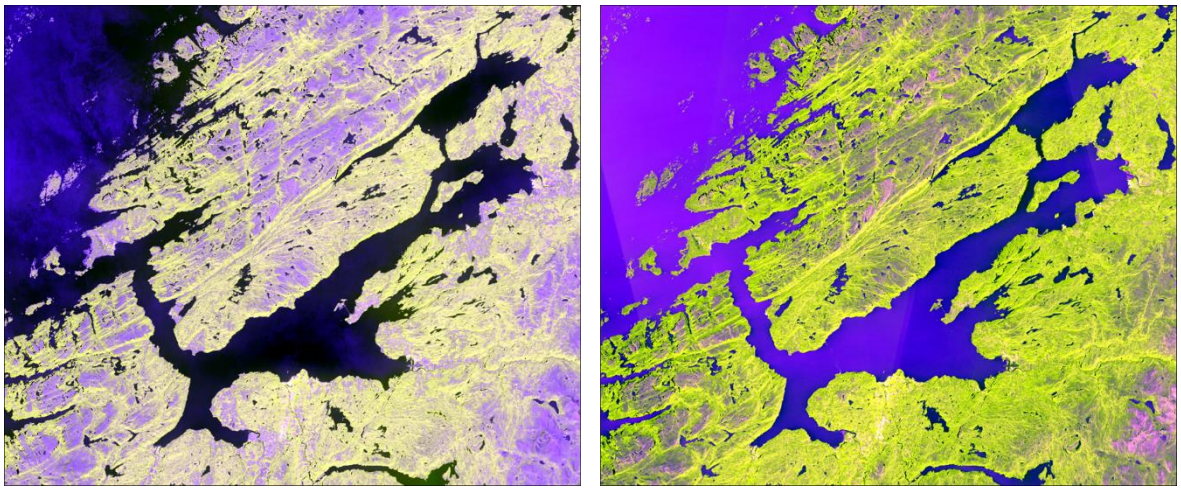

Figure 11. Low percentile (minimum, left) and high percentile (maximum, right) backscatter mosaics over Trondheimsfjorden. RGB=[VV,VH,NDI].

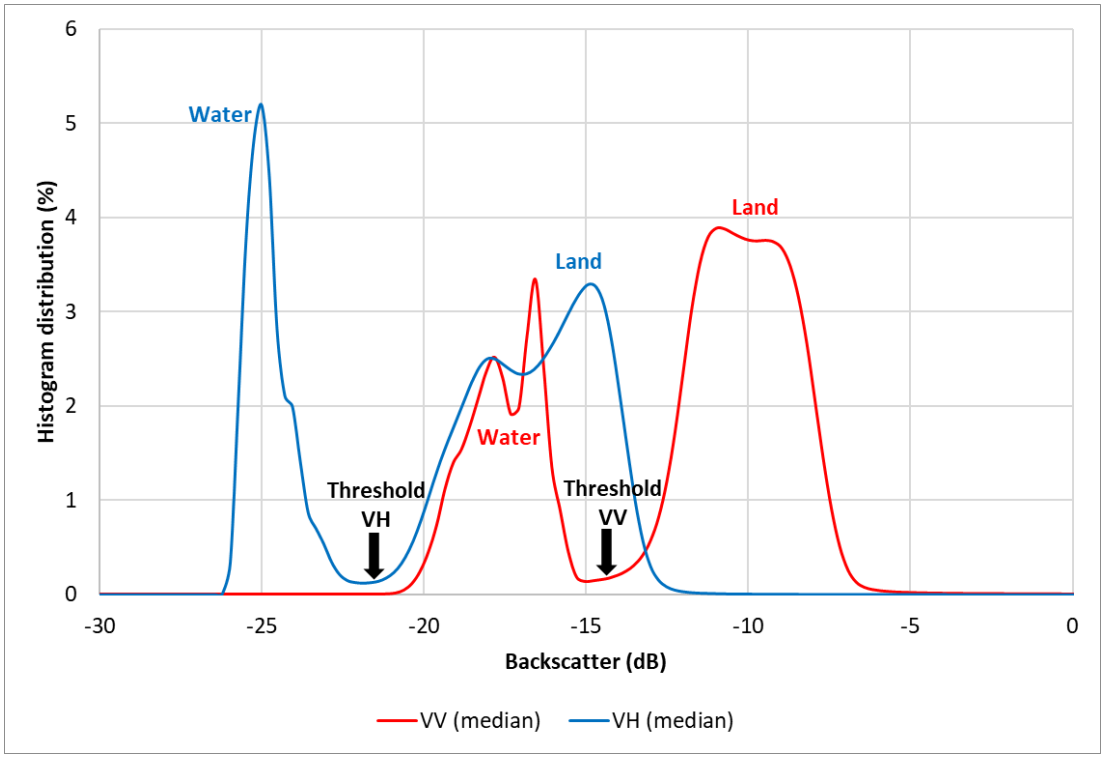

Figure 12. Median value (50 percentile value) VV and VH backscatter histogram over the Trondheimsfjorden area from Sentinel-1 2018 data. The left mode represents backscatter over water and the right mode, backscatter over land for both polarizations, VV and VH.

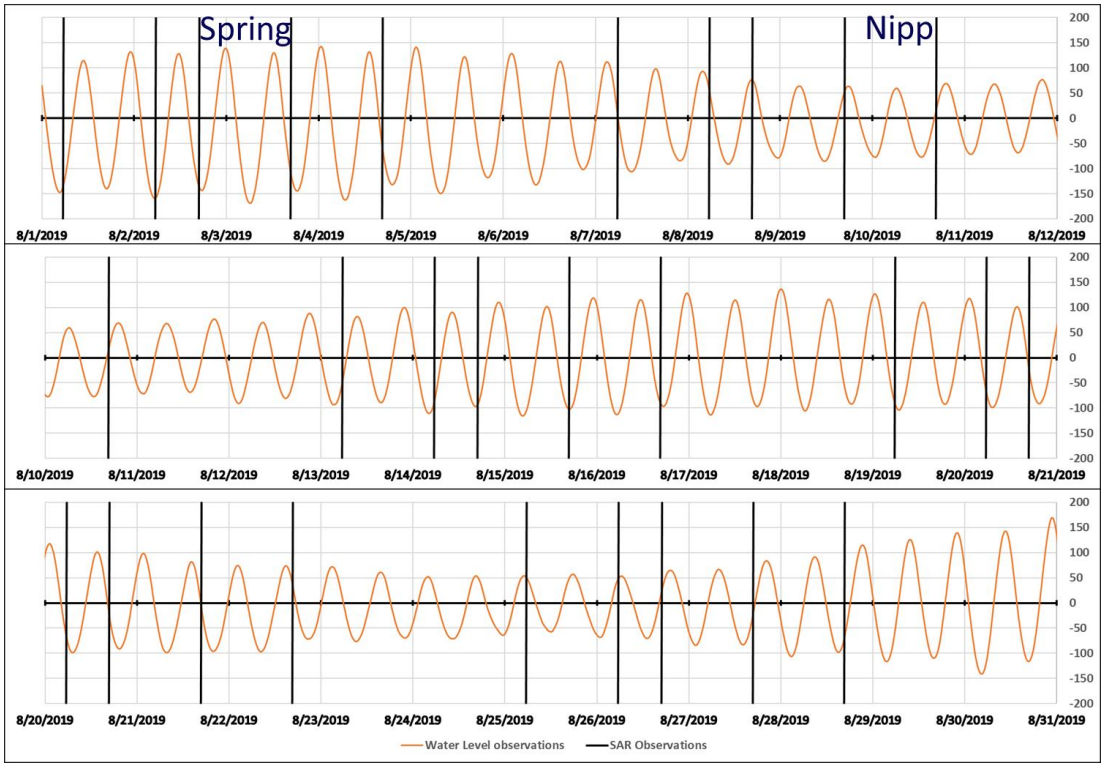

Figure 13. Tidal chart for Trondheim for August 2019 with the Sentinel-1 overpasses indicated with black bars.

The tidal chart (Figure 13) of Trondheim for August 2019 and the S1 acquisition marked as black bars illustrate the approach of using time series to extract different tidal level. The method can therefore be separated in 3 steps:

1) Preprocessing (geolocating, radiometric and topographic correcting) all Sentinel-1 data from a long time series
2) Statistical analysis of the backscatter time-series for each pixel, providing backscatter images that represent different percentiles of backscatter.
3) Extracting the high and low water lines by thresholding low and high percentiles, for example 2 and 98 percentile, respectively.

The intertidal zone is then the area between the highest and lowest waterlines extracted from the lowest and highest percentile backscatter, respectively. The more data is available, the longer the time series, the better is the statistical analysis. However, percentile extraction from times series is a mathematically and therefore process demanding operation. During this project the percentile extraction tool has been improved and included in the software. In order to exclude outliers, we use the 2nd and 98th percentiles extracted from a two-year time series in order to limit the speckle noise. As there is a risk of ice cover of some Norwegian fjord during winter, we have for the national mapping however used observations only from ice-free month from June to November, so twice 6 months accumulated.

Comparison with field data and high-resolution aerial data showed that water-land thresholds at low tides (high percentile, 98th percentile image) are in the range of [-8dB, -6dB] for the VV and [-21dB, -16dB] for the VH backscatter. For high tides (low percentiles, i.e. 2 percentile image), the

VV and VH thresholds are in the range of [-25dB, -18dB]. The minimum signal to noise level however is already around -22dB.

During the first phase of the project, the thresholds have been derived from the histograms, comparison with high resolution data and considering noise for the highest and lowest percentile.

Finally, the water land threshold for the 2nd percentile (2%) backscatter values have been determined to be -18.0 dB and -22.0 dB for VV and VH, respectively. The 2% backscatter water line corresponded also quite well to the land mask extracted from the 10m, thresholding at 10cm and represents in fact an update of the land mask. We thereby define the water line of the highest tide and the reference land mask by:

Land mask = (DEM > 0.5m) OR ((γ_{VV}(2 perc.) > -18dB) AND (γ_{VH}(2 perc.) > -22dB))

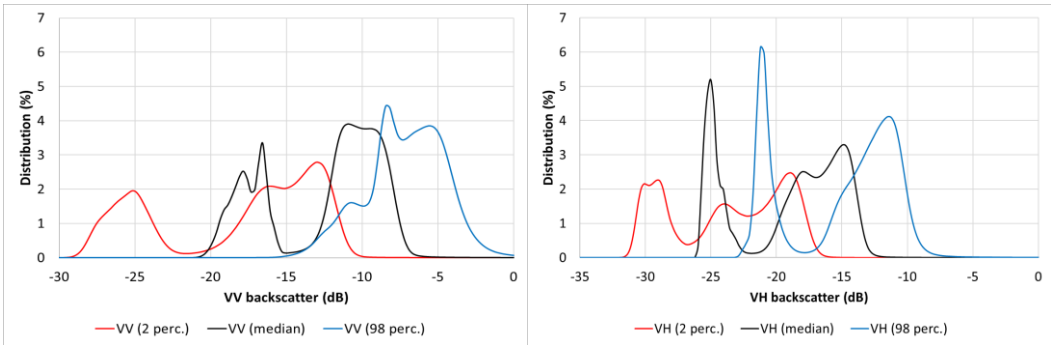

Figure 14. 2 percentile, median value (50 percentile) and 98 percentile Sentinel-1 VV and VH image histograms over the Trondheimsfjorden area from 2018 data.

The water land threshold for the 98th percentile (98%) backscatter values have been determined to be –6.4dB and -18.5dB for VV and VH, respectively. Note that these thresholds have been updated from Haarpaintner and Davids (2020) in order to reduce noise, especially from strong wind events over the ocean particularly at low radar incidence angles at near range. In Sentinel-1 data we therefore cut off the acquisitions taken at incidence angles lower than 33.8 degree (also updated from Haarpaintner and Davids (2020)).

The method is applied on percentile images from 10m-resolution pre-processed Sentinel-1 data, giving slightly more details than in the interpolated 10m from 20m pre-processing from Haarpaintner and Davids (2020).

The legend of the final results is shown in Figure 15.

Intertidal Zone Area		
Class	**Color Code**	**Pixel Values**
Water	(0,0,255)	0
Intertidal Zone Area	(255,0,0)	1
Land	(0,0,0)	8
No data	(255,255,255)	255

Figure 15. Legend of the Intertidal Zone Area products

3.2.2 Mapping atmospheric exposure with Sentinel-1 CSAR

Similar to the extraction of the water line at lowest and highest tide with thresholding high and low percentile images based on a statistical analysis, a water line extracted from thresholding a percentile image P of the backscatter time series corresponds to a certain atmospheric exposure time of [100% - f(percentile P)].

Figure 16 shows the tidal heights during S1 acquisitions in 2019 from five different satellite paths. As the satellite is sun-synchronous, each path has a specific acquisition time off the day every 12 day per satellite, so every 6 days from either S1A or S1B.

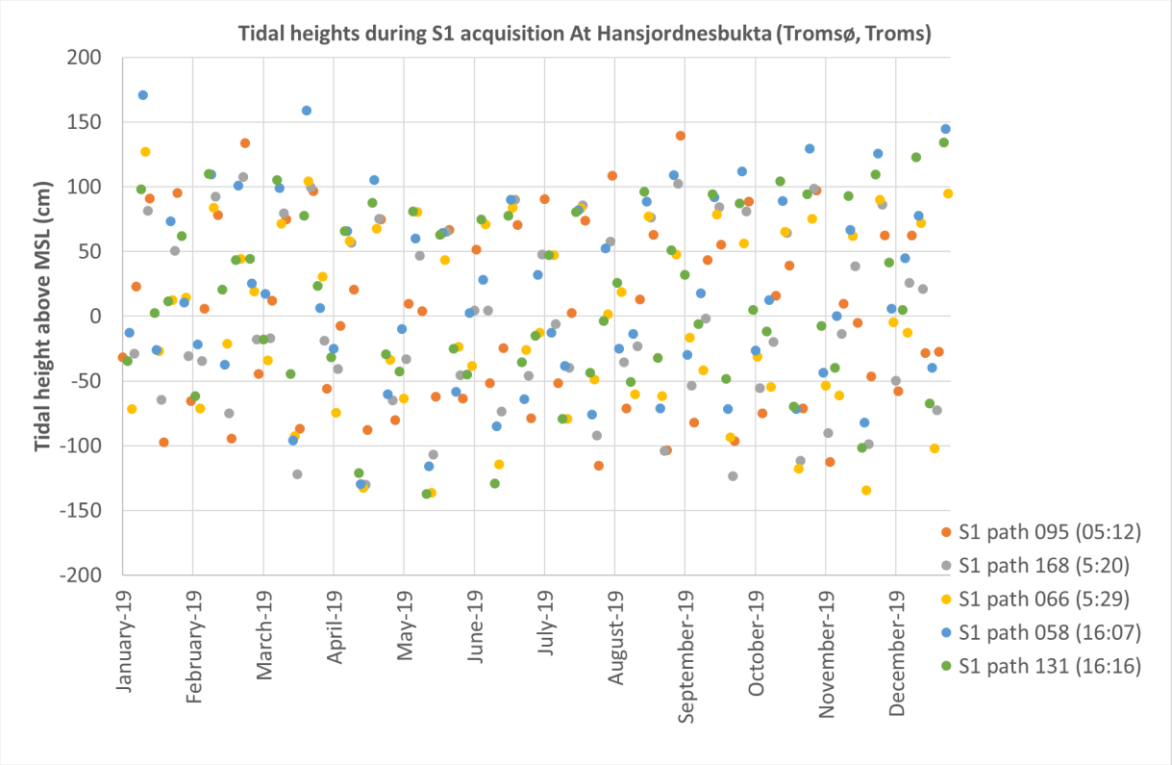

Figure 16. Tidal height over MSL during S1 acquisition times from five different satellite paths over Tromsø. The legend shows the path numbers at their corresponding overfly times.

Figure 17 shows the height corresponding to percentiles of 10min in-situ observation compared to percentiles from S1 observation acquisition times from 1 June to 30 November 2019. We assume that with taking acquisitions from two ice-free years, the slight bias in Figure 17 towards higher sea level will decrease. It is quite clear though that with using the 2nd and 98th percentile, we will always miss the highest and lowest tidal levels but should be able to map MLWS and MHWS. The 5th to 25th percentile interval corresponds quite well to the low tide range between mean spring and neap low tide level (MLWS and MLWN). The 75th to 95th percentile interval corresponds to the high tide range between mean neap and spring high tide (MHTN and MHTS). The errors are well in the range of the difference between predicted and observed tidal levels from kartverket.no.

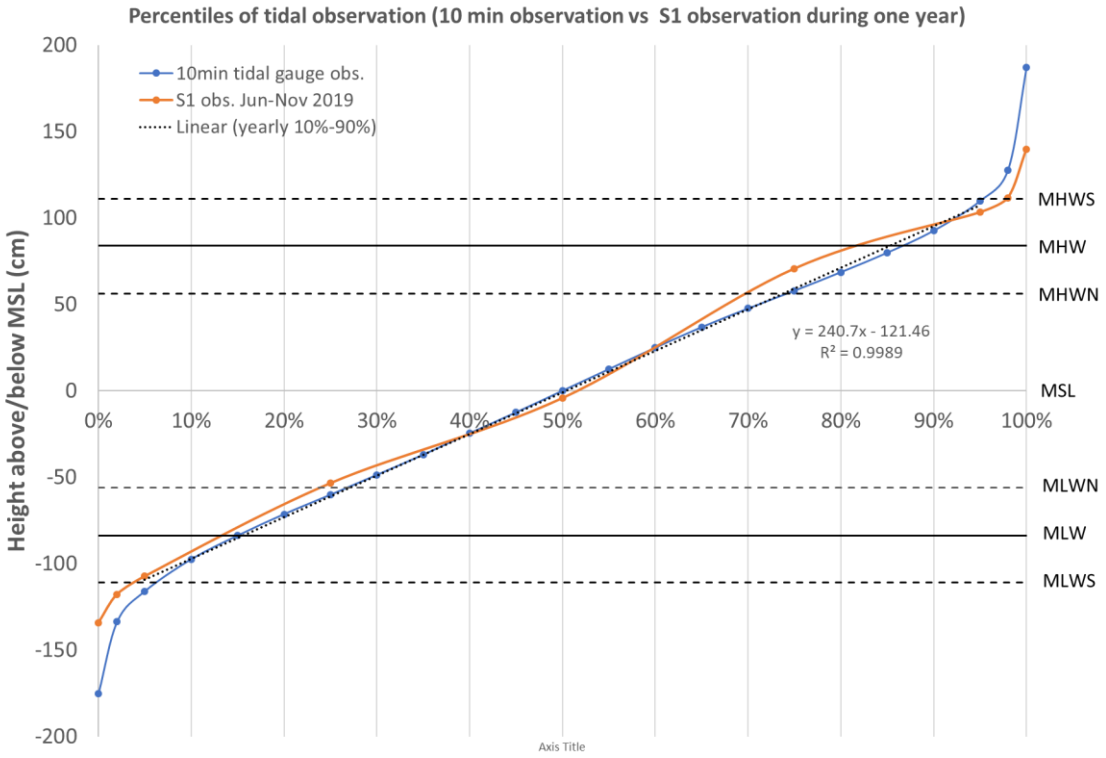

Figure 17. Tidal level heights corresponding to percentiles of time series of tidal level from 10min in-situ tidal gauges observation and from S1 observations acquisition times from 2019 at Hansjordnesbukta (Tromsø, Troms).

Logically, there is a direct correspondence between the water line extracted from the S1 backscatter percentiles images and tidal levels. From 3.2.1 we decided that the area between water lines extracted from the 2nd and 98th percentiles images correspond to the intertidal zone area. The water line extracted from the 5th, 25th, 50th, 75th, and 95th percentile backscatter images from a S1 time series correspond then to the tidal levels MLWS, MLWN, MSL, MHWN and MHWS, respectively.

Figure 18 and Figure 19 show the backscatter histograms over Trondheimsfjorden of VV and VH backscatter of these percentile images. Haarpaintner and Davids (2020) chose the thresholds by using the minimum between a water and land mode in these histograms. As we collected the water lines during fieldwork at these specific tidal levels, we updated the thresholds in order that the threshold contour lines in the percentile images best fitted the GPS tracks taken during these tidal levels at Langnes and Hillesøy, both in Tromsø Kommune, Troms. The final land-water thresholds γ_{VV}(perc.) and γ_{VH}(perc.) are summarized in Table 4. The maximum noise equivalent sigma zero (NESZ) of -22dB defined for the interferometric wide (IW) swath mode (De Zan and Guarniere, 2006) limits the lowest of our thresholds. Figure 20 shows the land-water thresholds as a function of percentile level. At low percentiles (2nd and 5th) the VV threshold is the main parameter to be considered and at high percentiles (95th and 98th), the VH threshold is the main parameter as significant noise can be induced from strong winds over the ocean in co-polarized SAR images (VV).

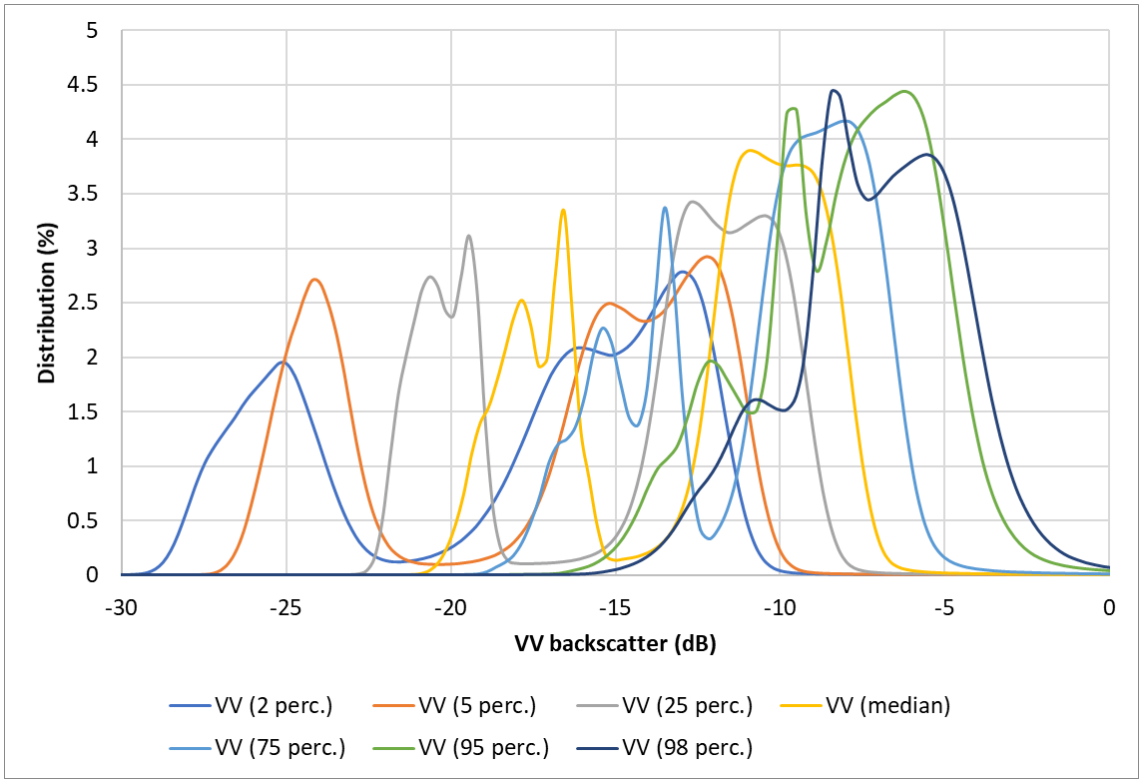

Figure 18. VV Backscatter distribution of percentile images at 2%, 5%, 25%, 50%, 75%, 95% and 98 % percentile around Trondheimsfjorden.

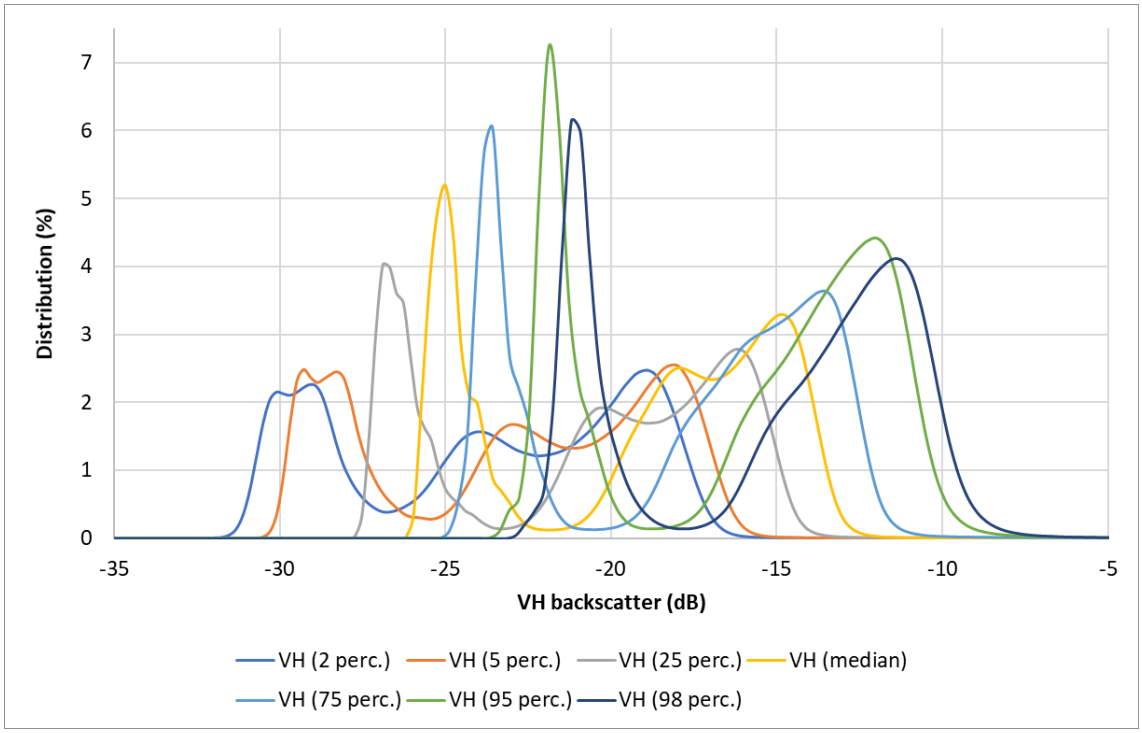

Figure 19. VH Backscatter distribution of percentile images at 2%, 5%, 25%, 50%, 75%, 95% and 98 % percentile around Trondheimsfjorden.

Table 4. Land-water threshold values for γ°(VV) and γ°(VH) backscatter for the percentile images at 2nd, 5th, 25th, 50th, 75th, 95th and 98th percentiles.

	2%	5%	25%	50%	75%	95%	98%
γ°(VV)	-18.0	-17.3	-15.0	-14.5	-12.7	-8.5	-6.4
γ°(VH)	-22.0	-22.0	-22.0	-21.7	-20.7	-19.8	-18.5

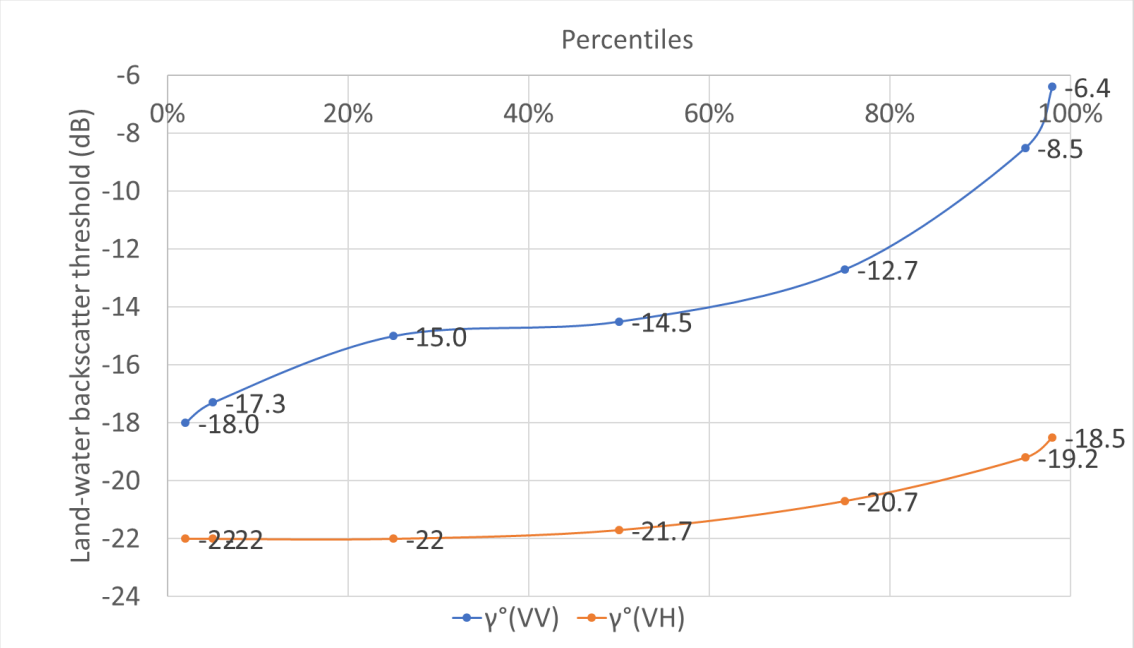

Figure 20. Land water threshold vs percentile image for VV and VH polarizations.

Therefore, for a certain percentile P, the corresponded land-water thresholds $\gamma_{VV}(P)$ and $\gamma_{VH}(P)$ each define the threshold of the atmospheric exposure AtmExp(100%-P). by

$$\textbf{AtmExp(i,j) > 100\%-P} \quad \textbf{if} \quad \gamma_{VV}(I,j) > \gamma_{VV}(P) \textbf{ OR } \gamma_{VH}(I,j) > \gamma_{VH}(P).$$

The method has been applied on the 10m-resolution percentile images and the legend of the results is shown in Figure 21.

ITZ - Atmospheric Exposure (Tørrleggingsvarighet)		
Class	**Color Code**	**Pixel Values**
No data	(255,255,255)	255
Land (DEM >50cm)	(0,0,0)	8
Land (mask from S1)	(139,69,19)	7
> 95%	(255,0,0)	6
75-95%	(218,165,32)	5
50-75%	(255,255,0)	4
25-50%	(173,255,47)	3
5-25%	(0,255,0)	2
<5%	(0,255,255)	1
Water	(0,0,255)	0

Figure 21. Legend of Intertidal Zone Atmospheric Exposure maps.

3.2.3 Intertidal zone area and type mapping with Sentinel-2

The methodology used for the analysis of Sentinel-2 data for the purpose of mapping tidal zones uses statistical parameters calculated from time series of vegetation and water indices and is inspired by the methodology presented by Murray et al. (2019). As discussed in previous sections, the reason behind using time series is that tidal zones are very dynamic areas, which are submerged some or most of the time. This makes it difficult to acquire satellite images at exactly low tides. By using cloud-free time series, the area is imaged at different tidal stages and the variation in index values with time is expected to help distinguish between permanent water, permanent land and tidal zones. The frequent cloud cover along the coast of Norway reduces the number of cloud free images available and the analysis is based on significantly fewer images than the S1 analysis; on the other hand, optical data also provides information from several meters below the water surface, which helps to identify the extent of the tidal zone even though no images are available during the lowest tides. To avoid images with very low sun angles and the presence of sea ice in the fjords, only images from the period between 1 May and 30 October have been used.

The processing workflow has been implemented in java script within Google Earth Engine (GEE; Gorelick et al., 2017), which provides cloud-based access to satellite imagery and enables the analysis of large datasets in the cloud.

Vegetation indices, such as the widely used Normalized Difference Vegetation Index (NDVI), provide information about the presence and type of vegetation and are influenced by biophysical characteristics, such as chlorophyll content, structure and leaf area, and color. Water indices on the other hand, e.g. the Normalized Difference Water Index (NDWI), provide information about the presence or absence of surface water. Vegetation changes during the season and these changes are reflected in the variation of the vegetation indices during the season. Similarly, the intertidal zone is characterized by changes in surface water cover during each tidal stage, which means that intertidal zones will show larger variation in water index values during the time series than areas that are permanently covered by water or permanently dry.

The statistical parameters of the time series are calculated for each pixel and include the mean, median, standard deviation and different interval means. The interval means help to describe the

variation in values over the time period of the time series (similarly to the percentile values used in the S1 analysis), which is illustrated in Figure 22. Figure 23 and Figure 24 show an example of how some of the interval means of the NDVI, NDWI, and SWIR1 vary across land, tidal zone and water.

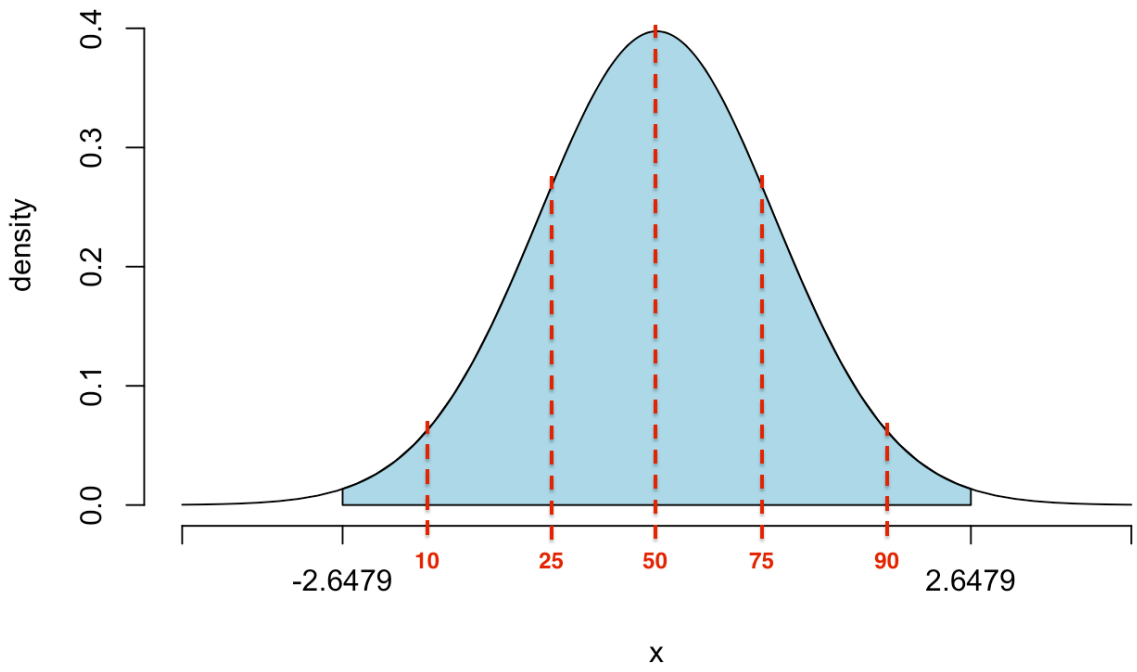

Figure 22. Illustration of the calculation of interval means. The graph shows a distribution of values, in our case this would be the values during the time series. In this graph, 50 is the same as the median value, and e.g. 10 is the 10th percentile. Interval Mean 1025 (intMn1025) is the mean value of the values between 10 and 25.

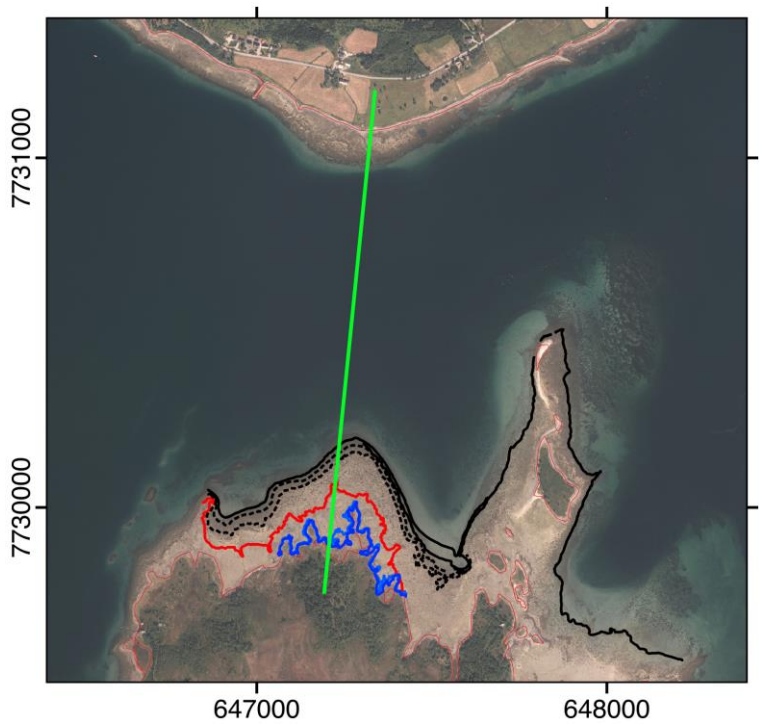

Figure 23. Location of the transect as shown in Figure 24.

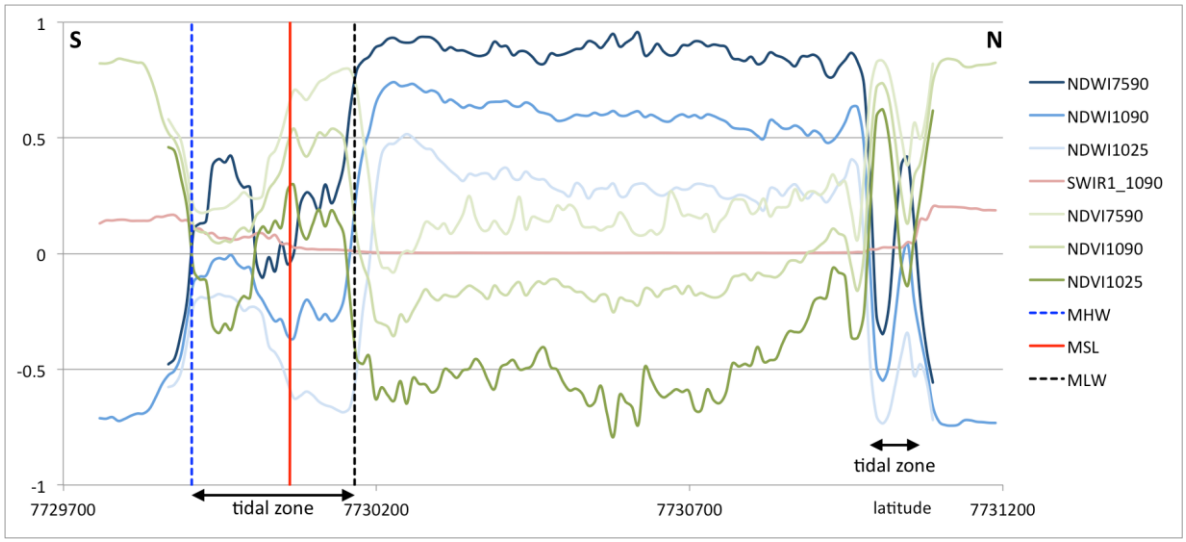

Figure 24. Variation of NDVI and NDWI inter means and SWIR1 mean along a transect from Grindøya nature reserve in the south (left) to Håkøya in the north (right) (Figure 23), across coastal land, tidal zones and permanent water. MLW = mean low water, MSL = mean sea level, MHW = mean high water.

There are 2 main types of methods to classify images: unsupervised classification and supervised classification. Unsupervised classification is purely based on the statistics of the input images without any a priori knowledge on possible classes. An advantage is therefore that this avoids any bias from the analyst. Supervised classification methods, on the other hand, use a priori knowledge of the classes to be mapped and is therefore strongly dependent on the quality of the training data. Unsupervised classification using Gaussian Mixture Modelling worked well in the

test area Trondheimsfjorden, but it is computer intensive and challenging to extend to a Norway wide mapping within the scope of this project. For this project, we have therefore chosen for a supervised classification using a training dataset that is based on the visual interpretation of the aerial photos available in the Norge I Bilder database in combination with S2 NDVI and NDWI images to ensure correct positioning of the training points. Additional information used to aid the visual interpretation include the field data and photos collected in the field and the mudflat database.

The diagram in Figure 25 summarizes the workflow used in this project and the different steps will be described in more detail below. All steps were carried out in GEE, training and validation data was prepared in QGIS and uploaded as assets in GEE to be used in the analysis.

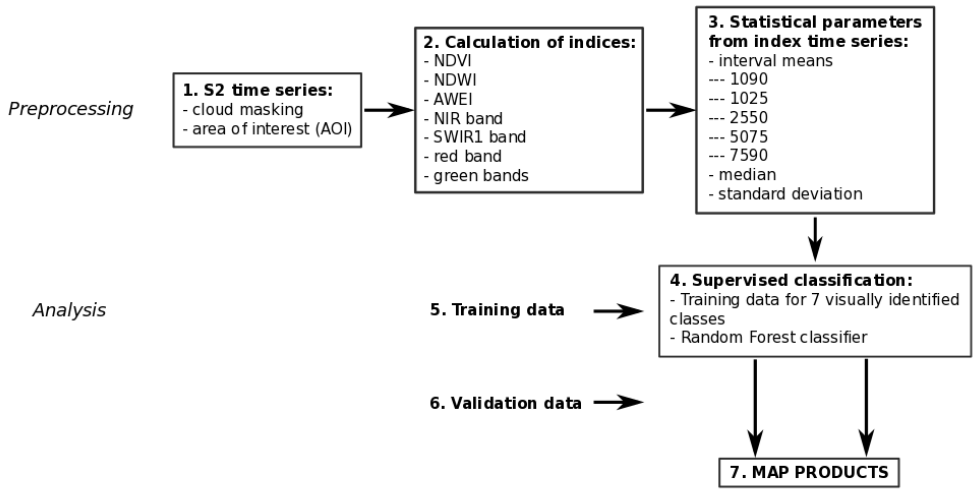

Figure 25. Processing workflow used for Sentinel-2.

1. Cloud masking and AOI. Optical satellite imagery is dependent on cloud free conditions and cloud covered areas will therefore need to be masked. Level 2-A S2 imagery has been atmospherically corrected and includes information on cloud cover in the QA60 band. The information in this band has been used to mask cloud covered pixels in all images used in the analysis. All available images in the period between 1st May – 30th October 2019, and with less than 50% total cloud cover, were used. Figure 26 shows that, after cloud masking, the majority of the pixels are covered by between 15 and 65 images, with some of the lowest number of cloud free images in the area north of Stavanger. In addition to cloud masking, all areas outside the tidal zone region were masked by creating an area of interest (AOI); the AOI is here defined as the zone within 5 km of the coastline, and at elevations of less than 0.5 m (based on the 10 m DEM from http://www.geonorge.no). The mask was created in QGIS, using a coastline vector downloaded from http://www.geonorge.no in combination with the 10 m DEM.

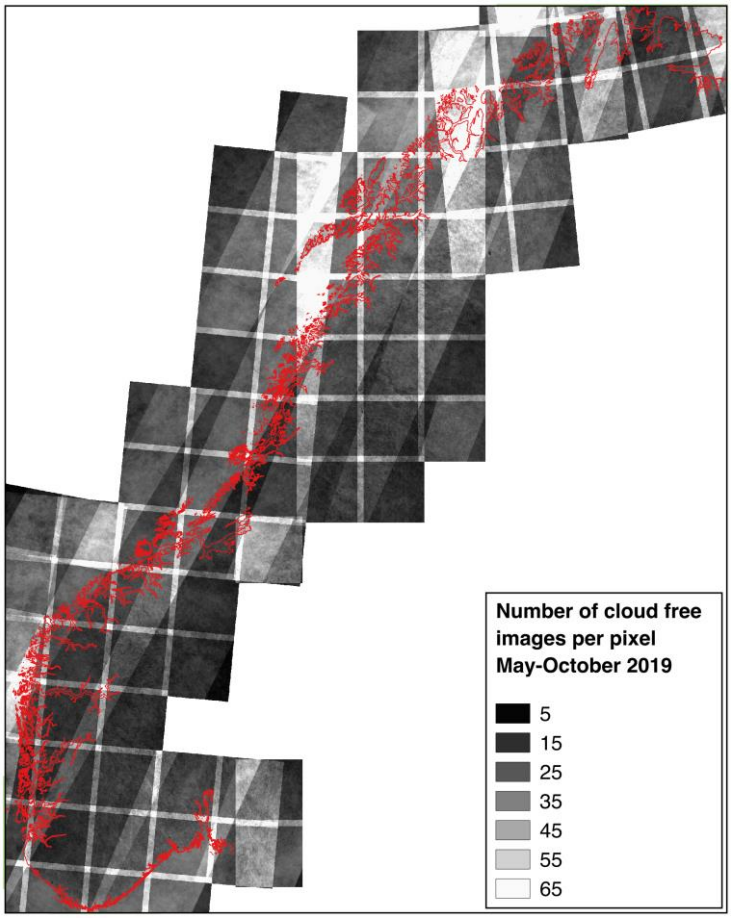

Figure 26. Number of cloud free images used in the analysis after cloud masking.

2. Calculation of water and vegetation indices. Two vegetation indices and three water indices were calculated for each image: the transformed normalized difference vegetation index (TNDVI), the normalized difference vegetation index (NDVI), the modified normalized difference water index (MNDWI), the normalized difference water index (NDWI), and the automated water extraction index (AWEI). These indices provide information about the presence and greenness of vegetation and the presence of surface water. In addition to the indices, the NIR band (band 8) and SWIR1 band (b11) are also included and help distinguish land and water and provide information on vegetation biomass. The vegetation and water indices are calculated using the following equations and band combinations (Table 2 described the different band numbers that are used):

(1): $TNDVI = \sqrt{\frac{(b8-b4)}{(b8+b4)} + 0.5}$

(2): $NDVI = \frac{(b8-b4)}{(b8+b4)}$

(3): $MNDWI = \frac{(b3-b11)}{(b3+b11)}$

(4): $NDWI = \frac{(b3-b8)}{(b3+b8)}$

(5): $AWEI = 4 \times (b3 - b11) - (0.25 \times b8 + 2.75 \times b12)$

3. Statistical parameters from time series. To reduce the amount of data and get different measures of the temporal variation of the indices, a number of statistical parameters were calculated from the time series: interval means, median and standard deviation (sd). An interval mean is the mean of the data within a percentile range; e.g. the interval mean 1090 (intMn1090) is the mean of the data in the percentile range 10 to 90. The interval means contain information about the shape of the distribution. All parameters used were subsequently scaled to between 0 and 1 prior to segmentation and classification.

After testing several combinations of indices, statistical parameters and bands, the final combination of indices and bands used is: MNDWI and AWEI (median, all interval means), SWIR1, NIR, red and green bands (only intMn1090).

4. Supervised classification. For the supervised classification, a database with training points was created based on visual interpretation of aerial photos (Norge-i-Bilder) (step 5). The training points were used to train a random forest classifier, which was subsequently applied to the whole dataset for all of Norway. A simple smoothing filter was applied to reduce some of the speckle. The intertidal zone types identified here are permanent water, shallow water, mud, rock, sand/gravel, seaweed, and land.

5. Training data. The training data is based on the visual interpretation of aerial photos in combination with NDVI and NDWI images. Eight classes were visually identified (land, urban, permanent water, shallow water, mud, sand/gravel, seaweed, and rock), and examples were digitized on screen to create a database with training data (Figure 27). A total of 750 points were digitized. The points were then converted into circle polygons with a radius of 5 m around the points, resulting in a dataset of 1376 pixels. This dataset is subsequently randomly split in 80% training data (1086 pixels) and 20% validation data (290 pixels). The dataset is, however, strongly biased to Troms and Finnmark due to more local knowledge in these areas.

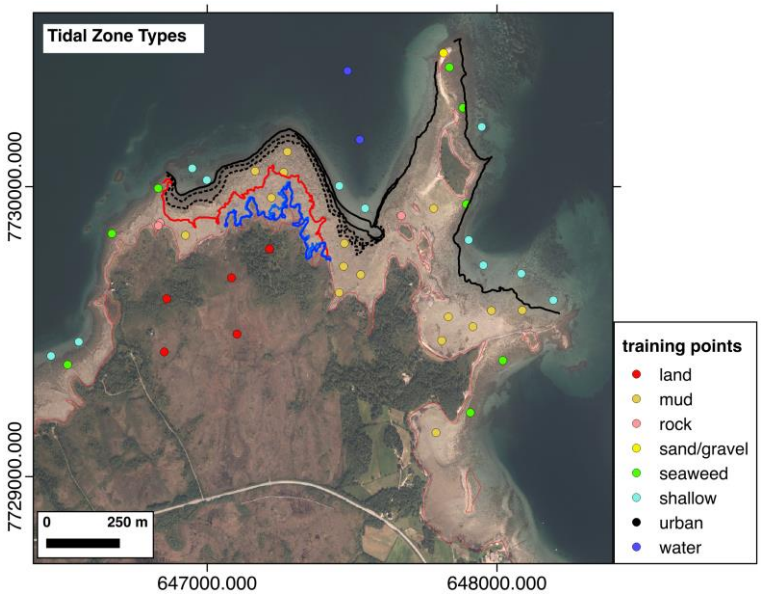

Figure 27. Example of training points in the field area around lille Grindøya, Tromsø.

6. Validation points. Initial validation is done visually against the aerial photos. In addition, a validation set was created by splitting the training points (see step 5.) into a training and a validation set. This resulted in a validation set of 284 pixels.

7. Map products. The final products are generated per county as indicated in Figure 28 and exported in GeoTIFF format and in UTM33N coordinate system via Google drive.

3.2.4 Use of aerial data

Aerial data from Norge-i-Bilder has been visually investigated, and it was concluded that the aerial data is not suitable for operational and large-scale monitoring of intertidal zones. There are several reasons for this:

1) The aerial data, as it is available on norgeibilder.no, only comes with a time stamp of the date, but not the exact time of the acquisition. That is also quite logic in the way that the aerial data is available as mosaics of aerial photography and not as single photographs. Since there are no time stamps, it is impossible to combine this data with modeled or observed tidal heights.
2) To map intertidal zones, it would be necessary to have acquisitions at both maximum low and maximum high tide, which has obviously not been considered in the strategy under the acquisition of the aerial data.
3) Tidal maximums can vary over relatively short distances because of the fjord systems along the Norwegian coast. So even if we would know the exact time at some position, it would be difficult to extract this over the whole region.
4) Aerial photos over Norway are of different quality and resolution, as they have been taken under different light conditions and with different cameras, which makes a consistent method difficult for nation-wide intertidal zone area mapping.
5) The access and quantity of the aerial data over all of Norway for processing would be very challenging for processing on a large scale. It would be either necessary to download the whole data or bring the method to the data in the cloud.
6) Investigating several aerial mosaics has also shown that it is nearly impossible to distinguish the water line in the optical data, especially under calm water condition. That is even the case when using aerial photos for validation of the results presented in this report.

Nevertheless, the high resolution of aerial data gives us important information to help distinguish different types of intertidal zone. It is therefore used to establish training data for classification of the intertidal zone and validation data for the results. Exact interpretation however is still challenging and the quality of any training and validation data set will still be dependent of the analyst's experience.

3.3 Mapping of intertidal zone changes

In this second phase, the focus was on producing a first national product of the intertidal zone and mapping changes will be done in future studies. This section therefore mainly repeats some general outcomes from Haarpaintner and Davids (2020).

Most of the intertidal zone definition, specifically the water level lines are all defined as “mean” values, which necessitates a certain integration period for defining natural changes. Rapid changes from anthropogenic activities and disasters should be detectable using shorter integration times, like on a monthly basis directly by comparing single SAR scenes; however likely to show noise at high resolution because of SAR speckle noise.

Yearly changes can be directly detected through comparison of specific percentiles over long time periods. The highest percentile should detect most changes. Changes above the highest water line, for example man made above-water constructions, should also be detectable at lower percentiles if they have occurred during the whole integration period. Otherwise, the level of percentile that detects the changes is directly related to the period since the change has occurred. This means that different percentiles could be used to approximately date the change.

A general threshold to detect changes used in SAR remote sensing is a 3dB difference between images of different periods for both VV and VH polarization. Lower thresholds of differences might detect noise and natural backscatter variations. Results from subtracting high percentile images of 2017 from 2018 in the demonstration site Trondheimsfjorden during the first phases of the project shows some example and man-made construction and changes are clearly detectable. Natural changes in the intertidal zone might occur on longer time scales and need therefore a longer acquisition and processing of Sentinel-1 data. On a national mapping basis, it was decided that this is out of scope of the current project due to the project’s limited budget and the processing and data load and has not been studied further during phase 2 of the project. Examples are shown in Haarpaintner and Davids (2020).

However, in order to detect changes between different years, a simple method would be to directly compare the S1 or S2 map products between these years. There will be some amount of natural change and uncertainty, but major changes should be detected. Visual interpretation may be needed to determine the type of change.

4. Nation-wide mapping of the intertidal zone for the Norwegian coast

4.1 Sentinel-1 processing for nation-wide mapping of the Norway coast

The intertidal zone atmospheric exposure (ITZ_AtmExp) mapping method has been scripted into a python module. The intertidal zone area product can be directly extracted by combining the different atmospheric exposure classes into one intertidal zone area class and is included in the same script.

The python module to map the atmospheric exposure and area of the intertidal zone has then been implemented in NORCE's operational processing system for SAR processing (GDAR), which already includes the pre-processing of S1 level-1 GRD images and a toolbox to mosaic, statistically analyze and calculate percentiles from SAR time series in an operational automatic manner, executable in parallel on multiple processors.

To map the complete coast of continental Norway, the whole area of a 10km wide band along the coastline has been divided into 20x20 km^2 tiles (Figure 5) summing up to 597 tiles for whole Norway. For each tile, a list of Sentinel-1 GRD level-1 products has been established and combined into a JSON file to process all 597 tiles. All together 6893 Sentinel-1 IWH GRD dual polarization single scenes have been used and processed, which sums to a total of more than 10TB of original satellite data to be processed and 482404 temporary partial processed products during the processing.

The complete processing has been done using 2-3 PCs parallel in-house with 8 cores each, 4 TB solid-state disks (SSD) for cache and temporary files. The complete processing took about 6 weeks, though including some down-time of the Alaska Satellite Facility where the Sentinel-1 data has been downloaded from. The processing steps can be summarized as:

1) Checking the in-house data archive for the required Sentinel-1 data.
2) Download missing data from the Alaskan Satellite Facility.
3) Preprocessing
4) Statistical analysis and percentile extraction
5) Intertidal zone atmospheric exposure and area mapping.
6) Cache for later use original S1 data and delete temporary files for later use.

The individual tiles have then manually been mosaicked into nine Norwegian county products (see section 5, with Oslo, Viken, Vestfold and Akershus in one product), in order to make them easier to compare with Sentinel-2 results generated from the Google Earth Engine.

4.2 Sentinel-2 processing for nation-wide mapping of the Norway coast

The processing of the optical Sentinel-2 data on a nationwide level is done in Google Earth Engine (GEE) using javascript, as described in 3.2.3. Prior to processing in GEE, a number of products were prepared using QGIS and uploaded as assets in GEE:

- Detailed coastline vector data was extracted from AR50 products downloaded from Geonorge
- A land mask was made, >0.5 m, based on digital terrain models (DEM10 products) from Geonorge.
- A training/validation set of 750 points (1376 pixels, see section 3.2.3), based on visual interpretation of aerial photographs from Norge I Bilder. The training/validation set is randomly split into 80% training and 20% validation. Each point is a circle of 10m diameter and can therefore contain between 1-4 pixels.

Processing is done for all of Norway at once, and the final county products, based on the same division as the Sentinel-1 products (Figure 28), are exported in GeoTIFF format from GEE to Google Drive.

5. Results

5.1 Sentinel-1

5.1.1 Nomenclature of files and data set from the Sentinel-1 processing

All together the whole Norwegian coast is covered by 597 20x20 km^2 tiles.

The file names for the ITZ Atmospheric exposure and ITZ area products based on S1 data are:

ITZ_AtmExp_N***E***_S1_2018-2019_10m_UTM33N_***.tif
ITZ_Area_N***E***_S1_2018-2019_10m_UTM33N_***.tif

Where N***E*** is the position of the lower left corner in 10km in UTM33N.

The products have been mosaicked into nine county products shown in Figure 28. Figure 29 shows an example of both the ITZ atmospheric exposure and ITZ area product derived. Table 5 summarizes the pixel and file size of the nine county products covering the Norwegian coast. The total size of the nine county products of about 4.5GB can be compressed to 60MB.

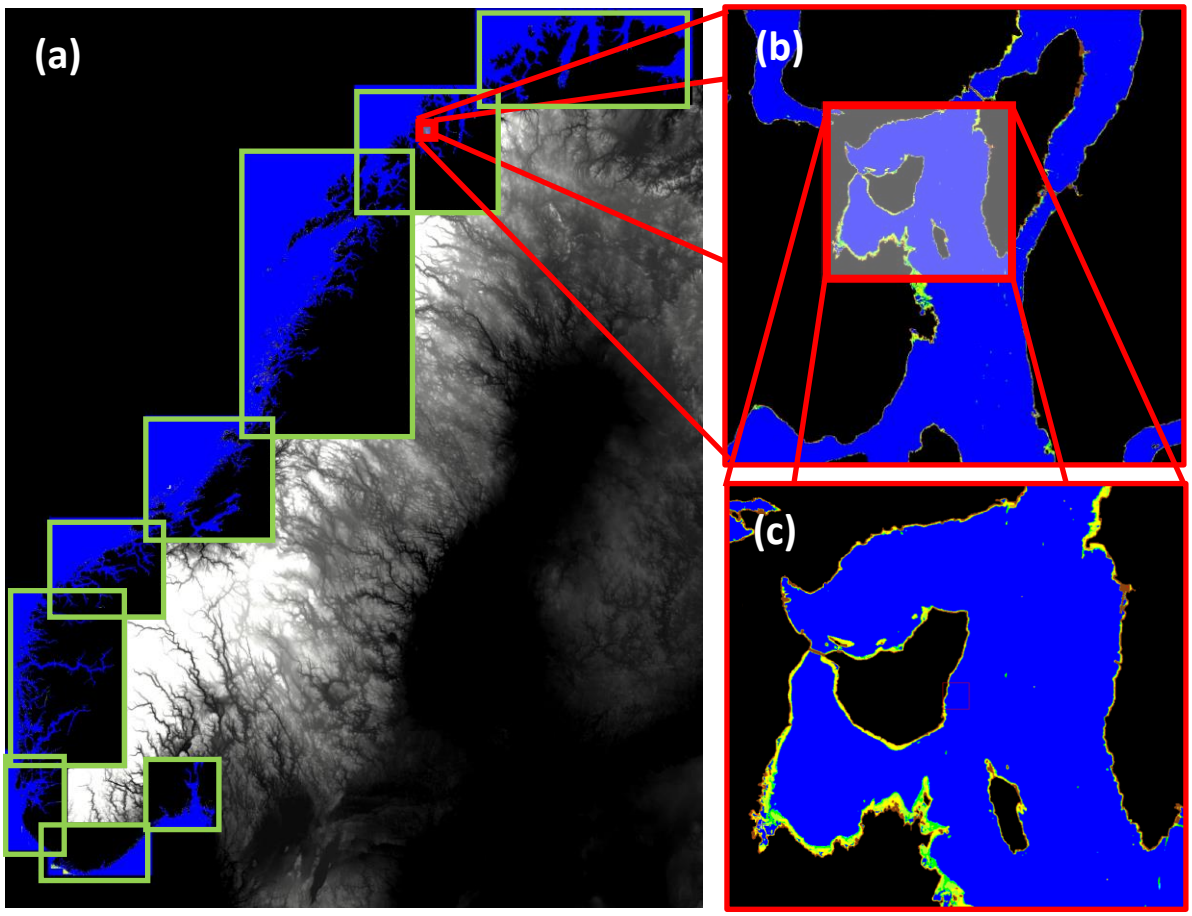

Figure 28. (a) The nine ITZ atmospheric exposure county products overlaid over the Norway DEM, (b) tile "772x64" and (c) a full resolution over Lille Grindøya and Langnes field sites.

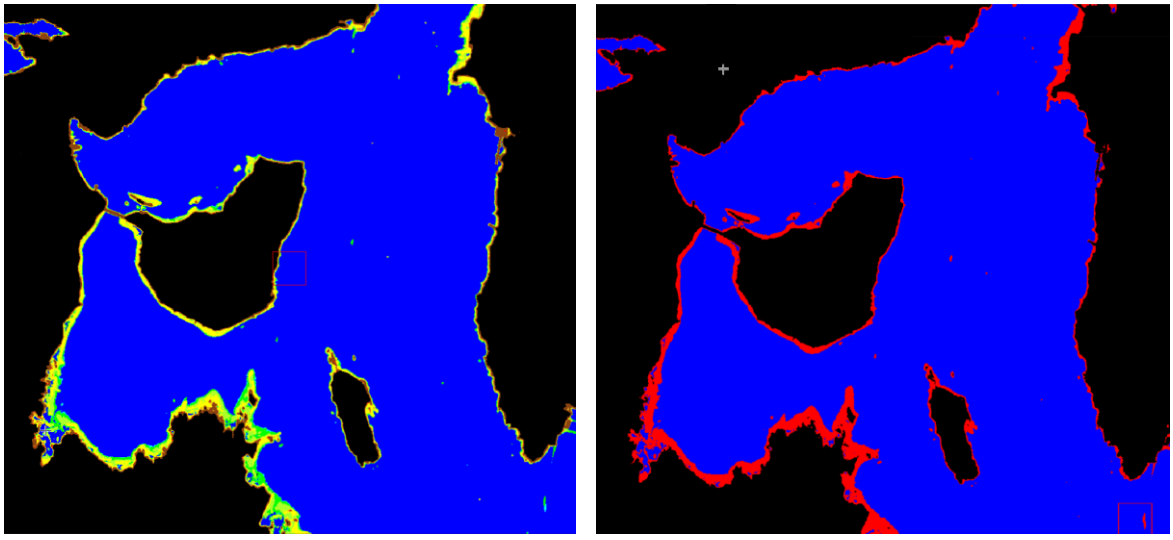

ITZ - Atmospheric Exposure (Tørrleggingsvarighet)		
Class	**Color Code**	**Pixel Values**
No data	(255,255,255)	255
Land (DEM >50cm)	(0,0,0)	8
Land (mask from S1)	(139,69,19)	7
> 95%	(255,0,0)	6
75-95%	(218,165,32)	5
50-75%	(255,255,0)	4
25-50%	(173,255,47)	3
5-25%	(0,255,0)	2
<5%	(0,255,255)	1
Water	(0,0,255)	0

Intertidal Zone Area		
Class	**Color Code**	**Pixel Values**
Water	(0,0,255)	0
Intertidal Zone Area	(255,0,0)	1
Land	(0,0,0)	8
No data	(255,255,255)	255

Figure 29. An example of the ITZ atmospheric exposure product (left) and the derived ITZ area product (right) south-west of Tromsø.

Table 5. Size in pixels and file size of the nine county products covering whole Norway.

County(ies)	Image Size (pixel)	Resolution	File Size (MB)
Agder	17900x9100	10m	163
Finmark	37400x16600	10m	621
Møre og Romsdal	19700x16800	10m	331
Nordland	29000x49000	10m	1421
Oslo, Viken, Vestfold og Telemark	12500x12500	10m	156
Rogaland	10800x17400	10m	188
Troms	26000x22000	10m	572
Trøndelag	22000x21200	10m	467
Vestland	20000x30300	10m	606
Total			**4525**

5.1.2 National mapping issues, sources of errors and limitations

Developing methods locally and applying them to large areas, like national mapping, reveals certain limitations, particular for varying regions like the Norwegian coast, involving different climate zone (polar, boreal and temperate) and societal (sparsely to densely populated) conditions. In addition, the tidal ranges along the Norwegian coast vary quite importantly with tidal ranges below 30 cm in the South to tidal ranges of above 2.5 m in the North (Figure 30). Satellite coverage is also variable with increasing satellite image overlaps towards the North. Here we will describe certain issues that have been already encountered while reviewing the results as well as some limitation of the method.

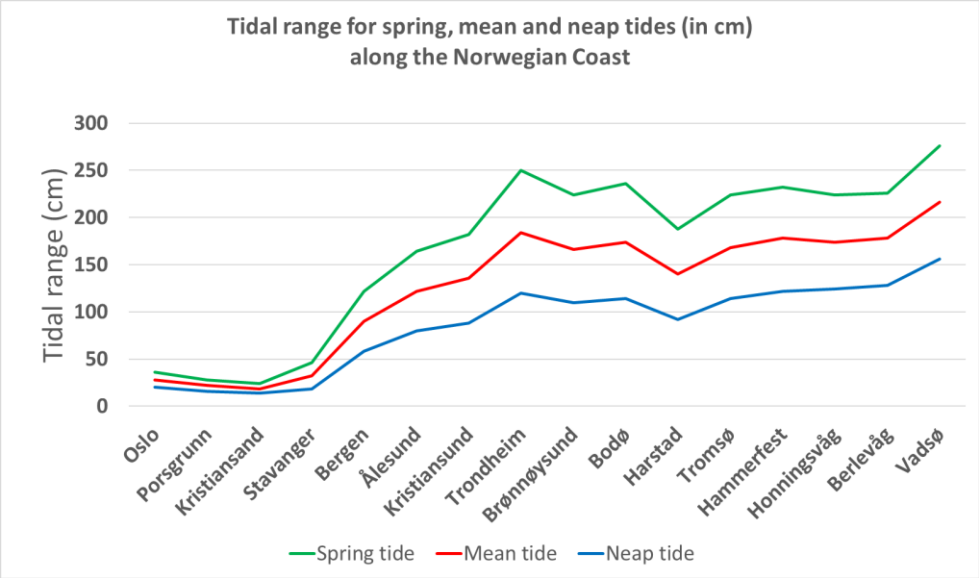

Figure 30. Tidal range in cities along the Norwegian coast from Oslo to Vadsø according to https://www.kartverket.no/til-sjos/se-havniva .

Sea ice in fjords

As some fjords in Northern Norway and maybe even some inner-fjords in mid-Norway can be ice covered during the winter months, we already avoided false detection of the intertidal zone because of sea ice by limiting the input data to ice-free months from June to November. We have not studied in detail how much sea ice would wrongly induce a detection of intertidal zone but have seen some effects while testing the methods on Troms Fylke. Ignoring the sea ice issue or masking out only potentially ice-covered fjords could make it possible to integrate over one complete year instead of processing two summer seasons. This might be relevant if interannual variations and changes need to be studied.

Harbor occupancy and boat traffic

As the coast in southern Norway is much more populated than in northern Norway, there is a lot more boat traffic and in particular recreational private boat traffic. As boat occupancy of harbors and boat traffic has only been a minor effect during the methods development in Trondheimsfjorden, this has not been paid attention to originally. Processing the whole Norwegian coast however shows that boat occupancy and traffic in and around harbors dominates

the detection of the intertidal zone as water pixels close to land are occupied temporarily by boats rather than by land as in the intertidal zone. Harbor constructions, like piers, that are not resolved in the original DEM will show up as the S1 derived land mask in brown. New construction should be easily detectable if the processed is repeated on a 1-2 yearly bases.

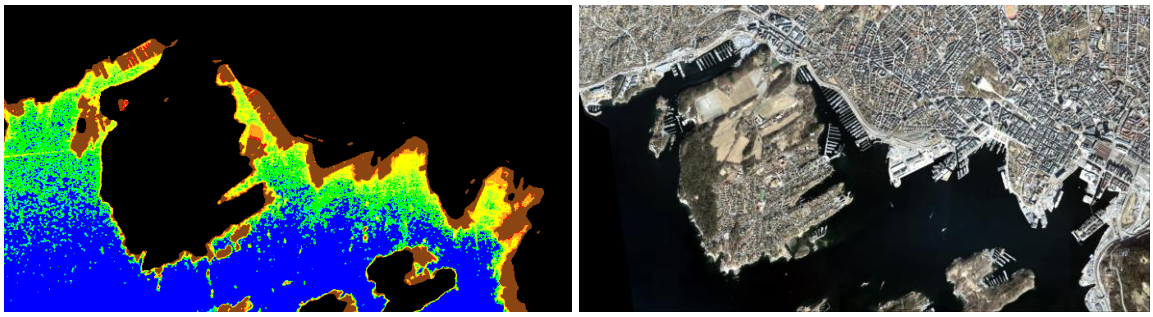

Figure 31. The ITZ atmospheric exposure product in Oslo harbour reflects the spatial occupancy of boats over the integration time instead of an intertidal zone.

Strong ocean winds and waves

We are quite confident that the mapping thresholds as well as the elimination of steep incidence angles at near range from the S1 satellite have been defined in a way to reduce errors induces by strong ocean winds and waves in the final products. Still some strong ocean noise has been detected at the south-western coast of Norway (Figure 32). It seems though that this has been the only place where this occurred to such a strong degree and a data issue could also be the course. However, at this time we cannot completely exclude that this source of error might occur in the products. However, visually it appears clearly as an error. Especially in this particular case the strong wind signature has been out in the ocean and not near land.

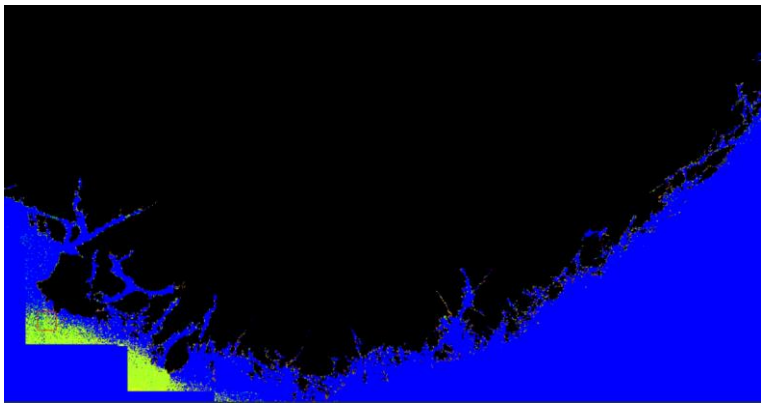

Figure 32. Falsely detected intertidal zone in green probably because of strong winds or waves at the south-western coast of Norway.

Radar echo from steep south- and north-faced mountain slopes.

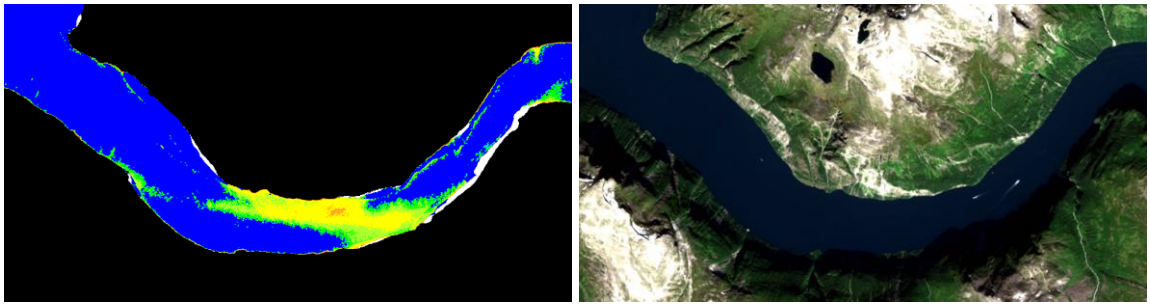

Figure 33. Falsely detected intertidal zones due to a SAR echo effect inside Geirangerfjord between two mountain slopes facing each other in the north-south direction.

Mountain slopes that are directed towards or against the satellite induce radar shadow and radar overlay effects, i.e. mainly east or westward slopes. They can be well masked calculating the local incidence angle using the satellite orbit parameters and the digital elevation model. However, it seems that there is also a backscatter echo effect from the radar signal side-lobe where mountain slopes are parallel to the emitted radar signal. This occurs especially in the cross-polarization band VH increasing the signal to the point that qualifies to falsely detect an intertidal zone inside the fjord. The backscatter from the radar signal side lobes reflected from the hill sides dominates the received radar signal compared to the low backscatter from water. One has therefor to be cautious when detecting intertidal zones in east-west directed fjords. Figure 33 shows an example of such an effect in Geirangerfjord in Møre og Romsdal Fylke.

Fish farms and aquaculture installation

Fish farms and aquaculture offshore installation will also be detected as intertidal zone (Figure 34), as these installations are not completely fixed and the backscatter signature from them can therefore be quite variable at different incidence angles from different satellite paths. Generally, these installations are easily recognizable by their geometric forms though. We assume also that a trained machine learning method could detect such sites as fish farms automatically.

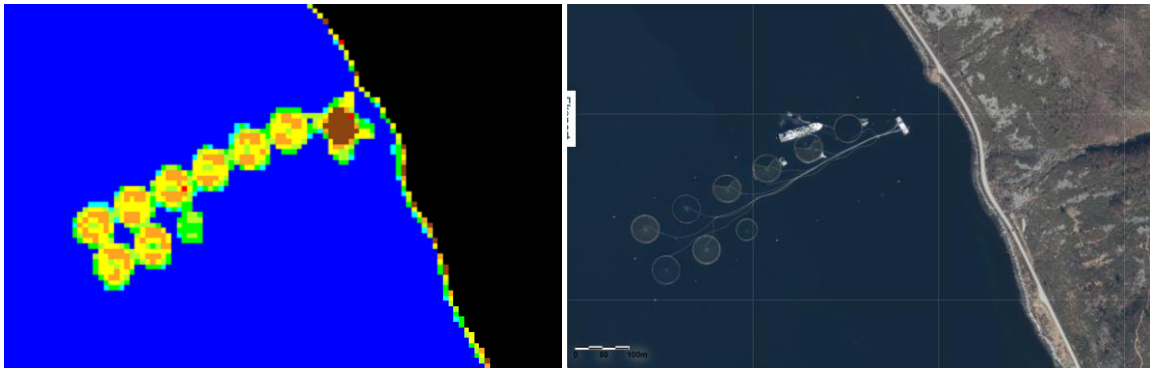

Figure 34. Salmon farm detected as intertidal zone I Vanylsvfjord in Møre og Romsdal Fylke.

Water saturated ground

It does not need a lot of water to reduce the radar signal to a minimum. Mudflats or sandy beach pools that are completely saturated by water and continue to have a smooth surface might therefore not reflect the radar signal enough to be detected as “dry” land inside the intertidal zones. Such areas can also occur as water areas enclosed by an intertidal zone area. It is therefore often a question of definition if such pools are part of the intertidal zone, intertidal pools. In optical images and in-situ observation such water saturated area would be interpreted as intertidal zone from most observers, although they are still covered by water. Figure 35 shows several of such water areas enclosed by an intertidal zone south of Lille Grindøya field site close to Tromsø.

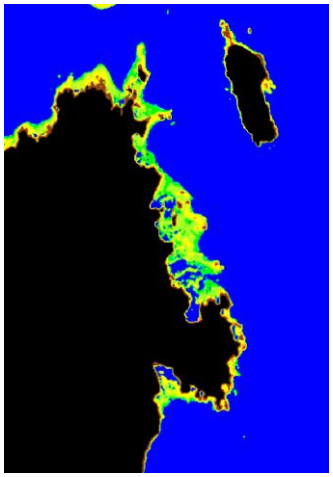

Figure 35. Water area enclosed in intertidal areas can be water saturated mudflats.

5.2 Sentinel-2 results

5.2.1 Nomenclature and datasets from S2 processing

The file names for the ITZ type products based on S2 data are:

SVC_S2_***_2019-2020_10m_UTM33N.tif

, where _***_ is the name of the county.

The products have a spatial resolution of 10 m and are given in the UTM33N coordinate system. Figure 36 gives an overview of the nine products covering Norway, with a detailed example of the tidal zone product. The total size of the nine products is 50.6 MB (Table 6). Figure 37 gives an example of the detail in the ITZ type product and how this can be converted into an ITZ area product (S2) by combining the mud, rock, sand/gravel and seaweed classes. The ITZ area product (S2) is used to produce the combined S1/S2 ITZ area product (see section 5.3).

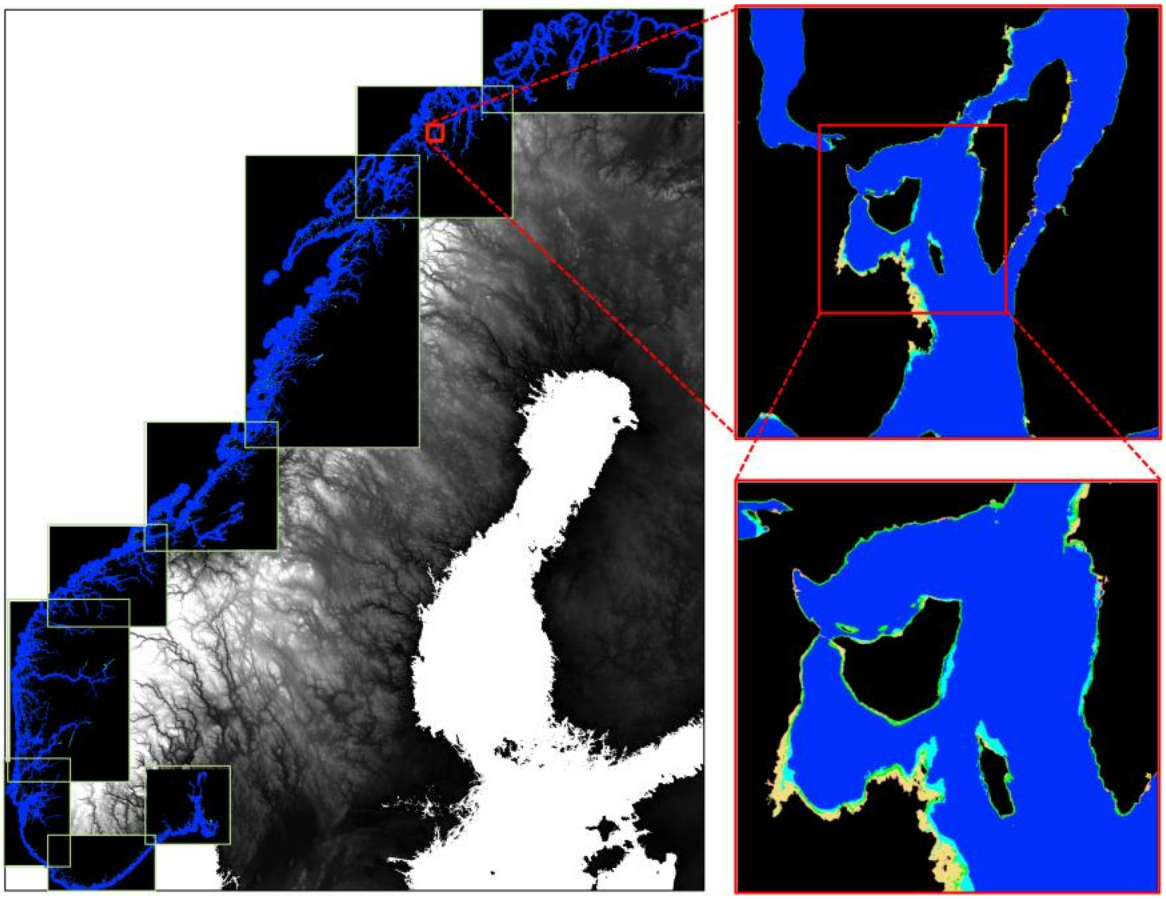

Figure 36. All nine S2 county products for Norway, with an example of a detailed image to the right.

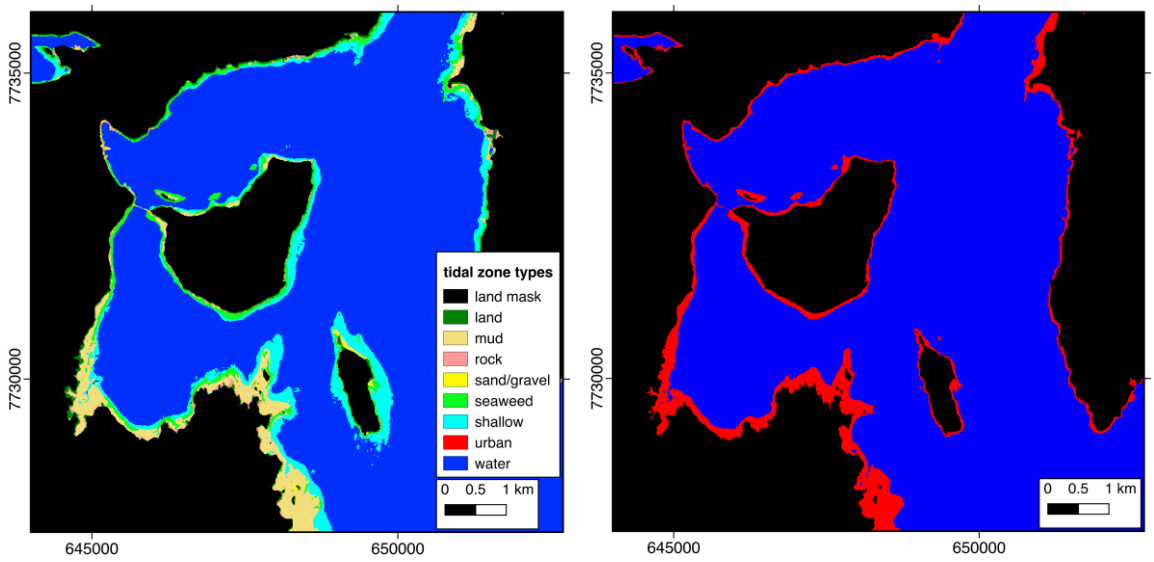

ITZ - Tidal Zone Type

class	colour code	pixel value
land	(0,130,0)	1
mudflat	(243,222,125)	2
rock	(251,154,153)	3
sand/gravel	(251,248,0)	4
seaweed	(7,253,32)	5
shallow	(0,255,243)	6
urban	(255,0,0)	7
water	(1,48,252)	8

ITZ - Area

class	colour code	pixel value
water	(0,0,255)	8
ITZ Area	(255,0,0)	2
land	(0,0,0)	1

Figure 37. Two different S2 products: the ITZ types (left), and the ITZ extent (right).

Table 6. Size in pixels and file sizes of the nine county ITZ type products for Norway. Compressed geotifs.

County	Image size (pixels)	Resolution	File size (MB)
Agder	17900x9100	10m	1.8
Finnmark	37400x16600	10m	6.5
Møre and Romsdal	19700x16800	10m	3.8
Nordland	29000x49000	10m	15.8
Oslo, Viken, Vestfold and Telemark	12500x12500	10m	2.0
Rogaland	10800x17400	10m	2.3
Troms	26000x22000	10m	3.2
Trøndelag	22000x21200	10m	5.8
Vestland	20000x30300	10m	7.0
Total		**10m**	**48.2**

5.2.2 Limitations and errors

Even though the general detection and classification of the tidal zones appears good (see also accuracy assessment in Table 9), the current products do show some errors in some areas. This will most likely improve by extending the training dataset; the current products are based on a training set of only 1092 pixels for all of Norway, with the vast majority of the training data currently collected from Troms and Finnmark. The following figures show the main misclassifications in the current products.

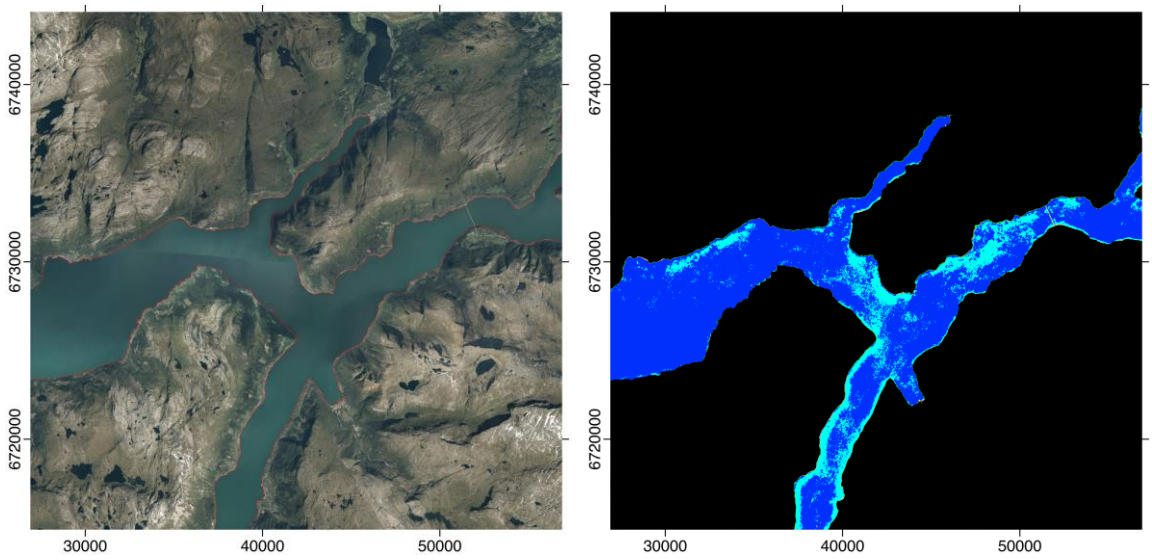

Figure 38. Water misclassified as shallow water in Hardangerfjord. In this case this is mainly the results of the presence of suspended sediments and can be improved with further training data.

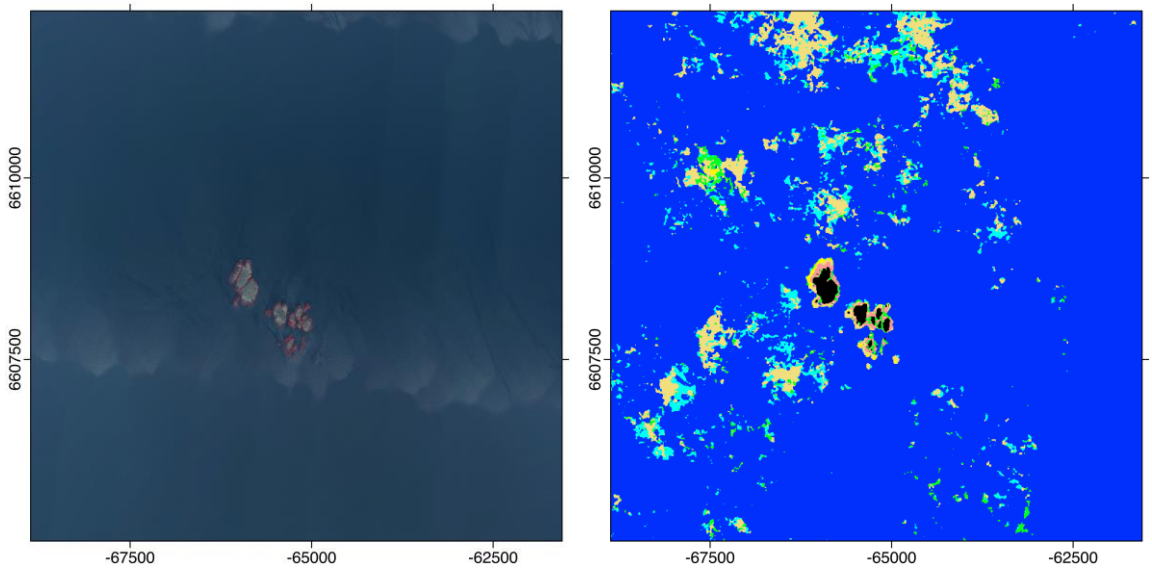

Figure 39. Water randomly misclassified west of Karmøy, Rogaland. This is the result of poor cloud masking and very few cloud free images available during the analysis period. In most of coastal Norway, there are enough images in the time series that any poor cloud masking has little influence on the result.

5.3 Combination of Sentinel-1 and Sentinel-2 for mapping the intertidal zone area.

From both the Sentinel-1 ITZ atmospheric exposure and the Sentinel-2 ITZ type products, the intertidal zone area is extracted independently. Combining these two independent products has two advantages:

1) The intercomparison between these two area products can be seen as an independent validation of both products and the area where they agree can be flagged as "highly accurate" and with high confidence.
2) The area where they disagree can be visually interpreted as areas where they either complement each other or confirm an erroneous detection of the intertidal zone area.

Table 7. Legend of the combined ITZ area product from S1 and S2.

ITZ - S1/S2 combined area product		
Class	**Color Code**	**Pixel Values**
No data	(255,255,255)	255
Land (mask from S1)	(0,0,0)	8
ITZ area (S1 and S2)	(255,0,0)	1
ITZ area (S1 only)	(46,139,87)	2
ITZ area (S2 only)	(255,255,0)	3
Shallow water (S2)	(0,255,255)	4
Water	(0,0,255)	0

Table 7 shows the legend of a combined S1 and S2 ITZ area product.

Four examples from this product are shown from Tromsø Kommune. Figure 40 shows the ITZ area around Lille Grindøya (Tromsø Kommune). Most of this area has stone beaches with a large occurrence of kelp. Clearly the ITZ area here from S1 corresponds well with the ITZ area from S2 (in red). Because of its higher temporal sampling, Sentinel-1 can detect a slightly lower tidal level, i.e. a slightly bigger intertidal zone (area in dark green) that is generally directly connected with the agreed intertidal zone. Small pools inside the intertidal zone and water-saturated mudflats however are ITZ areas that are missed by Sentinel-1 and detected by Sentinel-2 (in yellow). In the case of Troms county, about 60% of the ITZ area detected by only S2 are classified as mudflats by S2. Shallow water areas that surround the ITZ zone are well detected with Sentinel-2.

Figure 41 shows a typical mudflat area in the Målselv delta (Målselv Kommune, Troms). It seems that in the absence of stone and rocks and water saturated mudflats are difficult detectable by S1 but are well detected in with S2.

Figure 42 shows an example of the detection of fish farms in the product detected only by S1. Comparison with aerial photos shows that those fish farms can even be difficult to see in very-high-resolution photos.

Figure 43 shows an example of a false detection of ITZ area of both S1 and S2 in Kjosen south of Lyngen peninsula (Troms). S1 is due to the radar echo from the steep south-north ward mountain slope perpendicular to the east-west radar range. S2's false detection seems to be due to suspended sediments from a close-by sand-production facility and glacier river outflows.

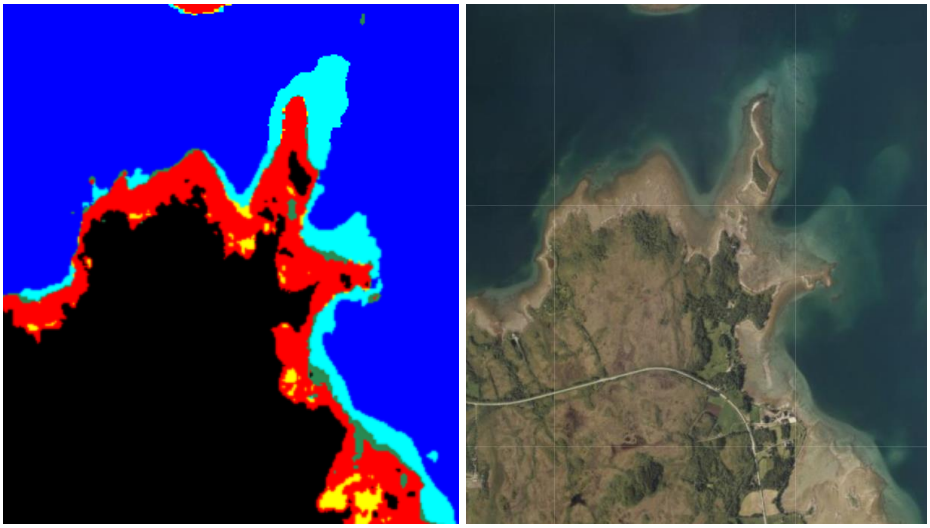

Figure 40. The S1/S2 combined ITZ area product around Lille Grindøya (Tromsø Kommune). The combined S1/S2 ITZ area product (left) and screenshot from norgeibilder.no (right).

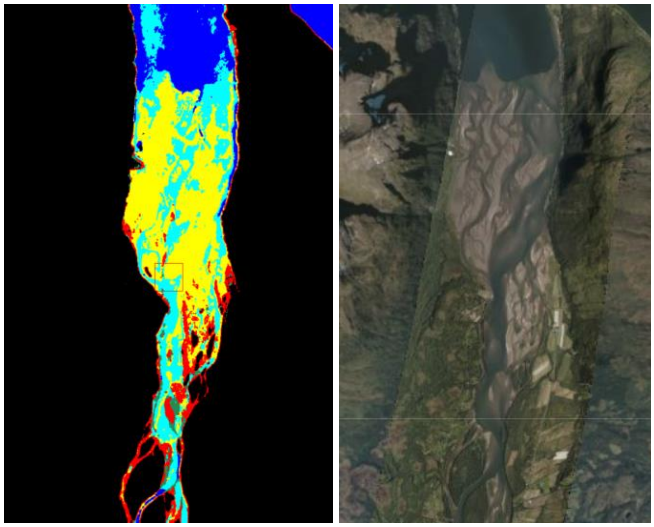

Figure 41. A typical ITZ mudflats area at the Målselv river delta (Målselv Kommune, Troms). The combined S1/S2 ITZ area product (left) and screenshot from norgeibilder.no (right).

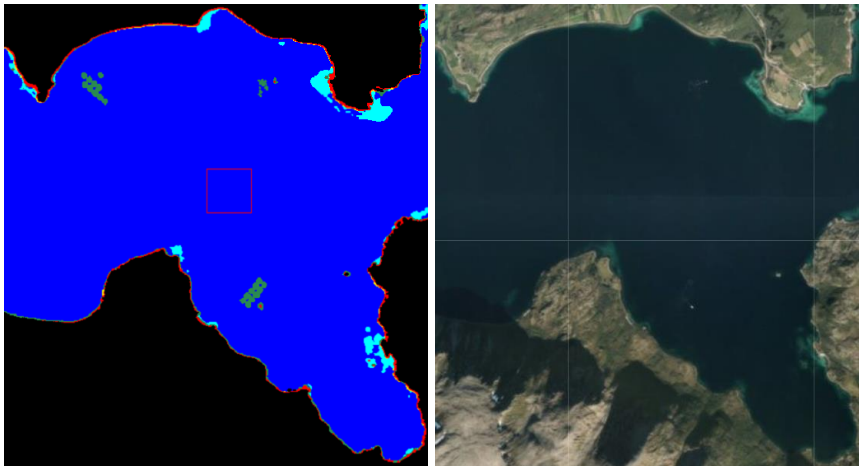

Figure 42. Detection of fish farms (in dark green, left) in the combined S1/S2 ITZ area product.

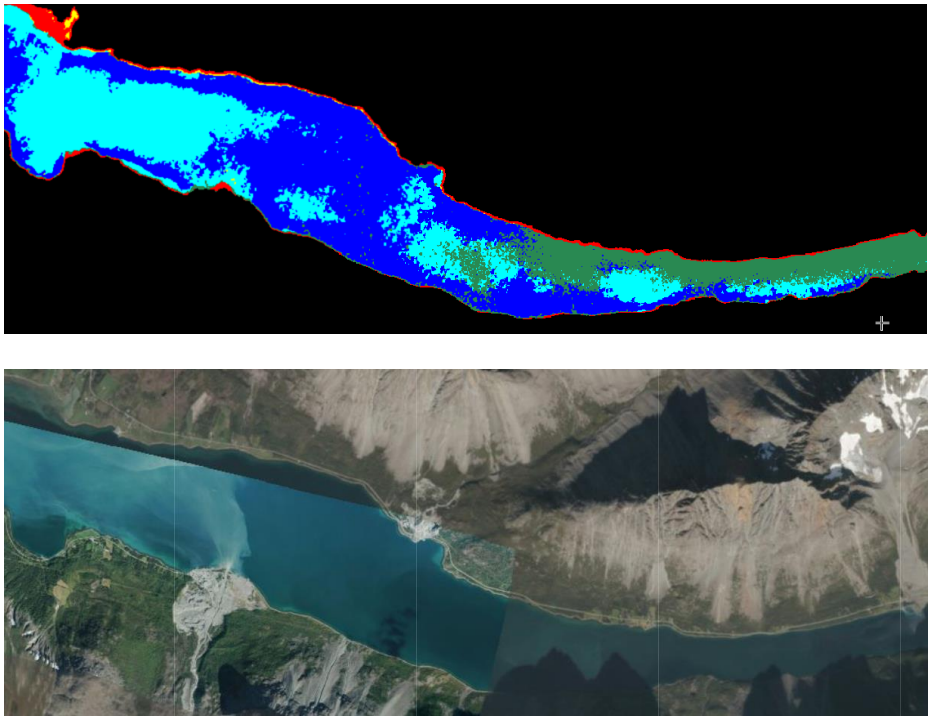

Figure 43. Example of false detection by both S1 (dark green) and S2 (cyan). The combined S1/S2 ITZ area product (top) and screenshot from norgeibilder.no (bottom).

The following figures, Figure 44 and Figure 45, show some examples of the different products from 2 areas around the island Vega in Nordland. The figures show the atmospheric exposure product

(sub figure b.), the type product (sub figure c.) and the combined S1/S2 area products (sub figure d.) and give the aerial photograph (sub figure a.) for visual comparison.

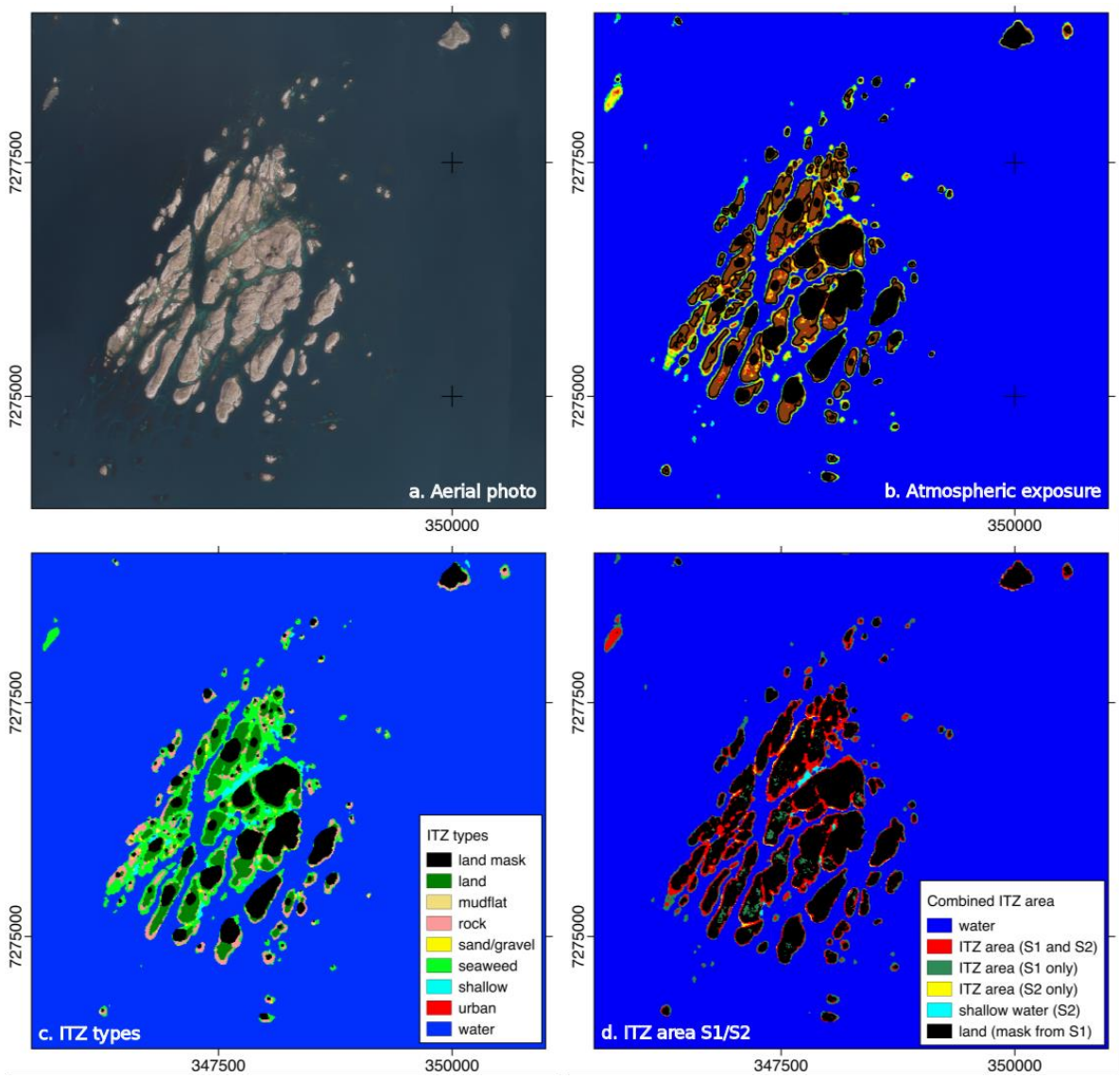

Figure 44. Example of the different products from Muddværet, south of the island Vega, Nordland. a. Aerial photo of the area; b. Atmospheric exposure product (section 5.1.1; see Figure 29 for colour code of the different exposure levels); c. Intertidal zone types product (section 5.2.1); and d. Combined S1/S2 intertidal zone area product (section 5.3).

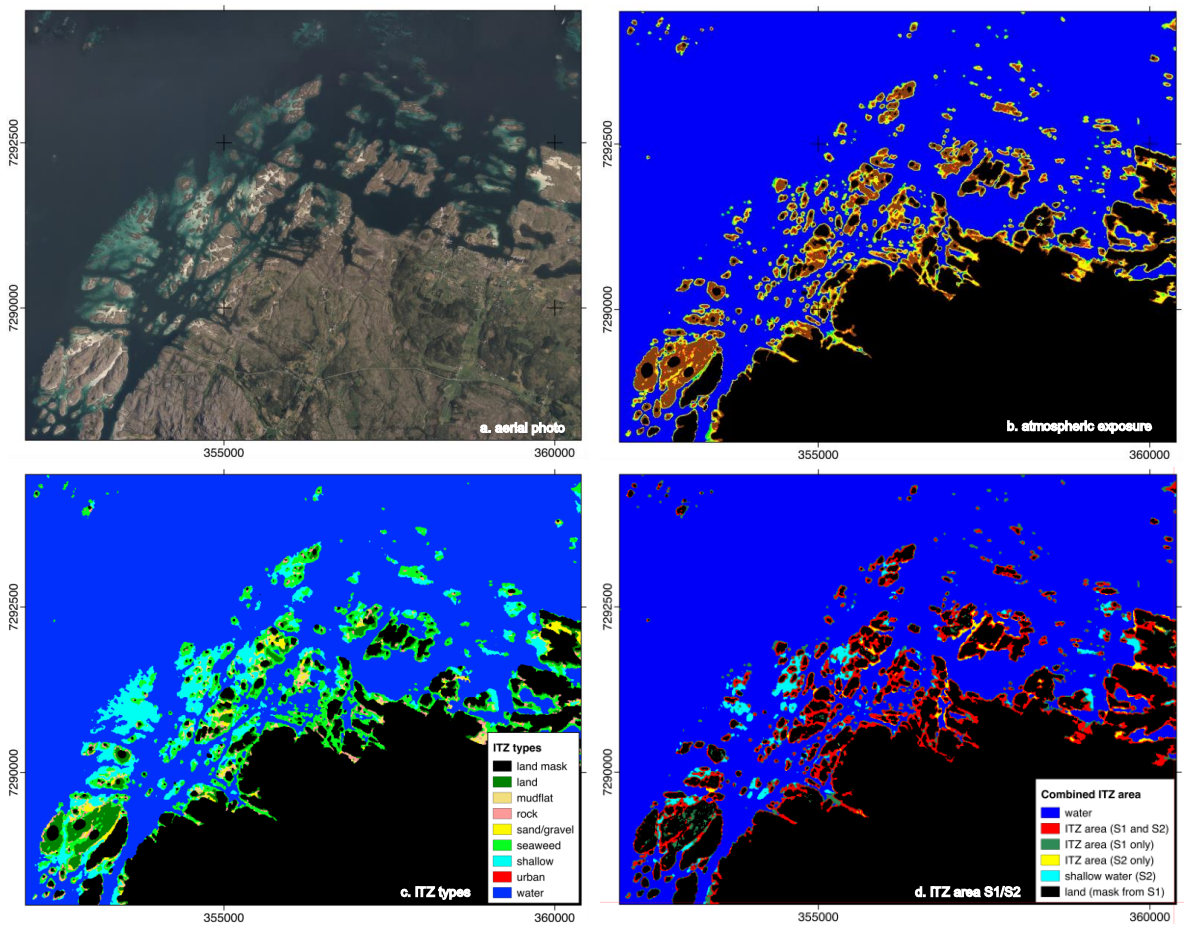

Figure 45. Example of the different products from the north-eastern part of the island Vega, Nordland. a. Aerial photo of the area; b. Atmospheric exposure product (section 5.1.1; see Figure 29 for colour code of the different exposure levels); c. Intertidal zone types product (section 5.2.1); and d. Combined S1/S2 intertidal zone area product (section 5.3).

6. Validation

To validate the products, several field visits have been undertaken in Tromsø Kommune. The collection of field data consisted mainly in collecting GPS tracks along the water line at different tidal levels using a mobile phone and ground photos of the type of intertidal zone for identification. The accuracy of the GPS when moving should be in the range of about 2 m.

6.1 Waterline observation accuracies

The water line can vary from being a well-defined line with centimeter accuracy at straight coastlines with a clear slope under calm conditions (Figure 46a) without water vegetation to a very diffuse area (Figure 46 b&c)with a gradient of areas above and below water at coastline with very flat areas with little slope, floating vegetation, small topographic changes, e.g. sand waves or from benthic activities, and waves. The diffuse water line areas are observed especially at tides below midwater. The position of the water line under diffuse areas is therefore highly dependent on the observer. Naturally though, areas where even just small sand patches are above water and where an observer can easily walk along with plastic boot are mostly interpreted as part of the intertidal zone even though if most of the area is below water on a cm scale. Considering a clear definition of intertidal zone being above water would therefore actually exclude these regions and lead to an over estimation of the intertidal zone or at least at this specific tidal level.

Another issue is that different tidal level water lines are often closer to each other than the pixel resolution of 10m of S1. The highest waterline or atmospheric exposure class should therefore dominate this pixel value.

a 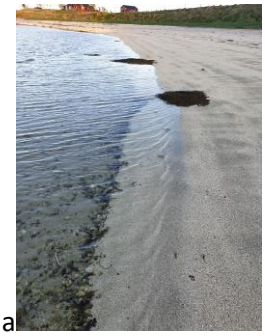 b  c 

Figure 46. Ground photos of the water line at (a) MSL, and (b&c) low tide (in Avløsbukta at Hillsøy, Tromsø Kommune, Troms.

6.2 Observation time accuracies

GPS track collection of hundreds of meters in slippery terrain takes of the order of 10-30min. The timing when collecting the GPS track has been decided according to the predicted time of the tidal levels (MLWS, MLW, MLWN, MSL, MHWN, MHW, MHWS). However, during some of these times, especially in flat areas (i.e., mudflats) the water line can move by some cm/s, which over a 10-30min period corresponds to an inaccuracy of several meters, which makes the data collection as well as the data filtering a challenging operation as timing of specific levels depend also on model

prediction of the tidal level. As there are no direct tidal gauge measurements at the field data collection sites, it is nearly impossible to obtain submeter accuracies in flat areas.

6.3 Field validation

Figure 47 - Figure 49 show different tidal level water lines from the three major field sites superimposed on the ITZ AtmExp product. The figures clearly show that even relatively small-scale patterns have been detected (see for example the 50-75% percentile class in Figure 47). High water lines (MHWN, MHW, and MHWS) often lie so close together that they are not resolved by the 10m S1 resolution. The MSL (Mean Sea Level) line is quite well represented in all cases by the 50% border between the 25-50% and 50-75% classes.

The intertidal zones at Langnes and Lille Grindøy are characterized by a clearer water line at low tides due to higher presence of SAR backscatter reflectors like stones, rocks and vegetation and a more defined slope than the mudflat in Avløsbukta at Hillesøy.

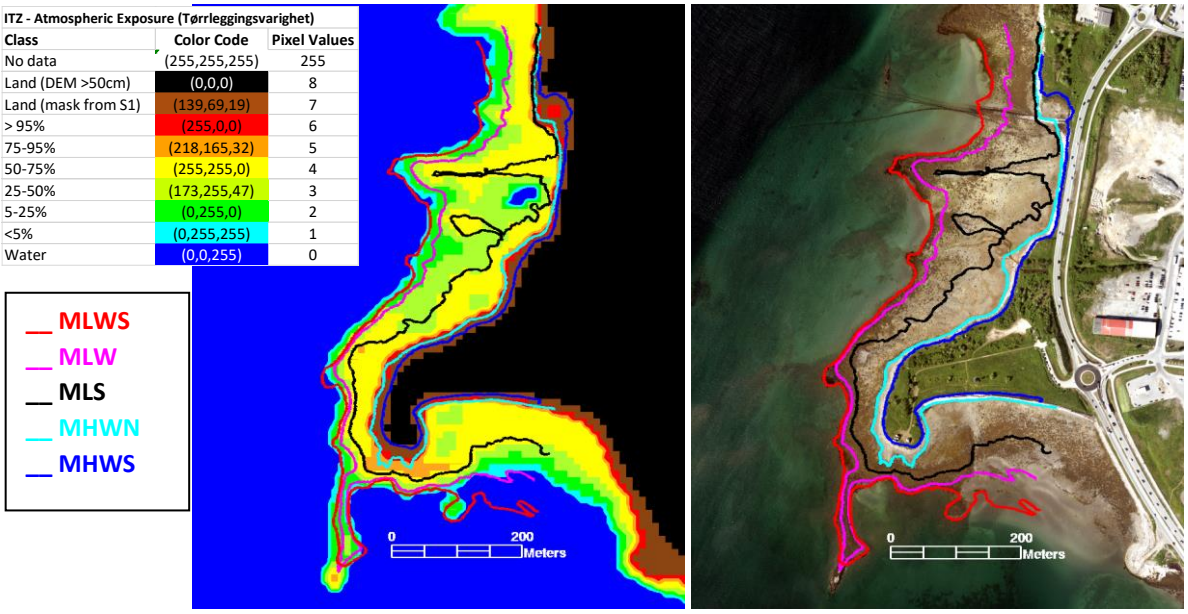

Figure 47. Different tidal water level lines superimposed on the ITZ-atmospheric exposure product at Langnes, Tromsø, Troms. The ITZ product is bilinear subsampled at 1m pixel size.

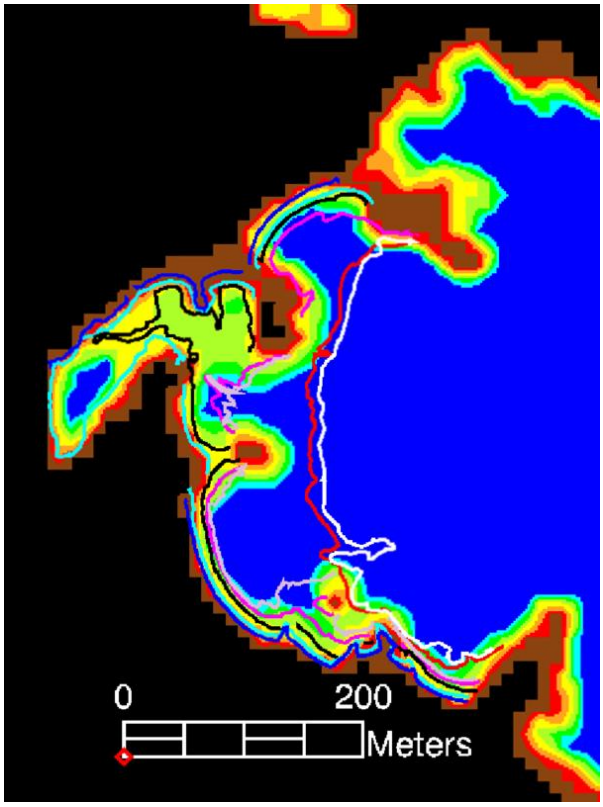

MinLWS
MLWS
MLW
MLWN
MLS
MHWN
MHWS

ITZ - Atmospheric Exposure (Tørrleggingsvarighet)		
Class	Color Code	Pixel Values
No data	(255,255,255)	255
Land (DEM >50cm)	(0,0,0)	8
Land (mask from S1)	(139,69,19)	7
> 95%	(255,0,0)	6
75-95%	(218,165,32)	5
50-75%	(255,255,0)	4
25-50%	(173,255,47)	3
5-25%	(0,255,0)	2
<5%	(0,255,255)	1
Water	(0,0,255)	0

Figure 48. Different tidal water level lines superimposed on the ITZ-atmospheric exposure product in Avløsbukta at Hillesøy, Troms. The ITZ product is bilinear subsampled at 2m pixel size.

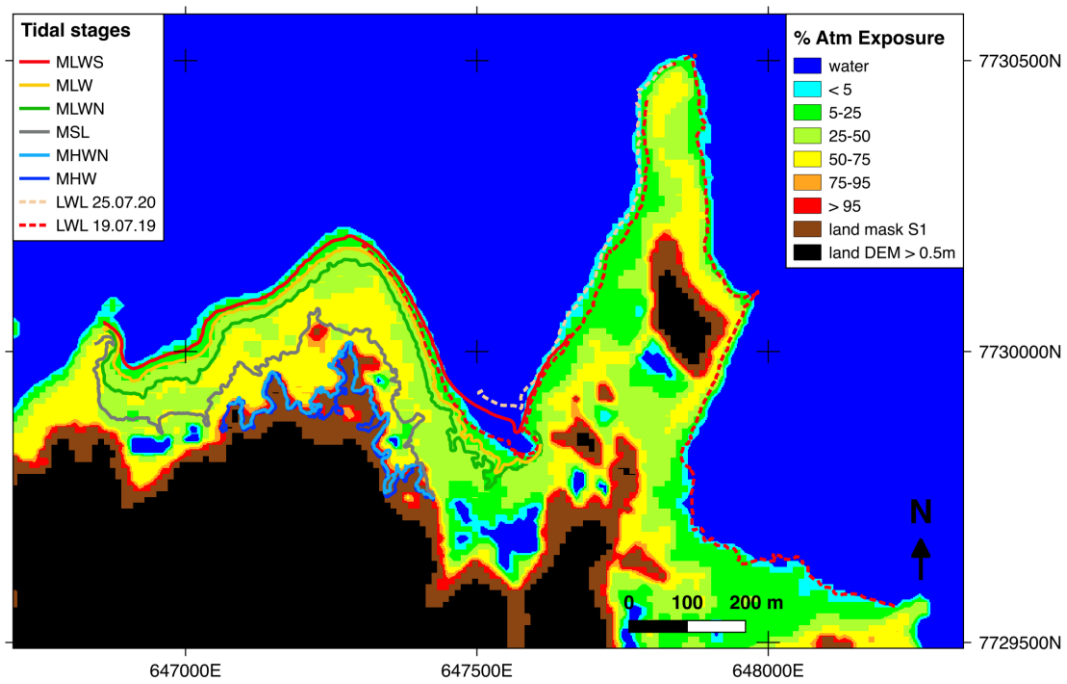

Figure 49. Different tidal water level lines superimposed on the ITZ-atmospheric exposure product in Lille Grindøya, Troms. The ITZ product is bilinear subsampled at 2m pixel size.

6.4 Validation against bløttbunn database

The 'bløttbunn' (mudflat) data available in Naturbase is based on manual on screen digitisation of identified mudflats. The dataset includes many of the mudflat areas in Norway but is not complete. The areas digitised as mudflats also include shallow water areas in some places as it can be difficult to identify the boundary between mudflat and shallow water in optical data. The data products produced in this project were visually compared with the mudflat dataset in known locations and Figure 50 and Figure 51show some examples where the products are compared. Figure 50 shows the area around Tromsø where the mudflat data includes the mudflats around lille Grindøya and Langnes but is missing the mudflats around Finnvika in the northern part of the image indicated by the larger green circle. The smaller green circle tidal zones along the southern coast of Håkøya that have been identified in the ITZ products, but these are more partially seaweed covered gravel rather than mudflats and are therefore not part of the mudflat database but are intertidal zones.

Figure 51 shows more detail in the different products using the Grindøya nature reserve as an example, as this area was used to collect field data on the water lines at different tidal stages. Here the mapped low water line (MLWS) shows that the mudflat data includes areas that remain submerged. These shallow water areas are distinguished in the ITZ type product and the combined S1/S2 product. In general, where mudflat data is available, the ITZ products agree well with the mudflat data, and are more accurate. As the mudflat data base is not complete and includes mudflats below the water surface, it is not directly comparable to the mudflat areas detected with S2.

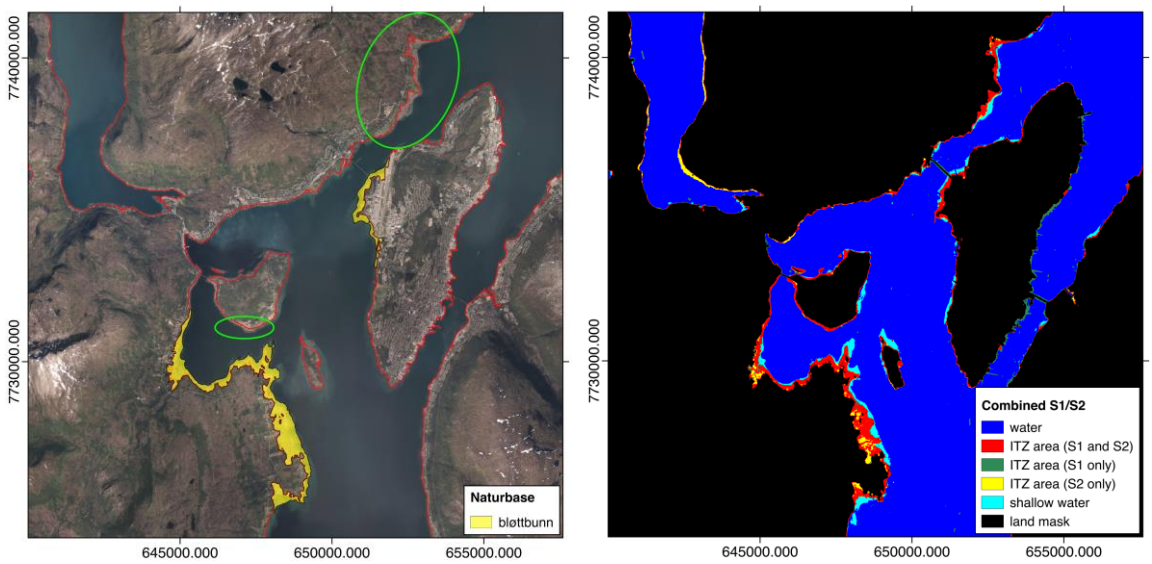

Figure 50. Comparison between the mapped mudflats in the mudflat database (Naturbase) (left) and the ITZ area mapped by S1/S2 (right).

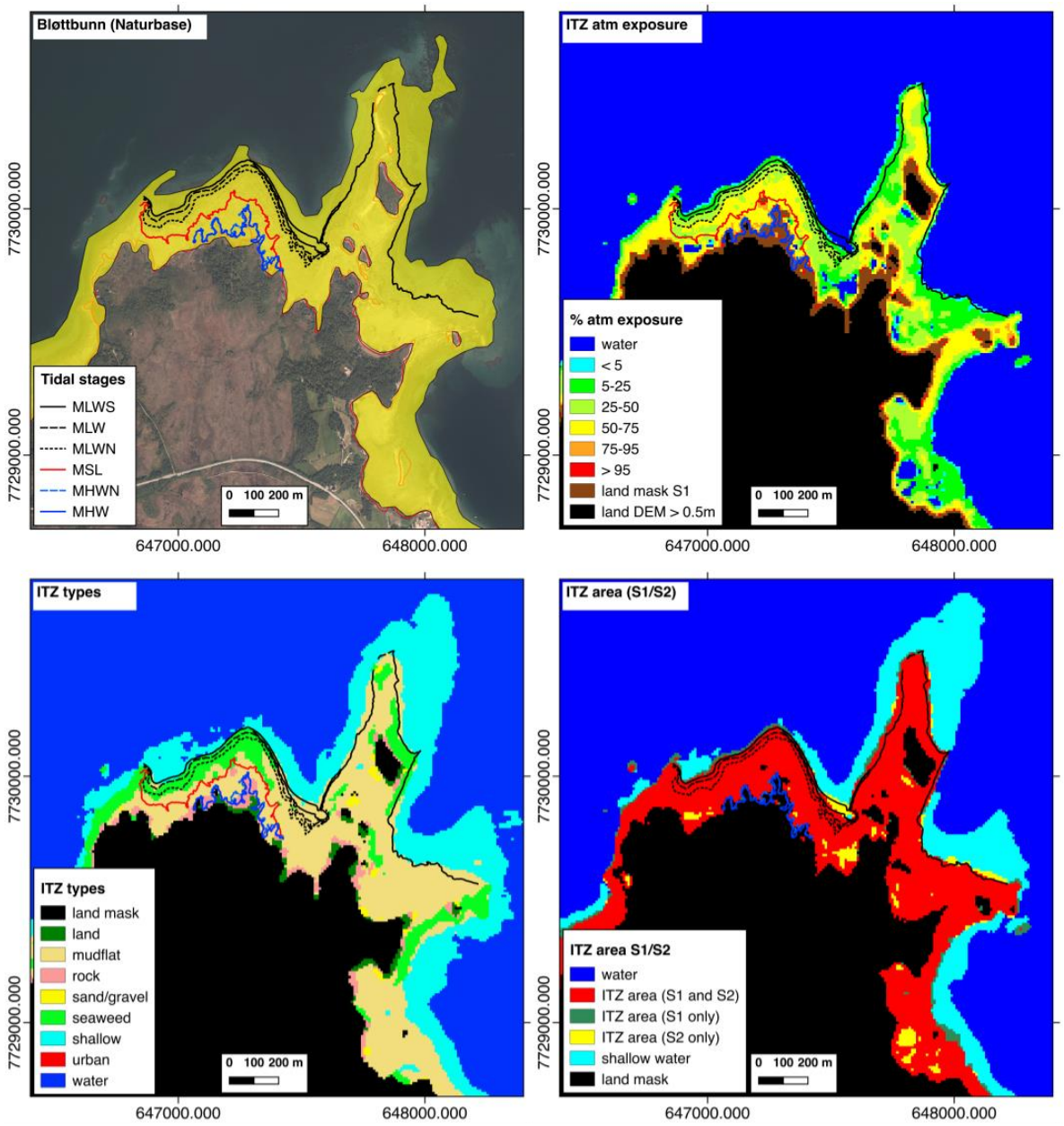

Figure 51. Detailed comparison between the bløtbunn data from Naturbase (top left) and the different products from this project: ITZ atmospheric exposure (top right), ITZ types (bottom right), and combined S1/S2 ITZ area (bottom right).

6.5 Accuracy Assessment

6.5.1 Atmospheric exposure products

The GPS tracks along the tidal level water lines have been transformed into a pixel validation set. As the distance between tidal level lines is often closer than the pixel size of 10m, we associated the pixel value with the highest water line present in this pixel, as the methods will also associate the highest atmospheric exposure percentile class.

Note that the classes do not correspond directly to each other. The different tidal level lines correspond mainly to the border between AtmExp classes. Only MLW and MHW correspond to the specific 5-25% and 75-95% classes, respectively.

Table 8 shows the confusion matrix using all collected water line GPS tracks from the 5 field sites. The table cells in grey in Table 8 are the results that we consider a correct classification of the tidal level lines. This corresponds to an overall accuracy of 49%. If we consider only 3 classes: low-tide area, mid-tide area and high-tide area, i.e. we consider the data inside the red rectangles correct classified into these classes, we obtain an overall accuracy of 74%.

Concerning the ITZ area accuracy, the method detects all intertidal areas above the MSL with a 99%-100% accuracy. With decreasing tidal level, MLWN, MLW, MLWS and observed lowest water line (MinLWS), the accuracy decreases from 93%, 84%, 64% to 47%, respectively.

If we disregard the lowest waterlines that we observed during fieldwork, which we know where well below MLWS, the overall accuracy of the detected ITZ area above MLWS is the average of the individual ITZ area accuracies, i.e. 91%.

		Ground	Truth	(Pixels)							
	Class	MinLWS	MLWS	MLW	MLWN	MSL	MHWN	MHW	MHWS	Total	User Acc.
	Water	120	378	82	25	5	3	0	0	613	
	<5%	11	105	26	1	1	1	1	0	146	79%
	5-25%	62	395	117	25	16	3	2	2	622	86%
	25-50%	27	122	196	186	99	1	6	5	642	44%
	50-75%	6	51	83	88	406	52	45	27	758	60%
	75-95%	0	9	13	4	36	49	27	32	170	64%
	95-99%	0	0	0	1	3	15	17	5	41	54%
	S1 Land	0	1	7	7	17	108	211	99	450	22%
	DEM>50cm	0	0	3	3	4	14	43	150	217	69%
	Total	226	1061	524	337	583	232	309	170	3442	
	Prod. Acc.	32%	47%	22%	63%	87%	44%	9%	80%		
	ITZ area acc.	47%	64%	84%	93%	99%	99%	100%	100%		

Table 8. Validation confusion matrix of the ITZ AtmExp. product versus GPS track along at different tidal levels. Note that the classes do not correspond to each other as the tidal level line correspond mainly to the border between classes.

6.5.2 Tidal zone type product

The accuracy assessment of the tidal zone type product was carried out as described in 3.2.3 by randomly splitting the database with interpreted points (750 sample points with a total of 1376 pixels; see section 3.2.3) in a 80% training set and 20% validation set. This resulted in a total of 290 pixels in the validation set. The confusion matrix is shown in Table 9. Due to the limited number of pixels, some of the classes, such as rock and urban, are not well represented, and the results for these classes have little meaning. More points would be needed to get better statistics. The land and urban classes are mostly masked out, but from a visual comparison it is clear that the remaining urban areas are often misclassified as rock. The results do indicate that the mudflat, seaweed, sand/gravel, shallow water and water classes are generally correctly classified with accuracies between 73% and 92%. The mudflat class is, however, quite varied and it can be difficult to identify the difference (and gradual transition) between mud, gravel, and sand in aerial photos. Similarly, there is a gradual transition in the amount of seaweed present on mudflats. The overall accuracy is 86%.

	class	ground truth (pixels)									
		land	mudflat	rock	sand/gravel	seaweed	shallow	urban	water	total	user acc.
	land	3	0	0	0	0	0	0	0	3	100%
	mudflat	0	55	0	0	5	4	0	1	65	85%
	rock	0	2	2	0	0	0	0	0	4	50%
	sand/gravel	2	5	2	24	0	0	0	0	33	73%
	seaweed	0	3	0	0	33	0	0	0	36	92%
	shallow	0	3	0	0	0	35	0	5	43	81%
	urban	0	0	0	0	0	0	0	0	0	NA
	water	0	0	0	2	0	7	0	97	106	92%
	total	5	68	4	26	38	46	0	103	290	
	prod. acc.	60%	81%	50%	92%	87%	76%	NA	94%		

Table 9. Confusion matrix for the tidal zone type product.

7. Outlook and future studies

This study has led to a first version of national intertidal zone products; the Intertidal zone area, type and atmospheric exposure. Clearly, the products reveal some distinct error sources and inaccuracies, some of which have already been specified and presented in sections 5.1.2 and 5.2.2. At the same time, some of the false detection has also revealed the potential of new products that can be further developed. In this outlook for follow up projects, we present therefore first further studies needed to improve the current products and to map also changes in the intertidal zone and secondly, we present some potential other products that could be of interest for environmental monitoring.

7.1 Improving the methods

7.1.1 Reduce errors and false detections of the intertidal zone.

Sections 5.1.2. and 5.2.2 revealed a first list of error source in the intertidal zone mapping. There is a need to study those errors sources in detail and develop methods to reduce them. This can be either done through the combination of different satellite data, starting with Sentinel-1 and Sentinel-2, but maybe also including other data, as well as through studying the satellite signatures. Using even longer time periods to be analyzed might also help to resolve some of the issues. Effective filtering of such errors however needs to be studied in detail.

Harbor occupancy and boat traffic should be reducible to a high extent by filtering out occurrences that are not attached to land and by using data bases of harbor locations from mapping, fishery or shipping authorities.

Noise from strong ocean winds generally shows up as very low atmospheric exposure area far away from land and could probably be filtered out to a large extent and have been already.

Fish farms seem to have a characteristic signature and pattern and seems to be only seen in Sentinel-1 data. Artificial intelligence and machine learning methods or pattern recognition methods could help to filter out their false detection as intertidal zone.

Radar echoes from steep north-south slopes in fjords occur only in Sentinel-1 data and could filtered out with Sentinel-2. The false detection due to suspended sediments by Sentinel-2 however could undermine the filtering in some cases. It could also be possible to simulate such areas by using the Norwegian DEM.

Misclassification of water as shallow water in the ITZ type products occurs locally in fjords and is likely caused by the presence of suspended sediments. This has already been much improved by increasing the training dataset, and it is expected that this can be further improved by adding further training data throughout Norway as the current training dataset is still mainly based on data from Troms - Finnmark. In addition, other methods, including filtering or thresholding, can be further investigated.

In some areas, particularly in coastal areas of Agder and Vestlandet, only few (<10) cloud free Sentinel-2 images were available for the analysis. With so few data, any issues with cloud masking

become important and can influence the analysis. Section 5.2.2 shows an example of misclassification due to poor cloud masking and limited data. Improved cloud masking methods may reduce this error, or filtering/thresholding based on additional indices or other data.

Water pools in the intertidal zone as well as water saturated mudflats are missed by Sentinel-1 and seem to be detected with Sentinel-2. However, in the combined ITZ area S1/S2 product, this adds further information on ITZ types, which can be of interest. It might need further investigation, however, to define better the low water, especially in cloud dominant regions.

Last but not least, a manual quality check and clean-up of the county products should be done in addition to ensure the high quality and reliability of a national product.

7.1.2 Operational monitoring on a yearly basis

The products presented here have been based on satellite data from two summers to avoid a potential issue of fjord and coastal sea ice that would be another source of false detection and still have the necessary sampling density of all tidal levels for the atmospheric exposure product. If yearly change mapping of the intertidal zone is a future requirement, the time period could be reduced to one year by applying a sea ice mask for Norway to avoid false detections. Such a national sea ice mask is currently not available though. Another option could be to reduce the integration time to one summer, which would probably lead to higher inaccuracies in general.

7.1.3 Mapping changes in the intertidal zone

Natural changes of the intertidal zone occur generally on a longer time scale than anthropogenic changes as constructions, which could also subsequently lead to natural changes in the intertidal zone due to, for example, a change of coastal currents. Construction induces in many cases double-bounce scatterers, i.e. corner reflection, and as fixed construction in the intertidal zone should be detectable at least on a yearly bases. A system to update the reference on a yearly basis would require a fully operational and automatic processing system to be put in place. Most tools in the Sentinel-1 processing line are generic and can be operationalized but need to be further automized.

7.1.4 Mapping other intertidal zone types

The current division in intertidal zone types in permanent water, shallow water, mud, rock, sand/gravel, seaweed, and land, is based on what can be relatively easily distinguished from aerial photos. However, it may be possible to identify other types of interest of good ground truth data exists or can be collected.

7.1.5 Operationally combine S1 and S2

Due to budget limitations, we have focused on the use of single sensors for the atmospheric and type product. Both sensors and their products, however, can be reclassified into simple intertidal zone area products; these have then been manually combined into a multi-sensor (S1/S2) area product flagging high confidence where the single sensor area products agree, and lower confidence where they do not. Nevertheless, it is clear that the area where they disagree actually complements the real intertidal zone area. It would therefore need a further study to investigate if it is possible to separate the disagreement in complementarity and error filtering with the aim to improve the combined area products. Furthermore, the combination of S1 and S2 could also be used to improve the atmospheric exposure and type products.

7.1.6 Improving by refining the current methods on a regional scale.

The methods have been developed originally on the study site Trondheimsfjorden (Haarpaintner and Davids, 2020) and further trained and verified with field observations around Tromsø Kommune. As the Norwegian coast is quite variable considering climate, geography and demography, and sun angle, as well as considering the tidal range and satellite data coverage, different regional trainings sets and regional refinement of the method parameterization would probably further improve the results on a local and regional scale.

7.1.7 Improving the accuracy assessment.

The results have mainly been validated with field data collected in Tromsø Kommune. To get a better idea of the accuracy on a regional scale, specific validation studies based on the collection of field data, should be done at several locations along the Norwegian coast. We suggest focusing on mid and northern Norway (Trøndelag to Finnmark), as the tidal range is more significant than in southern Norway. We consider a 1 to 2 week fieldwork necessary per county. An important issue is the water line at different tidal levels which can only be detected reliably in the field. Intertidal zone type can be partly collected with aerial photography from norgeibilder.no, but for example sand and mudflats will still be difficult to distinguish. Manual clean-up prior to an accuracy assessment should also be done.

7.2 New opportunities

A part of showing several sources of errors, this study also shows several potential bi-product and additional information that could be extracted from the analysis and be useful as other products to different authorities apart from the ITZ mapping.

7.2.1 Kelp forest

Kelp forests occur along the Norwegian coast and are an important but threatened ecosystem. Kelp forests, floating and submerged in shallow water, are visible in optical satellite data and several authors have shown that it is possible to map kelp forests: e.g. a Kelp Difference index was developed by Mora-Soto et al. (2020) to map Giant Kelp on a global scale using S2 imagery, while Volent et al. (2007) mapped kelp forest along the coast of Svalbard using airborne hyperspectral data. Kelp floating at the surface at low tides seems to be also visible in SAR data. This could be investigated in more detail in order to try to map kelp forest. There is already an ongoing project about mapping marine vegetation under the Norwegian Environment Agency (Høegh Bojesen, 2020) and it should be investigated how that study can be complemented by this study of the intertidal zone.

7.2.2 Suspended sediments

Suspended sediments are clearly visible in optical satellite images and cause occasional misclassification of water as shallow water in some of the products produced in this project. Optical satellite imagery has long been used to estimate and monitor suspended sediment concentrations and a range of methods have been developed (e.g. Normandin et al., 2019). ESA provides a Total Suspended Matter Concentration as a variable in ocean products from Sentinel-3, at 300 m resolution.

7.2.3 Fish farm detection

Off-shore fish farm installation are clearly detected as false detection in the intertidal zone atmospheric exposure products by S1. The patterns of fish farms are quite typical and easily distinguishable by visual interpretation. In the combined S1-S2 ITZ area products, they seem to be detected by S1 only. Using machine learning techniques, it should be possible to detect these directly as fish farms in order to operationally monitor them also on a yearly basis.

7.2.4 Boat traffic estimation

The ITZ atmospheric exposure product in harbors and close to dense population centers is dominated by boat occupancy especially around the big towns in southern Norway. It could also be investigated if such traffic and harbor occupancy statistics could be reliably extracted from such data and be useful for harbor, marine or other authorities.

8. Conclusion

This study shows that both Sentinel-1 and Sentinel-2 are in general well suited to map the intertidal zone on a national level when using very long time series to capture all states of the intertidal zone and different tidal levels. Sentinel-1 has the advantage that every acquisition is usable as it is not dependent on clear sky conditions, and the potential of acquiring close to the highest and lowest spring tides is therefore given. Frequent cloud cover and dark winters in Norway limit the number of available cloud free data from Sentinel-2; on the other hand, Sentinel-2 acquires spectral information also from several meters below the water surface and it is therefore possible to image the intertidal zone with fewer data.

Considering the budget limitation, we used Sentinel-1 to map the atmospheric exposure and the area of the intertidal zone, ITZ_AtmExp and ITZ_Area, respectively. We focus on Sentinel-2 to map the type of intertidal zone, i.e. ITZ_Type. Both S1 and S2 datasets were used to produce (in)directly ITZ area products, that have subsequently been combined in order to flag areas of agreement with a high confidence and areas where the 2 methods did not agree with a lower confidence. This combined S1/S2 ITZ area product clearly shows where the intertidal zone is mapped with confidence, but also shows complementary information such as the presence of intertidal pools.

The validation and accuracy assessments show that we have above 99% accuracy in detecting ITZ area above MSL (Mean Sea Level) and we detect intertidal areas and classify atmospheric exposure with S1 down to the MLW and MLWS water line with an accuracy of 84% and 64%, respectively. The MSL seems to be well detected in all field validations. Also the validation and accuracy assessment of the S2 ITZ type product shows good result with over 85% overall accuracy. Some of the misclassification is due to the gradual transition between mud and seaweed, or mud and rock/gravel/sand, which can be interpreted in different ways. Visual inspection of the products against aerial photos suggests that the accuracy assessments give a good indication of the accuracy of the products across Norway, but the actual accuracy numbers themselves need to be treated with some caution as the assessments are based on relatively few field data and on aerial photo interpretation, mainly in Troms County.

Field observations and their descriptions show in general the difficulty to identify the precise location of the water line at low tide levels, especially in very flat areas and smooth surfaces like mudflats, other water-saturated substrates and intertidal ponds, especially in the S1 results. Intertidal zone areas with rocks, stones and vegetation are generally well detected.

However, there are still errors in the products in some areas, most of which are visually easy to identify in the combined S1/S2 ITZ area product. This could be solved by manual post-processing, but may also be resolved in a more automatic way by further developing the methods.

We realized that in areas with steep topography, there are some unexpected challenges with Sentinel-1. SAR shadow and overlay areas towards and behind slopes can be masked as areas where we do not have a reliable SAR signal and are therefore not able to detect the intertidal zone. In addition, however, strong slopes parallel to the radar range direction reflect side lobes of the radar signal that will be visible in low backscatter areas, especially on water in fjords that are in the east-west direction. Such radar side lobes echoes will therefore show as intertidal zone in S1

high-percentile images, that are used to detect low tide area. It needs to be further investigated how this effect can be foreseen and hopefully be avoided.

Other limitations to detect the intertidal zone in Sentinel-1 time series are areas with considerable shipping traffic that strongly reflect the radar signal. This is especially the case in harbor areas and recreational areas where boats commonly anchor at fixed locations in southern Norway, where the tidal range is also quite small. The possible effect of sea ice in the detection of the intertidal zone has been foreseen and therefore only S1 and S2 data from ice free months have been used. Aquaculture installations are also detected as intertidal zone areas by S1 but are readily distinguished by their geometry. In certain areas, particularly in southwestern Norway, frequent cloud cover resulted in very few available images, and in this case poor cloud masking in one of the images can influence the overall statistics and cause misclassification.

The combination with Sentinel-2 however showed that S1 has difficulties to map water saturated mudflats. Sentinel-2 seems to detect those mudflats quit well.

The Copernicus Land Monitoring Service (CLMS) in cooperation with the Copernicus Marine Environment Monitoring Service (CMEMS) is working on a comprehensive coastal zone monitoring solution that can address the complex and dynamic situations found in coastal environments. “Intertidal flats” (7.2.3.) is a subcategory under “coastal water (7.2)” under “wetlands” defined as “Generally un-vegetated expanses of mud, sand or rock lying between high and low water marks; area between tide marks, basically composed by mud, rocks or boulders.” (Copernicus). The first delivery of these Coastal Zones products has just been released at the end of 2020 for the European countries, including Norway. The methods seem to have been based entirely on optical data using semi-automatic landcover/land (LC/LU) classification of VHR satellite data and computer assisted visual refinement, visual interpretation of LC/LU classes following the specific hot spot nomenclature. The product also concentrates on the entire coastal zone and the intertidal area is only mentioned as coastal wetland and subclassified as salt marshes, saline and intertidal flats. In view of the crude definition above, and methods based on few observations, we do not expect that such products will contribute to the methods presented here. We suppose that the methods from CLMS will not provide insight of the atmospheric exposure and different tidal levels as our method based on S1. However, we expect our methods to work also in central Europe, probably with longer integration periods because of lower satellite coverage and could therefore contribute also to the Copernicus efforts in the future to further define their intertidal zone. As satellite coverage increases with higher latitudes, the methods should work even better in the high Arctic like Svalbard. The longer presence of fjord ice, the polar night and the low sun angle need to be taken into consideration when adapting the methods to Svalbard.

In summary, even though we have met several challenges, this first version of three national ITZ maps at 10m resolution representing ITZ area, atmospheric exposure and type that have been produced in this project clearly represent the best and most consistent ITZ data set currently available for Norway. A quantitative validation has been limited to Troms County due to a lack of funding and Covid-19 travel restrictions. Qualitatively, several challenges however were identified, including by a rough inspection of the other county products. However, with some experience, a potential user of the products should be able to distinguish most of such misclassification visually. To further improve the products, future studies should focus on the collection of field data in order to train, refine and better validate the methods on a county level, including a manual final “clean-up” of the results. Due to a generally lower tidal range and therefore a less significant ITZ in southern Norway, priority should be given to mid and northern Norway counties. There might also

be room for improvement in the combination of S1 and S2. Furthermore, the methods need to be more automized if ITZ maps should be produced on a periodic bases in order to detect changes.

The current products can be used in the identification and delimitation of important ITZ areas. The bathymetry in the ITZ is clearly represented in the ITZ AtmExp product and could be used for planning boat landings and new constructions. High biodiversity areas can be associated with the presence of seaweed and mudflats in the ITZ type product. After a manual clean-up, the total area of ITZ per county should also be quantifiable. The position as well as the size of fish farms are clearly identifiable in the products. As boat traffic dominates detection of ITZ in southern Norway where the tidal range is relatively low, the products should be a lot less accurate than our accuracy assessment in Troms county suggests.

The study also revealed new potential opportunities to map fish farms, suspended sediments, kelp forest and to estimate boat traffic or harbour occupancy in populated areas.

9. Project limitation

The total budget of this project was very limited, and we estimate an overuse of funding of at least 50%. The production of national products over a vast area such as Norway must take several additional challenges into account. Also, just the processing time of Sentinel-1 data has to run over several weeks for best results at 10m resolution.

10. Acknowledgments

The authors wish to thank our colleagues at NORCE that have developed that SAR processing line and continuously improve it with adding new tools.

11. References

Copernicus Land Monitoring Service. Coastal Zones Production of Very High Resolution Land Cover/Land Use dataset for coastal zones of the reference years 2012 and 2018. Nomenclature Guideline. https://land.copernicus.eu/user-corner/technical-library/coastal-zone-monitoring

Copernicus. http://coastal.planetek.it/geocommunity/dwnld/CZ_Guideline.pdf

Davidson, N.C., and Finlayson, C.M., 2019. Updating global coastal wetland areas presented in Davidson and Finlayson (2018). *Marine and Freshwater Research. Doi: 10.1071/MF19010.*

Delegido, J., J. Verrelst, L. Alonso, J. Moreno. Evaluation of Sentinel-2 Red-Edge Bands for Empirical Estimation of Green LAI and Chlorophyll Content. *Sensors 2011, 11, 7063-7081.*

De Zan, F., & Guarnieri, A. M. (2006). TOPSAR: Terrain Observation by Progressive Scans. *Geoscience and Remote Sensing, IEEE Transactions on, 44(9), 2352–2360. doi:10.1109/TGRS.2006.873853*

Direktoratet for naturforvaltning, 2007. Kartlegging av marint biologisk mangfold. DN Håndbok 19-2001, revidert 2007. 51 s.

ESA, Sentinel Success Stories, https://sentinel.esa.int/web/sentinel/news/success-stories/-/asset_publisher/3H6l2SEVD9Fc/content/copernicus-sentinel-1-supports-detection-of-shoreline-positions?redirect=https%3A%2F%2Fsentinel.esa.int%2Fweb%2Fsentinel%2Fnews%2Fsuccess-stories%3Fp_p_id%3D101_INSTANCE_3H6l2SEVD9Fc%26p_p_lifecycle%3D0%26p_p_state%3Dnormal%26p_p_mode%3Dview%26p_p_col_id%3Dcolumn-1%26p_p_col_pos%3D1%26p_p_col_count%3D2

Gilvear, D., Tyler, A., and Davids, C., 2004. Detection of Estuarine and Tidal River Hydromorphology Using Hyper-Spectral and Lidar Data: Forth Estuary. *Estuarine Coastal and Shelf Science, 61: 379-392. Doi: 10.1016/j.ecss.2004.06.007*

Gorelick, N., Hancher, M., Dixon, M., Ilyushchenko, S., Thau, D., & Moore, R., 2017. Google Earth Engine: Planetary-scale geospatial analysis for everyone. *Remote Sensing of Environment, 202: 18-27. Doi: 10.1016/j.rse.2017.06.031.*

Haarpaintner, J. & C. Davids. Satellite Based Intertidal-Zone Mapping from Sentinel-1&2. Final Report. *NORCE Klima Report nr. 2-2020, Norwegian Environmental Agency, M-1646, March 2020.* Available online at https://www.miljodirektoratet.no/publikasjoner/2020/mars-2020/satellite-based-intertidal-zone-mapping-from-sentinel-12/

Haarpaintner, J., B. Killough, R. Mathieu, L. Mane, B. Gessesse Awoke (2019). Advanced Sentinel-1 Analysis Ready Data for Africa. *Presentation at 'ESA Living Planet Symposium 2019', Milan, Italy, 13-17 May 2019. https://drive.google.com/file/d/1JOsOYNa8XGHVjuIEhfTagFE0S3RpwPgJ/view*

Høegh Bojesen, M., Kartlegging av bløttbunn vegetasjon i Oslofjorden. Miljødirektoratet fjernmålingsseminaret 2020 (digital), 8.12.2020.

IPBES (2019). Summary for policymakers of the global assessment report on biodiversity and ecosystem services of the Intergovernmental Science-Policy Platform on Biodiversity and Ecosystem Services. *S. Díaz, J. Settele, E. S. Brondízio E.S., H. T. Ngo, M. Guèze, J. Agard, A. Arneth, P. Balvanera, K. A. Brauman, S. H. M. Butchart, K. M. A. Chan, L. A. Garibaldi, K. Ichii, J. Liu, S. M. Subramanian, G. F. Midgley, P. Miloslavich, Z. Molnár, D. Obura, A. Pfaff, S. Polasky, A. Purvis, J. Razzaque, B. Reyers, R. Roy Chowdhury, Y. J. Shin, I. J. Visseren-Hamakers, K. J. Willis, and C. N. Zayas (eds.). IPBES secretariat, Bonn, Germany. 56 pages.*

Larsen, Y.; Engen, G.; Lauknes, T.R.; Malnes, E.; Høgda, K.A. A generic differential InSAR processing system, with applications to land subsidence and SWE retrieval. *In Proceedings of the ESA FRINGE Workshop 2005, ESA ESRIN, Frascati, Italy, 28 November–2 December 2005.*

Lundberg, A., 2013. Havstrandnatur. Tilstand, overvåking. DN-utredning 6-2013. Direktoratet for naturforvaltning. 76 pages. *ISBN: 978-82-8284-105-4.*

Macreadie, P.I., Anton, A., Raven, J.A. et al. The future of Blue Carbon science. *Nature Commun. 10, 3998 (2019). https://doi.org/10.1038/s41467-019-11693-w* .

Mora-Soto, A., Palacios, M., Macaya, E.C., Gómez, I., Huovinen, P., Pérez-Matus, A., Young, M., Golding, N., Toro, M., Yaqub, M., and Macias-Fauria, M., 2020. A High-Resolution Global Map of Giant Kelp (*Macrocystis pyrifera*) Forests and Intertidal Green Algae (*Ulvophyceae*) with Sentinel-2 Imagery. *Remote Sensing, 12, 694.* doi:10.3390/rs12040694

Murray, N. J. et al, 2018. The role of satellite remote sensing in structured ecosystem risk assessments. *Science of the Total Environment 619–620, 249–257 (2018).*

Murray et al., 2019. The global distribution and trajectory of tidal flats. *Nature Research, 565(7738): 222-225. Doi:10.1038/s41586-018-0805-8.*

Normandin, C., Lubac, B., Sottolichio, A., Frappart, F., Ygorra, B., and Marieu, V., 2019. Analysis of suspended sediment variability in a large highly turbid estuary using a 5-year long remotely sensed data archive at high resolution. *JGR Oceans, 124: 7661-7682. Doi: 10.1029/2019JC015417.*

Oliver-Cabrera, Talib & Wdowinski, Shimon. (2016). InSAR-Based Mapping of Tidal Inundation Extent and Amplitude in Louisiana Coastal Wetlands. *Remote Sensing. 8. 393. 10.3390/rs8050393*

Pettorelli et al., 2016. Framing the concept of satellite remote sensing essential biodiversity variables: challenges and future directions. *Remote Sensing in Ecology and Conservation, ⅔: 122-131. Doi: 10.1002/rse2.15.*

Rebelo, L.-M., Finlayson, C.M., Strauch, A., Rosenqvist, A., Perennou, C., Tøttrup, C., Hilarides, L., Paganini, M., Wielaard, N., Siegert, F., Ballhorn, U., Navratil, P., Franke, J., and Davidson, N., 2018. The use of Earth Observation for wetland inventory, assessment and monitoring: An information source for the Ramsar Convention on Wetlands. *Ramsar Technical Report No.10. Gland, Switzerland: Ramsar Convention Secretariat.*

regjeringen.no. Online: https://www.regjeringen.no/en/topics/climate-and-environment/biodiversity/innsiktsartikler-naturmangfold/hav-og-kyst/id2076396/

Robbi Bishop-Taylor, Stephen Sagar, Leo Lymburner, Robin J. Beaman. Between the tides: Modelling the elevation of Australia's exposed intertidal zone at continental scale. *Estuarine, Coastal and Shelf Science, Volume 223, 2019, 115-128, ISSN 0272-7714, doi: 10.1016/j.ecss.2019.03.006.*

Sagar, S., Roberts, D., Bala, B., Lymburner, L., 2017. Extracting the intertidal extent and topography of the Australian coastline from a 28 year time series of Landsat observations. *Remote Sens. Environ. 195, 153–169, doi: 10.1016/j.rse.2017.04.009.*

Satellite-based Wetland Observation Service, https://www.swos-service.eu

Spinosa, A., Ziemba, A., Saponieri, A., Navarro-Sanchez, V. D., Damiani, L., & El Serafy, G. (2018). Automatic Extraction of Shoreline from Satellite Images: a new approach. *In 2018 IEEE International Workshop on Metrology for the Sea; Learning to Measure Sea Health Parameters (MetroSea)(pp. 33-38). IEEE. DOI: 10.1109/MetroSea.2018.8657864*

Ulander, L. Radiometric slope correction of synthetic aperture radar images. *IEEE Trans. Geosci. Remote Sens. 1996, 34, 1115–1122, doi:10.1109/36.536527.*

Vesterbukt, P., Aune, S., Grenne, S., and Johansen, L., 2013. Basiskartlegging etter NiN (Naturtyper i Norge) i 10 utvalgte verneområder i Østfold. Resultater. *Bioforsk rapport 8 (75) 2013. 79 s. ISBN: 978-82-17-01096-8.*

Volent, Z., Johnsen, G., and Sigernes, F. (2007). Kelp forest mapping by use of airborne hyperspectral imager. *Journal of Applied Remote Sensing, 1, 011503. Doi:10.1117/1.2822611.*

Zhao, C., Qin, C-Z., and Teng, J., 2020. Mapping large-area tidal flats without the dependence on tidal elevations: A case study of Southern China, *ISPRS Journal of Photogrammetry and Remote Sensing, 159, 256-270, doi: 10.1016/j.isprsjprs.2019.11.022.*

NORCE Norwegian Research Centre AS
www.norceresearch.no